BOKU

University of Natural Resources & Life Sciences

Department of Applied Genetics and Cell Biology

Elucidating structure-function relationships of distinct IgA1 and IgA2 glycoforms

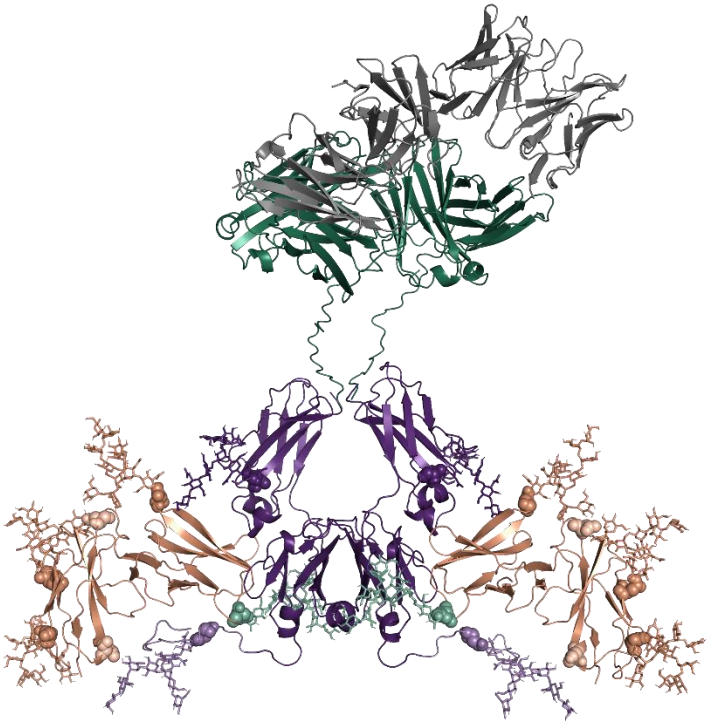

Ph.D. thesis

Dipl.-Ing. Kathrin Göritzer

Vienna, September 2019

Supervisor: Assoc. Prof. Dr. Richard Strasser
Co-supervisor: Univ.Prof. Dr. Christian Obinger

Für Fleischi – Entdecker und unermüdlicher Lebenskünstler

ACKNOWLEDGEMENTS

I would like to express my deepest gratitude to the many people who have accompanied me on this 4-year journey. Many of my colleagues have become dear friends and I am very grateful for all the many-faceted support during this challenging, educational and inspiring time.

First and foremost, I would like to thank Richard Strasser for being an exceptional supervisor and mentor, who has always been perfectly supportive. I also want to thank Gernot Beihammer, Julia König, Yunji Shin, Jenny Schoberer, Ulli Vavra and Christiane Veit for providing such a comfortable environment to concentrate on the thesis and advance in research as well as for all the fun and inspiration in my daily work at the institute. Special thanks go out to my great students Iris Goet, Stella Duric,, Marco Cvijic and Lukas Narendja for their constant and committed support for the project.

I would also like to thank my co-supervisor Christian Obinger and my PhD program coordinator Christa Jakoptisch for providing scientific input (or a beer) whenever needed. Furthermore, I would like to acknowledge Elisabeth Lobner and Irene Schaffner who have been a constant source of expertise and friendship throughout my Master's degree and PhD studies.

For the indispensable help with glycan analysis I would like to thank Daniel Maresch, who never looked too annoyed when I walked into his office with a massive number of new samples.

I would like to express my gratitude to Jan Novak, for his warm welcome and for giving me the opportunity to work at his lab in Birmingham, which has been a great time for professional advancement and personal growth.

Last but definitely not least, I would like to thank my family – especially my mum and my grandma – who have always been my biggest cheerleaders although they can't make head nor tail of where I got my enthusiasm for biology and chemistry from. Thank you Wolfi for your patience, pep talks (although I didn't always accept them) and loving support.

ABSTRACT

Immunoglobulin A (IgA) serves as a first line of defense against invading pathogens and is increasingly gaining attention as a biopharmaceutical for the treatment of infectious diseases and cancer. However, the full potential of recombinant IgAs as therapeutic antibodies is not explored yet, also owing to the fact that structure-function relationships of these extensively glycosylated proteins are not well understood. To study the influence of glycosylation on the biophysical and immunological properties, homogeneously glycosylated IgA is required. Therefore, human monomeric IgA1 and IgA2 variants of the HER2-binding clinical antibody trastuzumab were transiently expressed in *Nicotiana benthamiana* ΔXT/FT plants, in which enzymes responsible for generating non-human *N*-glycan structures are eliminated. By co-infiltration of the respective mammalian glycosylation enzymes, IgAs carrying homogeneous oligomannosidic, paucimannosidic, complex terminally galactosylated or sialylated *N*-glycans were generated. To verify the capacity of the plant-based system to produce functional IgA, the constructs were additionally expressed in human embryonic kidney (HEK293) cells. Plant- and HEK-produced IgA variants were then subjected to detailed characterization to assess site-specific glycosylation, overall structure and stability as well as binding to the antigen HER2 using a broad set of biochemical and biophysical methods. Furthermore, the influence of glycosylation for the thermodynamics and kinetics of complex formation of IgA with four different FcαRI glycoforms was investigated. We demonstrated that distinctly different *N*-glycan profiles do not influence antigen binding or the overall structure and integrity of the IgA antibodies but affect their thermal stability. Furthermore, we could show that not IgA but FcαRI glycosylation influences the antibody receptor interaction. We also noted that full-length IgA and FcαRI form a mix of 1:1 and 1:2 complexes tending toward a 1:1 stoichiometry due to different IgA tailpiece conformations that can hinder binding of a second receptor molecule.

KURZFASSUNG

Immunglobulin A (IgA) dient als erste Abwehrbarriere gegen die Invasion von Krankheitserreger und gewinnt als mögliches Biopharmazeutikum zur Behandlung von Infektionskrankheiten und Krebs zunehmend an Bedeutung. Das Potenzial von rekombinanten IgAs als therapeutische Antikörper ist jedoch noch nicht vollkommen erforscht, unter anderem weil die Struktur-Funktionsbeziehungen dieser stark glykosylierten Proteine erst unzureichend verstanden werden. Um den Einfluss der Glykosylierung auf die biophysikalischen und immunologischen Eigenschaften zu untersuchen, ist homogen glykosyliertes IgA erforderlich. In der vorliegenden Arbeit wurden humane monomere IgA1 und IgA2 Varianten des HER2-bindenden klinischen Antikörpers Trastuzumab in *Nicotiana benthamiana* ΔXT/FT transient exprimiert. In diesem pflanzlichen Expressionssystem wurden Enzyme, die für nicht-humane *N*-Glykan Strukturen verantwortlich sind, eliminiert. Durch Co-Expression der jeweiligen Säugetier-Glykosyltransferasen konnten IgAs mit homogener oligomannosidischer, paucimannosidischer, komplexe terminal galactosylierter oder sialylierter *N*-Glykosylierung erzeugt werden. Um zu verifizieren ob das pflanzliche System funktionelle IgA produzieren kann wurden die Konstrukte zusätzlich in einer humanen Zelllinie (HEK293) expremiert. Die IgA-Varianten wurden anschließend einer detaillierten Charakterisierung unterzogen, um den Glykosylierungsstatus, die Gesamtstruktur und -stabilität sowie die Antigenbindung mithilfe einer breiten Palette an biochemischen und biophysikalischen Methoden zu analysieren. Darüber hinaus wurde der Einfluss der Glykosylierung auf die Thermodynamik und Kinetik der Komplexbildung von IgA mit vier verschiedenen FcαRI-Glykoformen untersucht. Dabei konnten wir zeigen, dass unterschiedliche Glykosilierungen weder die Antigenbindung noch die Gesamtstruktur und Integrität der IgA-Antikörper beeinflussen, aber deren thermische Stabilität und dass nicht IgA-, sondern FcαRI-Glykosylierung die Antikörper-Rezeptorwechselwirkung beeinflusst. Weiteres haben wir festgestellt, dass IgA und FcαRI eine Mischung aus 1:1 und 1:2 Komplexen bilden, wobei eine Tendenz zur 1:1 Stöchiometrie zu beobachten ist. Dieses Phänomen lässt sich vermutlich auf unterschiedliche Konformationen des flexiblen C-terminalen Endstückes von IgA zurückführen, die die Bindung eines zweiten Rezeptormoleküles behindern können.

TABLE OF CONTENTS

INTRODUCTION

Immunoglobulin A (IgA) is the second most prevalent serum immunoglobulin after IgG and is the predominant antibody class in the external secretions of mucosal surfaces, where it serves as a first line of defense by neutralizing invading pathogens. The body expends a considerable amount of energy producing IgA thereby exceeding the daily production of all other immunoglobulin classes combined [1]. This already indicates its critical role in immune defenses for which it is equipped by unique structural attributes of its heavy chain and by its ability to polymerize.

IgA is an immune glycoprotein

Like all immunoglobulins, the basic monomeric structural unit of IgA comprises two identical heavy and light chains. These chains are arranged into two Fab arms responsible for antigen recognition and an Fc part that mediates effector functions linked by a flexible hinge region. Each heavy and light chain is folded into four (V_H, C_H1, C_H2, C_H3) and two (V_L, C_L1) globular domains, respectively, and each domain adopts the characteristic "immunoglobulin fold".

In humans, two subclasses IgA1 and IgA2 have been characterized, of which the latter occurs as two major allotypes [IgA2m(1) and IgA2m(2)]. Each of these subclasses comprises distinct structural features (**Figure 1A**). While the light and heavy chains of IgA1 and IgA2m(2) are linked by disulphide bridges, these are generally lacking in IgA2m(1). Instead, the light chains form a disulphide bridge and the association with the heavy chains is mediated through non-covalent interactions[2]. Another notable difference is the extended hinge-region of IgA1 that increases the flexibility of its Fab arms possibly allowing the simultaneous binding of more distant epitopes[3]. This elongation features a 13 amino-acid insertion rich in proline, serine and threonine with 9 putative *O*-glycosylation sites of which usually 3 to 6 are occupied. The *O*-glycans are very heterogeneous with a combination of mucin-type core 1 structures consisting of N-acetylgalactosamine (GalNAc) with β1,3-linked galactose and one or both saccharides can be sialylated [4-7] (**Figure 1B**). The *O*-linked glycans are very likely to affect the structure adopted by the hinge by decreasing its conformational variability [8]. The lack of the hinge-region in IgA2 leads to a reduced susceptibility to bacterial proteases, which might explain the higher prevalence of the IgA2 subclass in mucosal secretions while serum IgA is mostly comprised of IgA1 [9, 10].

Furthermore, all subclasses have a varying number of *N*-glycosylation sites. IgA1

exhibits a C_H2-resident *N*-glycan site at the sequon "NLT" and at the flexible tailpiece with the sequon "NVS", while the IgA2m(1) and IgA2m(2) isotypes have even further sugars attached (**Figure 1A** and **B**), making IgA one of the most heavily glycosylated antibody classes [5-7]. The glycosylation profile of the different IgA subclasses is very heterogeneous consisting mostly of complex-type *N*-glycans comprising a heptasaccharide core with varying levels of terminal sialic acid, core-fucose and branched structures. In addition, there are indications for site-specific glycan processing as core fucosylation in the *N*-glycans from the tailpiece of IgA1 but not in the C_H2-resident glycans has been observed in serum IgA, as well as CHO-, HEK- and plant-produced recombinant IgA. Furthermore, the NVS glycosylation site in the C-terminal tailpiece comprises more highly branched complex *N*-glycans with incomplete galactosylation and sialylation [6, 7, 11-13]. Thus, site-specific differences between the individual *N*-glycosylation sites of IgA can be observed, however, distinct structural features of the *N*-glycans at the respective sites in the different subclasses seem to be conserved among isotypes and different hosts (**Figure 1B**).

Interestingly, it has also been reported that the glycosylation status of IgA depends on its tissue location with considerable higher levels of terminal sialic acid in the *N*-glycans linked to serum IgA compared to IgA in secretions, where also small amounts of oligo-mannosidic *N*-glycans could be observed [4, 13, 14].

Structural studies showed that unlike the IgG and IgE *N*-glycans, which are found between the upper Fc domains, the C_H2-resident *N*-glycans of IgA are solvent-accessible and located on the external surface of the protein (**Figure 1C**) [15-17]. The presence of this glycan in IgG is important to maintain an open conformation of the Fc domain and influences properties like conformational and thermal stability [18, 19]. Furthermore, distinct sugar modifications of IgG can drastically influence serum half-life and binding affinity to FcγIIIa to modulate the immune response. The absence of the core-fucose promotes increased carbohydrate-carbohydrate interactions with the *N*-glycans of the receptor leading to enhanced antibody dependent cellular cytotoxicity. In contrast to the broad acceptance of the importance of the IgG glycans on structure-function relationships, the roles of the glycans attached to IgA are still relatively unexplored. IgA generally has a very short half-life due to rapid clearance by the asialoglycoprotein receptor (ASGPR) expressed on hepatocytes in the liver and due to the lack of FcRn binding as seen in IgG. However, increased serum half-life could be achieved with higher sialic acid content, which circumvents fast clearance of IgA by ASGPR [20]. Furthermore, it was shown that the higher number of *N*-glycans in the IgA2 subtype contributed to faster clearance from circulation by this receptor compared to IgA1. Another study showed

the importance of terminal sialic acid on *N*-glycans of IgA for inhibition of influenza A and other sialic-acid-binding viruses [21]. However, how glycans influence other properties of IgA and binding to various cellular receptors remains to be elucidated.

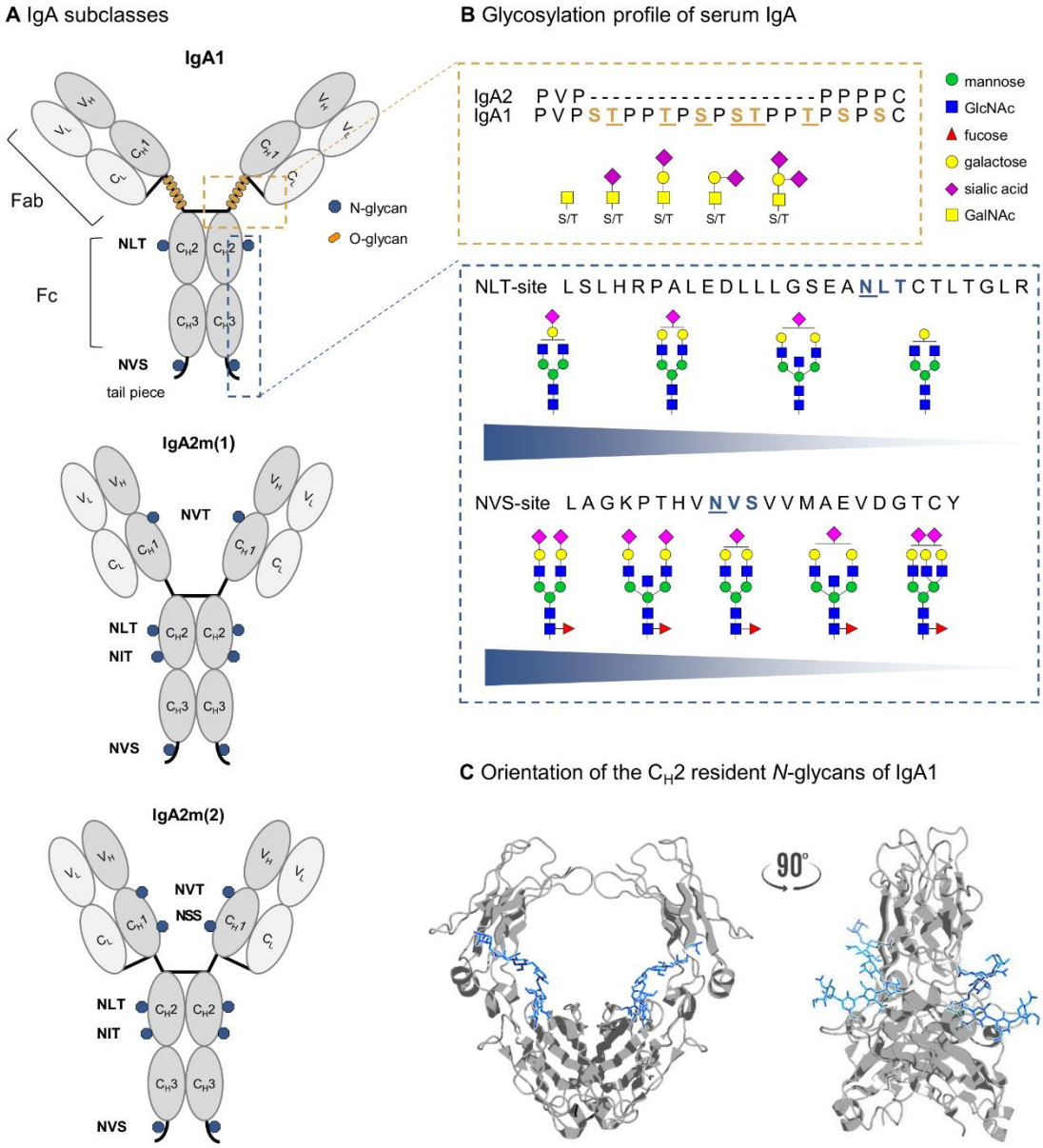

Figure 1: Illustration of the monomeric structural units of IgA. A) Schematic illustration of the structure and glycosylation sites of the IgA isotypes IgA1, IgA2m(1) and IgA2m(2). The light chain is colored in light gray and the heavy chain in dark gray. *N*-glycans found in the different isotypes are indicated by blue dots. The *O*-glycans in the elongated hinge-region of IgA1 are marked by orange dots. **B)** Heterogeneity and site-specific difference of *O*- and *N*-glycosylation of IgA1 from human serum. The symbols for the monosaccharaides are drawn according to the nomenclature from the Consortium for Functional Glycomics. **C)** Crystal

structure of the IgA1-Fc lacking the tailpiece (PDB-ID: 1OW0). The *N*-linked glycans resolved by the structure are marked in blue and the heavy-chains of IgA1-Fc are colored in gray.

Molecular forms of IgA

As mentioned in the previous section, serum IgA is predominantly monomeric and is produced by local plasma cells in the bone marrow, spleen and lymph nodes. Secretory IgA at mucosal surfaces is a product of local synthesis by the gut-associated lymphoid tissue where it is produced as a dimer, although small amounts of monomers, trimers and tetramers can also be present [2, 22] (**Figure 2**). Dimeric IgA (dIgA) is composed of two monomers that are linked by a disulphide bridge of one of the heavy chains of each monomer with the joining chain (J-chain) [23, 24]. The J-chain is a highly conserved polypeptide that is incorporated in dIgA, larger IgA polymers and pentameric IgM. It has an *N*-linked glycan of biantennary complex structure, which along with the IgA tailpiece *N*-glycan contributes to correct dimer formation [23, 25]. Furthermore, the polypeptide comprises eight cysteine residues of which six form intra-chain disulphide bridges and the remaining two (Cys14 and Cys68) form covalent links to the penultimate residue of the IgA tailpiece [25]. Newly synthesized dimeric IgA can associate with the pIgR receptor that is expressed as integral membrane protein on the basolateral side of epithelial cells lining mucosal surfaces, after which it is transported across the epithelium and released into the lumen. At the luminal side, pIgR is cleaved and a part referred to as secretory component (SC) remains attached thereby forming SIgA [26, 27]. This secretory component is a hydrophilic and highly glycosylated negatively charged molecule with a molecular weight of 80 kDa and 7 *N*-glycosylation sites, which protect SIgA from degradation in the luminal secretions and can directly interact with various host cell receptors and pathogens [28]. Therefore, secretory and serum IgA are produced by cells with different organ distributions and have different biochemical and immunochemical properties. Different methods of immunization can induce serum or secretory IgA responses or a combination of both.

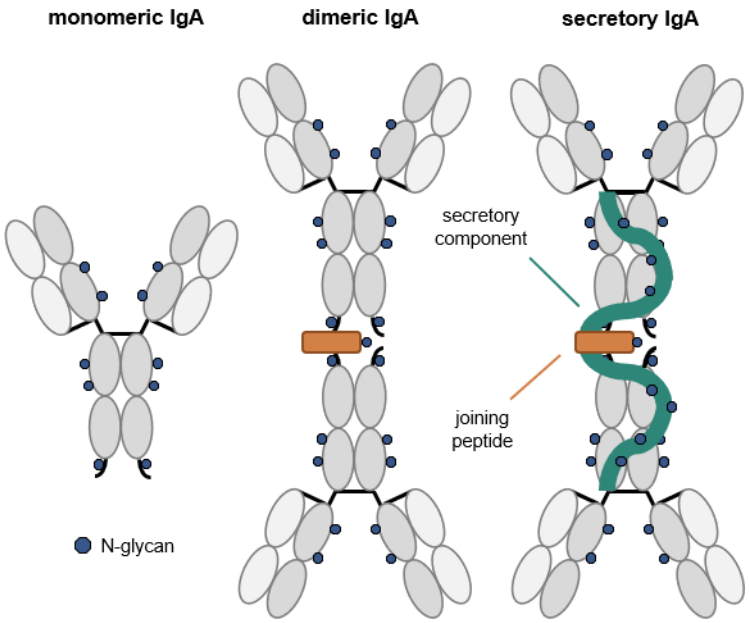

Figure 2: Schematic representation of different molecular forms of IgA (e.g. IgA2m(2)). Dimeric IgA consists of two IgA molecules that are linked with a J-chain (orange). Secretory IgA contains an additional molecule, the secretory component (green). *N*-linked glycans are marked with blue dots.

Interaction of IgA with host cell receptors

IgA can mediate a variety of protective functions such as phagocytosis, respiratory burst, cytokine release and antibody-dependent cellular cytotoxicity through interaction with various receptors that are presented on host (immune) cells. So far, the major IgA receptor FcαRI is the best characterized one. For some of the IgA receptors an understanding of their mode of interaction has been developed, but for many it is less clear and remains to be elucidated.

FcαRI is the major IgA receptor

Structure and expression of FcαRI

The FcαRI, also known as CD89, is a key mediator of IgA effector functions. It is expressed constitutively on the cells of the myeloid linage including neutrophils, eosinophils, monocytes, macrophages and Kupffer cells [29-31]. It is a member of the Fc receptor immunoglobulin superfamily and although the ligand-binding chain of FcαRI is structurally related to the alpha chains of IgG Fc receptors and the high-affinity IgE receptor, its gene maps to chromosome 19 and shares higher homology with leucocyte Ig-like receptors [32, 33]. The FcαRI comprises two Ig-like extra cellular domains, a transmembrane region, and a short cytoplasmic tail (**Figure 3A**). The two extracellular domains EC1 and EC2 are oriented in a 90° angle to each

other. Furthermore, the receptor is heavily glycosylated comprising 6 *N*-glycosylation sites and several putative *O*-glycosylation sites. Although the molecular mass of the receptor is 32 kDa the molecular weight varies between 55 and 75 kDa on neutrophils and monocytes, or up to 100 kDa on eosinophils due to extensive and differential glycosylation in different cell types [10, 34, 35]. However, the nature and composition of the glycosylation profile of FcαRI is not known.

Molecular basis of the FcαRI-IgA interaction

The binding site for IgA on FcαRI is located in the extracellular domain EC1 and involves mostly hydrophobic residues, while Fcε and Fcγ receptors bind their ligand in EC2. The interaction interface on IgA is found between the C_H2 and C_H3 domains and corresponds to the FcRn and Protein A rather than the FcγR binding sites on IgG [36]. Due to steric hindrance by the secretory component, FcαRI is not able to bind SIgA [16, 37] (**Figure 3B**). Both dIgA and monomeric IgA on the other hand can bind the receptor with moderate affinity [38].

Ligand binding to FcαRI is regulated through inside-out signaling. Resting FcαRI is serine phosphorylated in its cytoplasmic tail and has low capacity to bind IgA. However, stimulation with cytokines leads to dephosphorylation switching inactive FcαRI into an active, ligand binding receptor. The increased affinity upon cytokine stimulation has been suggested to be caused by release of the receptor from cytoskeletal anchoring which might allow bivalent ligand binding or might result from lateral movement to increase avidity as described for integrins [39-41].

Indeed, crystallographic studies demonstrated that one IgA can bind two FcαRI molecules [16, 42] (**Figure 3C**). This contrasts with Fcγ and Fcε receptors for which a 1:1 stoichiometry with their respective ligands was described [43, 44]. Several conformational changes in the receptor regions that are involved in binding were reported, however the relative orientation of EC1 and EC2 is unaffected [45, 46]. In solution the C_H2 domain of IgA exhibits a considerable degree of motion relative to the C_H3 domain. Binding to FcαRI on one side induces conformational changes across the dimer interface to the opposite heavy chain and thus might cause negative cooperativity for binding of a second FcαRI molecule. Furthermore, the crystal structure implicates a possible role of the FcαRI glycans on the IgA-receptor interaction. The *N*-glycan at position N58 comes into proximity of the interaction surface and forms two potential hydrogen bonds and a van der Waals contact [16] (**Figure 3C**). So far, studies primarily focused on the role of antibody glycosylation for the antibody-receptor interaction.

However, recent studies have also suggested an active role of receptor-associated oligosaccharides to mediate and control differential binding of immunoglobulins. Mutational studies of the N58 in FcαRI to E58 resulted in a variant that is lacking the *N*-glycosylation at this position and showed a 2-fold increase in binding affinity and a desialylated variant even exhibited a 4-fold increase [47]. The importance of receptor glycosylation in antibody-receptor interaction was further demonstrated for IgG and FcγRIIIa. It was shown that FcγRIIIa carrying oligomannosidic *N*-glycans bound IgG1-Fc with 12-fold greater affinity than FcγRIIIa with complex-type and highly branched structures [48]. So far very little information on the exact nature of receptor glycosylation in different tissues is available, due to the limited accessibility of receptors from native sources and the lack of high sensitivity and resolution methods. However, recent studies indicate a possible role of the glycosylation modification for the function of different receptors including the FcαRI and the receptors are differentially glycosylated in different tissues.

FcαRI function in vivo

To initiate effector functions upon binding of FcαRI to its ligand, association with the FcR γ-chain is necessary (**Figure 3D**). FcαRI does not have any signaling motifs in its cytoplasmic tail and thus has to associate with the FcR γ-chain, which is usually co-expressed with the receptor and contains an immunoreceptor tyrosine-based activation motif (ITAM) in its intracellular domain [49, 50]. If the γ-chain is not expressed, as it has been observed in monocytes and some neutrophil subpopulations, functionality is limited to ligand binding and receptor recycling in early endosomes [51, 52]. Complex formation with FcR γ-chain is also essential for other Fc receptors such as the IgE receptor and the IgG receptors FcγRI and FcγRIIa [53]. The cellular response that follows triggering of the FcαRI-FcR γ-chain complex depends on the nature of the ligand and leads to either pro-inflammatory or anti-inflammatory responses. Cross-linking of FcαRI-FcR γ-chain with multimeric IgA immune complexes transiently redistributes the receptor to plasma membrane rafts. Tyrosines in the ITAM are then phosphorylated and act as docking sites for signaling molecules and induce robust pro-inflammatory responses such as phagocytosis, antibody-dependent cellular cytotoxicity, respiratory burst, degranulation, antigen presentation and release of cytokines [29].

Alternatively, it was demonstrated that inhibitory signals can also be transduced via the FcαRI-FcR γ-chain complex. FcαRI-binding of non-targeted monomeric serum IgA results in partial phosphorylation of the FcR γ-chain and causes formation of cytoplasmic clusters

referred to as “inhibisomes”. Inhibisomes impair activation of Fc receptors via a process referred to as inhibitory ITAM (ITAMi) receptor signaling. ITAMi initiates an anti-inflammatory response to dampen pro-inflammatory responses induced by other Fc receptors [32]. Taken together, the hypothesis is that activating FcαRI-FcR γ-chain complexes can lead to either pro- or anti-inflammatory responses, depending on the valency of the ligand.

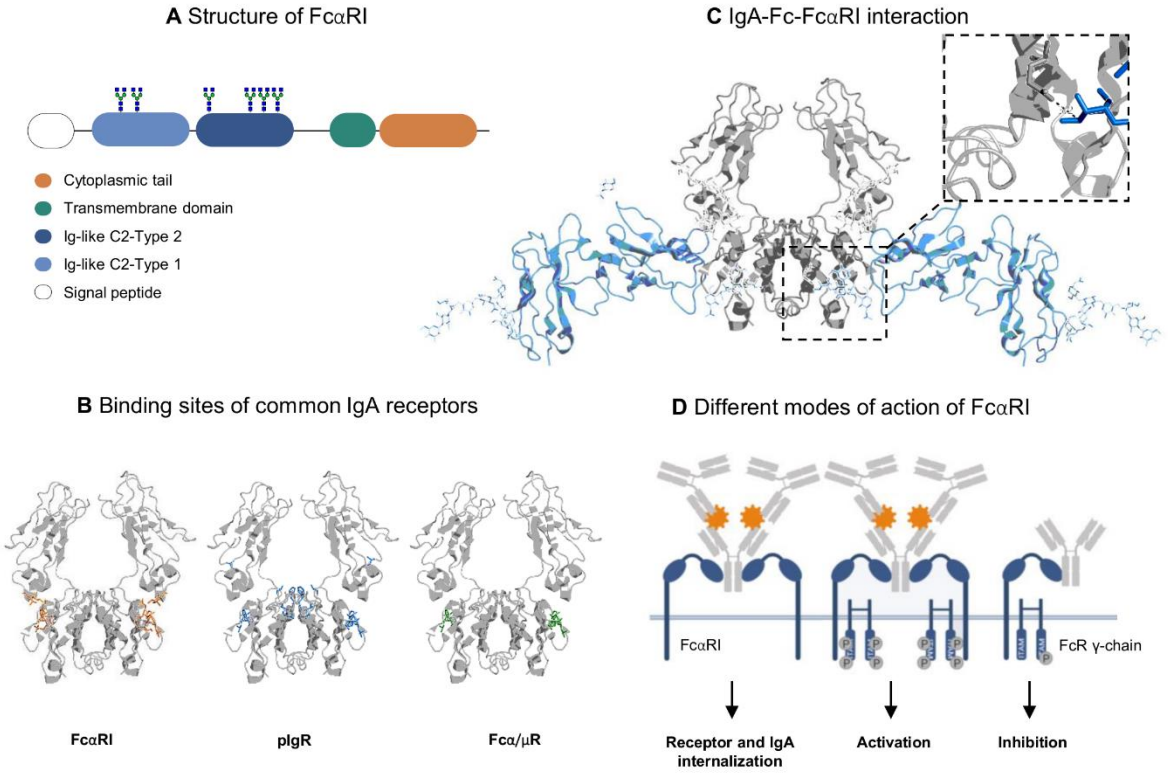

Figure 3: Interaction of IgA with its receptors. A) Schematic representation of the structure of the FcαRI and attached *N*-glycosylation sites. **B)** Partial overlapping of interaction interfaces on IgA1-Fc of different IgA receptors. Interaction surfaces are highlighted in color. **C)** Crystal structure of the IgA1-Fc-FcαRI 1:2 complex. Attached *N*-glycans are shown as sticks. The *N*-glycan at position N58 of FcαRI approaches the IgA1-Fc backbone within 3.2 Å. **D)** FcαRI can mediate different modes of action depending on the ligand.

pIgR

The polymeric immunoglobulin receptor (pIgR) is a transmembrane protein present on the basolateral side of epithelial cells and mediates transport of dimeric IgA to the apical site of the mucosal tissue where it is released as secretory IgA (as described in a previous section). The presence of the J-chain in dimeric or polymeric IgA is required for non-covalent binding of pIgR within the C_H3 domain of IgA [54, 55]. Binding to dIgA can be further stabilized by a

disulphide bond, however, this interaction is absent in some SIgA complexes [56]. Upon transcytosis the extracellular domain of pIgR is proteolytically cleaved creating the secretory component (SC). The human pIgR contains 7 *N*-glycosylation sites which very likely do not affect binding to dIgA [57]. *N*-glycosylation of pIgR may however be required for efficient transport of pIgR and release of the ectodomain during transcytosis [58], while *N*-glycosylation of dIgA did not affect these processes. Furthermore, the many glycosylation sites on the secretory component protects SIgA from proteolytic degradation and are important for the interaction with pathogenic bacteria such as *H. pylori*, *E. coli* and *Shigella* spp, commensal bacteria *Lactobacillus* and *Bifidobacteria* or host protein IL-8, and therefore contribute to microbiota homeostasis of the intestinal mucosa [59, 60]. Furthermore, the secretory component has an overlapping binding site with the FcαRI leaving one available for the receptor. Binding of FcαRI to SIgA was reported to be possible only when Mac-1 I co-engaged thereby triggering respiratory burst in neutrophils [61].

Transferrin receptor

The transferrin receptor (TfR) is a membrane glycoprotein which is upregulated in cultured mesangial cells (HMC) and patients with IgA nephropathy (IgAN). It was reported that it primarily binds polymeric IgA1 and that *O*-glycosylation as well as *N*-glycosylation are involved in the interaction. In these studies, pIgA1 from IgAN patients displaying aberrant IgA1 *O*-glycosylation showed increased binding to the receptor while binding capacity was lost after *N*-deglycosylation [62]. Furthermore, it was also identified as a receptor for SIgA immune complexes that mediates their retrograde transport back to the lamina propria during celiac disease [63].

Dectin-1

Dectin-1 is a C-type lectin that has been identified to be essential for the reverse transcytosis to the lamina propria of SIgA-antigen complexes by intestinal M cells with Siglec-5 as a possible co-receptor. It was reported that binding on SIgA occurs at the C_H1 domain region as well as at terminal sialic acid residues of the *N*-glycans of the secretory component. The transcytosed SIgA is taken up by dendritic cells (DCs) via the DC-SIGN receptor in the lamina propria [64].

DC-SIGN

Upon retro transcytosis by Microfold cells (M cells) SIgA-antigen complexes associate with sub-epithelial dendritic cells through interaction with the dendritic cell-specific intercellular adhesion molecule-grabbing non-integrin (DC-SIGN) that probably interacts with mannose

residues on the secretory component. It was speculated that this serves as a surveillance mechanism to assess luminal antigens and possibly promotes tolerance against commensal bacteria and dietary components [65].

FcRL4

Only recently, Fc receptor-like protein 4 (FcRL4) was identified as an inhibitory low affinity receptor for IgA [66]. It is a member of the FcRL family of cellular receptors that show homology to FcγRI and are predominantly expressed on a unique subset of tissue memory B cells concentrated in the subepithelial and marginal zones of mucosal lymphoid tissue and also accumulate in the joints of patients with rheumatoid arthritis [67]. It was suggested that the receptor is involved in the regulation of the mucosal IgA response and $FcRL4^+$ positive memory B cells are involved in the link between mucosal and joint autoimmunity [68].

ASGPR

The asialoglycoprotein receptor is a lectin domain containing receptor that is expressed by hepatocytes in the liver and is responsible for clearance of glycoproteins of which terminal sialic acid residues on *N*-glycans have been removed and terminal galactose residues are exposed. In previous studies it was shown that due to increased numbers of *N*-glycans on IgA2 these isotypes are eliminated more rapidly compared to IgA1 contributing to the characteristic distribution of IgA isotypes observed in human serum. Furthermore, it was observed that dimeric IgA is more rapidly cleared than monomeric IgA [20, 69].

Fc alpha/mu receptor

The Fc alpha/mu receptor is a transmembrane protein that is able to bind IgM with high and IgA with medium affinity [70]. It is expressed in Penth cells in the lamina propria, follicular dendritic cells in tonsils and on macrophages [71, 72]. It maps closely to pIgR on the human chromosome 1 and its *N*-terminal Ig-like domain shares homology with domain 1 of pIgR [73]. However, the receptor only interacts with polymeric forms of IgA and IgM, but the presence of the joining chain does not seem to be essential. The binding site on dIgA lies in an exposed loop in the C_H3 domain and thus is partially overlapping with the docking site of the FcαRI and pIgR. Indeed, it was shown that the secretory component and bacterial IgA-binding proteins can inhibit the dIgA-Fcα/μR interaction. Furthermore, it was shown that dIgA glycosylation did not affect binding [74, 75]. However, the functions of this receptor remain to be elucidated.

The different roles of secretory, dimeric and serum IgA

Secretory IgA serves as a first line of defense against invading pathogens by performing a variety of protective functions and providing passive immunity. The presence of hydrophilic amino acids and the abundant glycosylation of the heavy chains and secretory component make SIgA a very negatively charged molecule that can surround microorganisms with a hydrophilic shell and thereby block their entrance into the intestinal lumen. Furthermore, SIgA can agglutinate microbes by interacting with the flagella and is able to neutralize bacterial products such as enzymes and toxins. Thus, SIgA is a neutralizing anti-inflammatory antibody with the main function to maintain homeostasis on mucosal surfaces [76]. Recently, it was described that SIgA can also be transported back into the lamina propria. This is facilitated through a retrograde transport process by M cells located in the Peyer's Patches upon binding of SIgA to Dectin-1 receptor. The retro transported SIgA immune complexes can bind to the DC-SIGN receptor and are then taken up by dendritic cells (DC). This mechanism is thought to be important for monitoring the antigenic status of the intestinal lumen [64, 77].

Due to the abundant presence of microbial flora and food components, antigens still continuously reach the lamina propria through diffusion or transcytosis. Dimeric IgA that is produced by local plasma cells in the lamina propria can already interact with these antigens and the antigen-dIgA immune complexes are subsequently transported back to the lumen via the pIgR receptor. En route through the epithelial cells, dIgA also has the ability to interact with viruses and redirect them into the lumen [78, 79]. Once pathogens have breached through the epithelial barrier, they are opsonized by dIgA, which can engage neutrophils via interaction with the FcαRI. Upon recognition of dIgA by the receptor the cells can phagocytose dIgA-opsonized bacteria and recruit further neutrophils until clearance of the invading pathogens has been achieved [80, 81] . The ability of dIgA to recruit neutrophils functions as a second line of defense. Also, FcαRI^{+} dendritic cells were shown to bind dIgA opsonized particles suggesting a protective adaptive immune response that is initiated during mucosal infections (**Figure 4A**).

Still, intestinal proteins and microorganisms can leak into the tissue and enter the bloodstream where they can be recognized by monomeric serum IgA. In the liver they then encounter Kupffer cells which express the FcαRI and are able to eliminate IgA-immune complexes from the blood stream thereby representing a third line of defense [31] (**Figure 4B**).

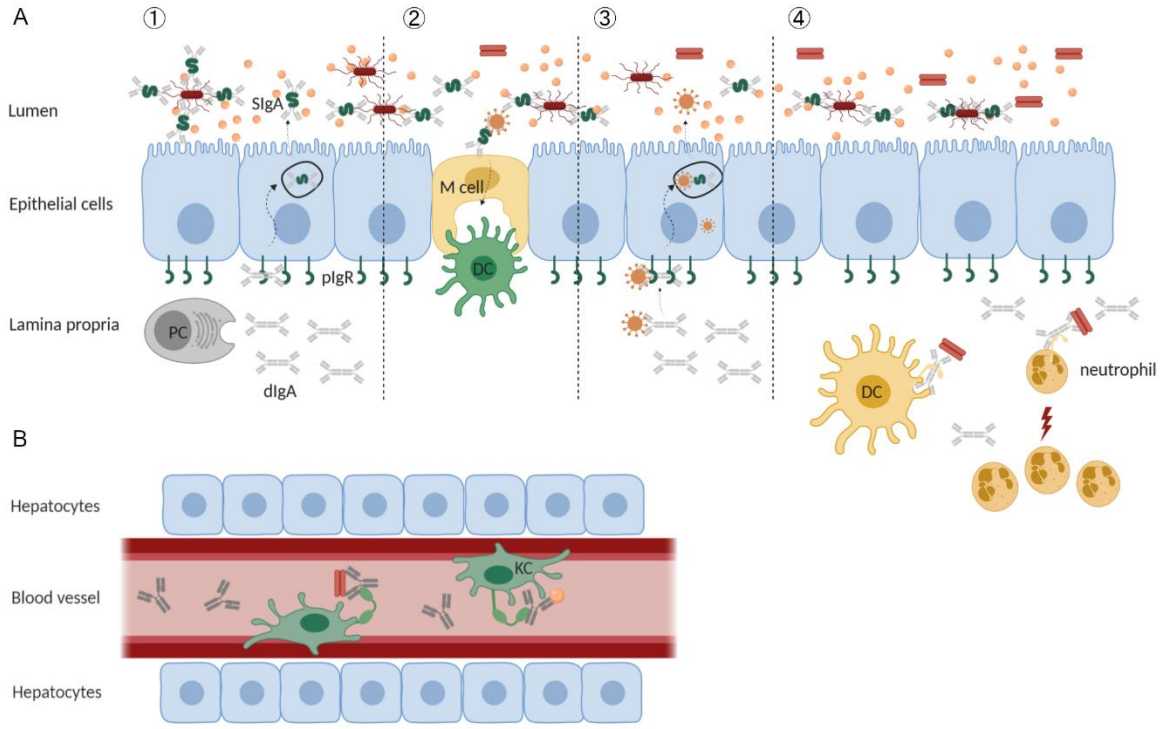

Figure 4: Roles of different molecular forms of IgA. A) Dimeric IgA is produced by local plasma cells (PC) in the lamina propria from where it is then transported to the intestinal lumen by binding to the polymeric immunoglobulin receptor (pIgR). In the lumen it is released as secretory IgA (SIgA) where it can coat bacteria. (2) Microfold cells (M cells) can facilitate retrograde transport of SIgA-coated pathogens back to the lamina propria where they are taken up by dendritic cells (DC). (3) Infiltrated antigens and pathogens are opsonized by dIgA and are transported back into the lumen. En route dIgA can bind, neutralize and eliminate viruses. (4) Breached pathogens in the lamina propria that are coated with dIgA can be taken up by FcαRI-expressing dendritic cells and neutrophils, which can attract more neutrophils until the infection is cleared. **B)** IgA-opsonizes bacteria which have leaked into the circulation are taken up by FcαRI-expressing Kupffer cells (KC) in the liver.

In contrast to the activating properties of complexed serum IgA, monomeric serum IgA is also capable of downregulating cell responses through ITAMi signaling. Via monomeric IgA targeting of FcαRI anti-inflammatory effects are promoted to protect against enhanced IgE- or IgG-, Fc-receptor-mediated signaling [9, 82].

Therefore, it has been suggested that during the normal physiological state monomeric IgA can downregulate activation of other Fc receptors to dampen excessive immune responses [32]. However, cross-linking of FcαRI during infection with dIgA or serum IgA-opsonized

pathogens results in potent pro-inflammatory responses including degranulation, phagocytosis, chemotaxis and antibody-dependent cellular cytotoxicity [83]. The dual role of IgA to passively and actively inhibit or initiate inflammatory responses makes it a very interesting target for the treatment of infections and cancer.

The potential of IgA for the treatment of infectious diseases and cancer

Currently most of the therapeutic monoclonal antibodies on the market are of the IgG type, which can mediate potent effector functions such as ADCC through the interaction with the FcγRIIIa expressed on natural-killer cells. However, recurrence of polymorphisms in FcγRs and co-engagement of the inhibitory FcγRIIb and FcγRIIIb receptors can dampen the potent ADCC response. Therefore, IgA was handled as a promising addition to therapeutic strategies, especially when IgG is less suitable. IgA mAbs could be superior over IgG when active or passive mucosal immunity is required. Furthermore, IgA can exert potent pro-inflammatory effector functions, such as induction of oxidative burst, phagocytosis and ADCC through engagement of the FcαRI expressed on polymorphonuclear (PMN) cells which are the most abundant effector cell population in the blood and can not be efficiently recruited by IgG [84, 85].

The multifaceted functions of IgA ranging from neutralization to active immune suppression and pro-inflammatory responses could be exploited in the design and generation of IgA mAbs with distinct functional activities.

AIMS OF THE THESIS

Immunoglobulin A (IgA) is increasingly gaining attention as a possible biopharmaceutical for treatment of infectious diseases and cancer [84]. However, the full potential of recombinant IgAs as therapeutic antibodies is still not fully explored, owing to the fact that robust recombinant production is challenging and a detailed understanding of structure-function relationships is still lacking. IgAs are extensively glycosylated. Despite the recognized importance of glycosylation for IgG function [86] comparatively little is known about the role of glycosylation for the structure of the various IgA formats as well as for their biophysical and immunological properties. The two IgA isotypes (IgA1 and IgA2) carry two to five *N*-glycosylation sites on the heavy chain. In addition, the IgA1 hinge region is elongated and modified with up to 6 O-linked oligosaccharides.

To assess the impact of glycosylation on structure-function relationships of the various IgA formats, an expression platform is needed which allows the production of IgA variants bearing defined glycans. In that terms, the tobacco-related species *Nicotiana benthamiana* has emerged as promising host for expression of recombinant glycoproteins with custom-made human-like *N*- and *O*-glycan modifications [87].

First a robust platform for the transient expression of monomeric IgA1 and IgA2 variants of the HER2-binding clinical antibody trastuzumab in *N. benthamiana* plants had to be established. Therefore, expression vectors and subcellular targeting signals for optimal expression conditions had to be assessed. To compare the capacities of plant-based and mammalian-based expression systems, IgA variants had to be additionally produced in HEK 293 cells. A suitable purification strategy for the recombinant IgA antibodies had to be established and correct assembly, integrity and purity had to be carefully analyzed by SDS-PAGE, immune blotting, size exclusion chromatography combined with multi-angle light scatter (SEC-MALS) and differential scanning calorimetry (DSC). Furthermore, the glycopeptides had to be subjected to LC-ESI-MS analysis to determine the *N*- and *O*-glycan composition.

Subsequently, common human glycoforms of IgA (lacking core fucose, high content of sialic acid etc.) should be generated by co-expression of mammalian glycosylation enzymes and other proteins required for sialylated complex *N*-glycan formation in the plants. Then the influence of differential glycosylation on the overall structure and homogeneity as well as conformation and thermal stability using a broad set of biochemical and biophysical methods

should be analyzed. Furthermore, the impact of glycosylation on the binding modes, binding stoichiometries and thermodynamics of the IgA interaction with its primary receptor FcαRI should be elucidated using surface plasmon resonance spectroscopy (SPR) and isothermal titration calorimetry (ITC). To also assess possible carbohydrate-carbohydrate interactions in the antibody-receptor interaction as it has been described for IgG and FcγRIIIa, different receptor glycoforms had to be generated and tested as well.

Taken together, this study aimed to establish a robust plant-based expression system for IgA glycoforms in order to systematically evaluate the impact of glycosylation on structure and function of the different IgA isotypes and to elucidate the role of glycosylation in the IgA-FcαRI interaction.

PUBLICATIONS

Exploring Site-Specific N-Glycosylation of HEK293 and Plant-Produced Human IgA Isotypes

Göritzer K., Maresch D., Altmann F., Obinger C., Strasser R.

Research article

J Proteome Res. 2017 Jul 7;16(7):2560-2570. doi: 10.1021/acs.jproteome.7b00121

.

Journal of proteome research

Article

pubs.acs.org/jpr

Exploring Site-Specific N-Glycosylation of HEK293 and Plant-Produced Human IgA Isotypes

Kathrin Göritzer,[†] Daniel Maresch,[‡] Friedrich Altmann,[‡] Christian Obinger,[‡] and Richard Strasser*[,†]

[†]Department of Applied Genetics and Cell Biology, University of Natural Resources and Life Sciences, Muthgasse 18, A-1190 Vienna, Austria

[‡]Department of Chemistry, Division of Biochemistry, University of Natural Resources and Life Sciences, Muthgasse 18, A-1190 Vienna, Austria

Supporting Information

ABSTRACT: The full potential of recombinant Immunoglobulin A as therapeutic antibody is not fully explored, owing to the fact that structure−function relationships of these extensively glycosylated proteins are not well understood. Here monomeric IgA1, IgA2m(1), and IgA2m(2) variants of the anti-HER2 antibody (IgG1) trastuzumab were expressed in glyco-engineered *Nicotiana benthamiana* plants and in human HEK293-6E cells. All three IgA isotypes were purified and subjected to biophysical and biochemical characterization. While no differences in assembly, antigen binding, and glycosylation occupancy were observed, both systems vary tremendously in terms of glycan structures and heterogeneity of glycosylation. Mass-spectrometric analysis of site-specific glycosylation revealed that plant-produced IgAs carry mainly complex-type biantennary N-glycans. HEK293-6E-produced IgAs, on the contrary, showed very heterogeneous N-glycans with high levels of sialylation, core-fucose, and the presence of branched structures. The site-specific analysis revealed major differences between the individual N-glycosylation sites of each IgA subtype. Moreover, the proline-rich hinge region from HEK293-6E cell-derived IgA1 was occupied with mucin-type O-glycans, whereas IgA1 from *N. benthamiana* displayed numerous plant-specific modifications. Interestingly, a shift in unfolding of the CH2 domain of plant-produced IgA toward lower temperatures can be observed with differential scanning calorimetry, suggesting that distinct glycoforms affect the thermal stability of IgAs.

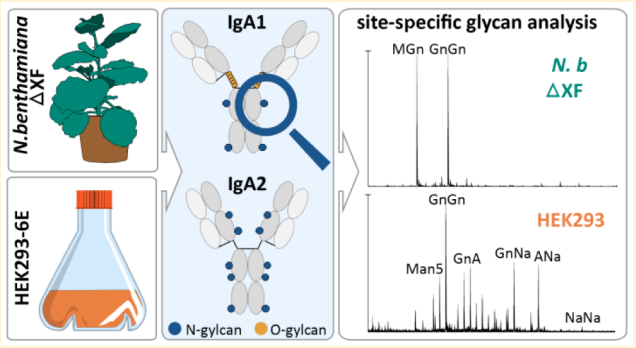

KEYWORDS: *glycosylation, IgA, HEK293-6E, HER2, Nicotiana benthamiana, monoclonal antibody, recombinant glycoprotein*

INTRODUCTION

Therapeutic monoclonal antibodies are the fastest growing class of recombinant biopharmaceuticals. Apart from the most commonly used immunoglobulin G (IgG), other antibody isotypes like IgAs have gained attention as potential candidates for treatment of cancer.[1−3] Human IgA occurs in two subclasses, IgA1 and IgA2, and for IgA2 there are two major allotypes (IgA2m(1) and IgA2m(2)). The different human IgA subtypes differ mainly in the length of their hinge region, disulfide bridges, type, and number of attached glycans.

Notably, all immunoglobulins are glycosylated to varying degrees and glycosylation is an important posttranslational modification that affects many properties of proteins including folding, stability, subcellular fate, and interaction with other proteins. The IgG1 heavy chain has a single asparagine (N)-linked glycan at Asn297 in the CH2 domain. Different types of IgG glycans are well known to modulate antibody function by affecting the binding affinity to receptors on immune cells. Nonfucosylated IgGs display increased affinity for the human FcγIIIA receptor and thus have enhanced effector functions like antibody-dependent cell-mediated cytotoxicity.[4,5] Heavily sialylated IgG antibodies, on the contrary, display an anti-inflammatory and immunomodulatory activity.[6] Therefore, the composition of the Fc glycans is highly important for a specific immunotherapy and a critical parameter of product quality for the biopharmaceutical industry.[7]

Surprisingly, despite the great importance of IgG glycosylation, little is known about the role of glycans for other Ig isotypes. In contrast with IgGs, the other Ig classes including both IgA subclasses are more heavily glycosylated with IgA1, IgA2m(1), and IgA2m(2) carrying two, four, and five N-glycans. Additionally, human IgA1 exhibits up to six O-glycans within its extended hinge region (Figure 1). While IgD, IgE, and IgM have a conserved N-glycosylation site that shares a similar glycan−polypeptide interaction as described for Asn297 from IgG1, an analogous N-glycan appears absent from the IgA alpha chain.[8] Instead of stabilizing intramolecular interactions between the two alpha chains, the N-glycan in the IgA1 CH2 domain is located at the surface of the protein and may have a

Received: March 3, 2017
Published: May 18, 2017

DOI: 10.1021/acs.jproteome.7b00121
J. Proteome Res. 2017, 16, 2560−2570

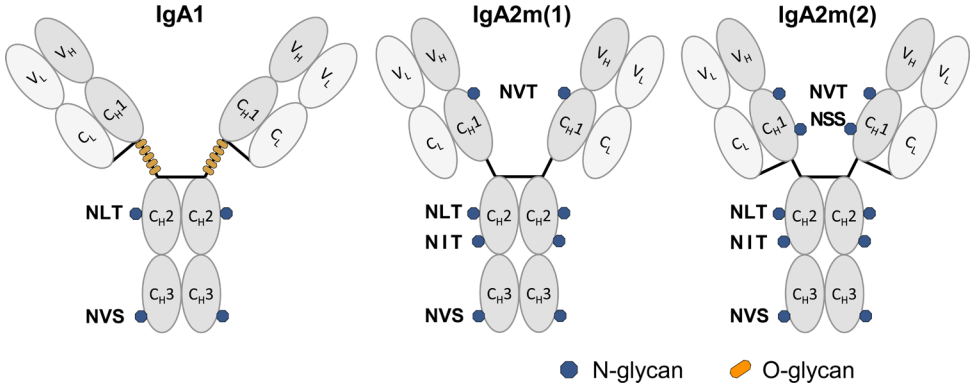

Figure 1. Schematic illustration of structure and glycosylation sites of the IgA isotypes IgA1, IgA2m(1), and IgA2m(2). The light chain is colored in light gray and the heavy chain in dark gray. N-glycans found in the different isotypes are indicated by blue dots. The O-glycans specific for the elongated hinge-region of IgA1 are indicated by orange dots.

completely different biological function. Interestingly, recombinant IgAs are rather short-lived in serum, which is a major drawback for therapy.[9] Similar to other glycoproteins, the rapid clearance depends on the exposure of distinct terminal glycan residues and their recognition by lectin-type receptors. The Ashwell-Morell and other endocytic lectin receptors may be responsible for the fast clearance of IgAs as part of a constitutive mechanism for protein turnover.[10−12] A specific role of glycans for IgA in vivo stability is consistent with a recent report that found an extended serum half-life of recombinant IgAs when the sialic acid content was increased.[13] While the O-glycans in the IgA1 hinge region may also contribute to in vivo stability,[9] it has been proposed that the O-glycans provide additional rigidity[14,15] and are involved in the interaction with endogenous receptors or pathogens.[16,17]

Aside from these findings, little is known about the biological role of individual glycans on the different IgA subtypes. Several recent studies have addressed the IgA glycosylation and its relation to function in the context of therapeutic applications.[13,18−20] These recombinant monomeric IgAs were derived from different expression hosts including plant-based and mammalian-cell culture expression systems. However, the capacity of different expression hosts was not systematically analyzed for the different IgA subtypes, and an in depth site-specific N-glycosylation analysis of all recombinant IgA subtypes is missing. Importantly, MS-based glycopeptide analysis of different heavily glycosylated Ig subtypes revealed pronounced site-specific glycan heterogeneity.[21−24]

For glycan structure−function studies as well as for glycoengineering attempts to improve the efficacy of glycoprotein therapeutics, the information about site-specific N-glycosylation is absolutely essential. This approach is more challenging but reveals important information that is completely lost when glycans are released from the protein for subsequent analysis. Here we produced recombinant anti-HER2 IgA1, IgA2m(1), and IgA2m(2) allotypes in two well-established expression hosts. We expressed all three IgA variants in the widely used human embryonic kidney (HEK293) cells and the glycoengineered *Nicotiana benthamiana* plant-based system, that is, for example, used to manufacture the ZMapp antibody cocktail against Ebola virus infections.[25] The recombinant IgA subtypes were purified, biochemically and biophysically characterized, and subjected to comprehensive site-specific glycosylation analysis to reveal common features as well as differences that may have implications for their function.

MATERIALS AND METHODS

Construct Design and Cloning

The codon-optimized genes of the heavy chains and light chain required for expression of the three different IgA isotypes in *N. benthamiana* and HEK293-6E cells were synthesized by GeneArt (Thermo Fisher Scientific, USA). Therefore, the variable regions of IgA1 (AAT74070.1), IgA2m(1) (AAT74071.1), and IgA2m(2) (AAB30803.1) heavy chains (α-HC) and the kappa light chain (κ-LC) (AAA5900.1) were replaced with the variable regions of the HER2-binding IgG-antibody Trastuzumab (1N8Z_A, 1N8Z_B).[26] Sequences for expression in *N. benthamiana* were flanked with the signal peptide from barley alpha-amylase (AAA98615) and the restriction sites XhoI and AgeI. The synthesized DNA was then amplified by PCR with the primers "Strings_7F (CTTCCGGCTCGTTTGACCGGTATG)/Strings_8R (AAAAACCCTGGCGCTCGAG)", and the constructs were separately cloned into the AgeI/XhoI sites of the binary vector pEAQ-HT.[27] Sequences of the heavy chains and the kappa light chain used for the expression in HEK293-6E were flanked with the signal peptides "MELGLSWIFLLAILKGVQC" and "MDMRVPAQLLGLLLLWLSGARC", respectively, and the restriction sites *Xba*I and *Bam*HI. The synthesized DNA was amplified by PCR with the primers "Strings_9F (CTTCCGGCTCGTTTGTCTAGA)/Strings_2R (AAAAACCCTGGCGGGATCC)". The corresponding genes for the heavy chains and the kappa light chain were then separately cloned into the *Xba*I/*Bam*HI sites of the mammalian vector pTT5 (National Research Council of Canada).[28]

Recombinant Production of IgA Isotypes in *N. benthamiana*

The pEAQ-HT plant expression vectors containing the alpha chains and the kappa light chain were transformed into *Agrobacterium tumefaciens* strain UIA143. Agrobacteria were grown overnight and diluted in infiltration buffer (10 mM MES, 10 mM $MgSO_4$, and 0.1 mM acetosyringone) to an OD_{600} of 0.15. Syringe-mediated agroinfiltration was used for transient cotransfection of the kappa light chain and the corresponding alpha heavy chain of 5 to 6 weeks old *N. benthamiana* ΔXT/FT plants.[29] For purification of the different IgA isotypes, 50 g of leaf material was harvested 4 days post-infiltration, snap-frozen in liquid nitrogen, and grinded. Homogenized leaf material was transferred to 200 mL of ice-cold extraction buffer (0.1 M TRIS, 0.5 M NaCl, 1 mM EDTA, 40 mM ascorbic acid, 2% (w/

DOI: 10.1021/acs.jproteome.7b00121
J. Proteome Res. 2017, 16, 2560−2570

v) immobilized polyvinylpoly pyrrolidone (PVPP), pH 6.8). The crude leaf extract was centrifuged at 25 000*g* for 20 min at 4 °C, passed through a Miracloth filter (Merck Millipore, Germany), and centrifuged again. The clarified extract was additionally filtrated through filters with pore sizes of 12−8 μm, 3 to 2 μm (Rotilabo round-filters, Roth, Germany), and 0.45 μm (Durapore membrane filter, Merck Millipore, Germany).

Recombinant Production of IgA Isotypes in HEK293-6E Cells

The HEK293-6E cell line that constitutively expresses the Epstein−Barr virus nuclear antigen 1 of the Epstein−Barr virus was licensed from the National Research Council (NRC) of Canada.[28] The suspension cells were cultivated and transfected according to the manufacturer's manual in F17 medium supplemented with 0.1% Pluronic F-68, 4 mM L-glutamine (Life Technologies, Germany), and 50 mg/L G418 (Biochrom, Germany). The cells were maintained in shaker flasks at 37 °C in a humidified atmosphere with 5% CO_2 on an orbital shaker never exceeding a cell density of 2×10^6 cells/mL. For transient transfection of a 200 mL culture, cells were brought to a concentration of 1.7×10^6 cells/mL. High-quality plasmid preparations of the pTT5 vector coding for the kappa light chain and the different alpha heavy chain were obtained using the PureYield Plasmid Midiprep System (Promega, USA). A total of 200 μg plasmid-DNA, consisting of 100 μg light chain and 100 μg of the respective heavy chain, were mixed with 10 mL of fresh medium. Another 10 mL of fresh medium, containing 2.5 μg/mL linear polyethylenimine (PEI) (Polysciences, Germany), was added to the DNA solution and incubated for 10 min. After adding the DNA/PEI mixture, the cells were incubated for 48 h, supplemented with 0.5% (w/v) tryptone N1 (Organotechnie, France) and further cultivated for 72 h. Supernatant containing the secreted soluble protein was harvested by centrifugation at 25 000*g* for 30 min at 4 °C and additionally filtrated (0.45 μm Durapore membrane filter, Merck Millipore, Germany).

Purification of Recombinant IgAs

Clarified leaf extract from *N. benthamiana* and supernatant of HEK293-6E suspension cells were subjected to a HiScale 16/20 column (GE Healthcare, USA) packed with 3 mL of CaptureSelect IgA affinity resin (Thermo Fisher Scientific, USA) equilibrated with phosphate-buffered saline (PBS) pH 7.4. Proteins were eluted with 0.1 M glycine pH 2.8, followed by immediate addition of 6 μL of 2 M Tris pH 12 to each 1 mL fraction to neutralize the acidic pH from glycine elution. Highly concentrated fractions were pooled and dialyzed against PBS at 4 °C overnight using SnakeSkin Dialysis Tubing with a MWCO of 10 000 kDa (Thermo Fisher Scientific, USA). Finally, the column was regenerated with 0.1 M glycine pH 2.5 and washed with PBS. Pooled protein fractions were then further concentrated using Amicon centrifugal filters with a MWCO of 10 000 kDa (Merck Millipore, Germany) and subjected to size-exclusion chromatography (SEC) on a HiLoad 16/600 Superdex 200 pg column (GE Healthcare, USA) equilibrated with PBS supplemented with 200 mM NaCl.

SDS-PAGE

For reducing or nonreducing SDS-PAGE a total of 5 μg of purified protein was loaded on a 4−15% Mini-PROTEAN TGX gel (Bio-Rad Laboratories, USA) and visualized with Coomassie Brilliant Blue staining.

Binding to Antigen HER2

The purified extracellular domain of human HER2 (residues 1−631), which was used for antigen-binding experiments, was generously provided by Elisabeth Lobner (BOKU Vienna). Each well of a medium binding MICROLON 200 96-well plate (Greiner Bio-One Intern., Germany) was coated with 0.5 μg HER2 overnight at 4 °C in coating buffer (0.5 M sodium carbonate/bicarbonate, pH 9.8). Plates were then blocked with PBS plus 2% (w/v) BSA and 0.05% (v/v) Tween 20. Purified IgA1, IgA2m(1), and IgA2m(2) antibodies were diluted to 500 ng/mL in blocking solution, added to the wells in normalized concentrations, and incubated for 1.5 h at room temperature. HRP-labeled antihuman IgA (A0295, Sigma-Aldrich, USA) was added to the wells and incubated 1 h at room temperature. The plates were developed using 5 mg *O*-phenylenediamine dihydrochloride in 10 mL of stable peroxidase substrate buffer (all Sigma-Aldrich, USA). After 20 min of incubation the plates were read on a Wallac 1420 VICTOR2 microplate reader (PerkinElmer, U.K.) at 492 nm.

Size Exclusion Chromatography−Multiangle Light Scattering (SEC−MALS)

To verify the molar mass of purified IgAs, high-performance liquid chromatography (HPLC) coupled to a size-exclusion chromatography column was combined with multiangle light scattering. HPLC (Shimadzu prominence LC20) was equipped with MALS (WYATT Heleos Dawn8+ QELS; software ASTRA6), refractive index detector (RID-10A, Shimadzu), and a diode array detector (SPD-M20A, Shimadzu). Samples were centrifuged (15 000*g*, 10 min, 4 °C) and filtrated through a 0.1 μm Ultrafree-MC filter (Merck Millipore, Germany), and a total of 25 μg protein was injected on a Superdex 200 10/300 GL column (GE Healthcare, USA) equilibrated with Dulbecco's PBS plus 200 mM NaCl, pH 7.4. All experiments were performed at a flow rate of 0.75 mL/min at 25 °C. The performance of molar mass calculation by MALS was verified by the determination of a sample of bovine serum albumin.

Differential Scanning Calorimetry

The thermal stability of the IgA variants was analyzed by differential scanning calorimetry (DSC) using a MicroCal VP-Capillary DSC (Malvern, U.K.). Purified samples were diluted to a concentration of 5 μM and were measured in the temperature range from 20 to 110 °C with a heating rate of 1 °C/min. Buffer baselines were subtracted, normalized for protein concentration, and fitted with a non-2-state thermal unfolding model using the Origin 7 software.

N- and O-Glycan Analysis

Between 5 and 10 μg of purified proteins was loaded on a SDS-PAGE under reducing conditions, and Coomassie Brilliant Blue stained bands were excised, S-alkylated, and digested with trypsin (Promega USA). Glycopeptides were then analyzed by capillary reversed-phase chromatography and electrospray mass spectrometry using a Bruker Maxis 4G Q-TOF instrument. The peptide mixture was dissolved in 15 μL of water, and a volume of 5 μL was analyzed using a Dionex Ultimate 3000 system directly linked to a QTOF instrument (maXis 4G ETD, Bruker) equipped with the standard ESI source in the positive ion, DDA mode (= switching to MSMS mode for eluting peaks). MS scans were recorded (range: 150−2200 *m*/*z*, spectra rate: 0.5 Hz) and the six highest peaks were selected for fragmentation (CID mode). Instrument calibration was performed using ESI calibration mixture (Agilent). For

DOI: 10.1021/acs.jproteome.7b00121
J. Proteome Res. 2017, 16, 2560−2570

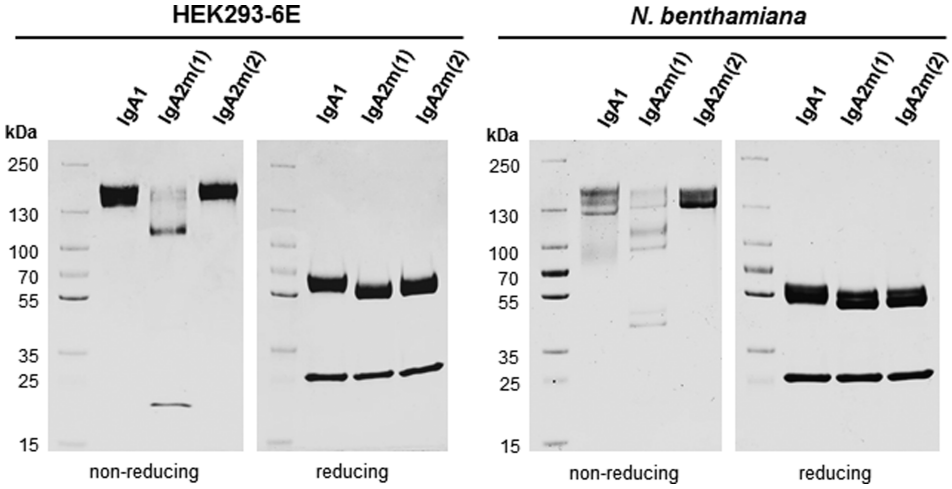

Figure 2. Purity and assembly of recombinantly produced IgA1, IgA2m(1), and IgA2m(2). Purified IgAs produced in *N. benthamiana* and HEK293-6E cells were run on an SDS-PAGE under reducing and nonreducing conditions. Proteins were then detected by Coomassie Brilliant Blue staining.

separation of the peptides a Thermo BioBasic C18 separation column (5 μm particle size, 150 × 0.320 mm) was used. A gradient from 97% solvent A and 3% solvent B (Solvent A: 65 mM ammonium formiate buffer, pH 3.0 (formic acid supplied by Carl Roth; ammonia supplied by VWR BDH Prolabo), B: 100% ACCN (VWR BDH Prolabo)) to 32% B in 45 min was applied, followed by a 15 min gradient from 32% B to 75% B at a flow rate of 6 μL/min at 32 °C.

The analysis files were converted using Data Analysis 4.0 (Bruker) to MGF files, which are suitable to perform MS/MS ion searches with MASCOT (embedded in ProteinScape 3.0, Bruker) for protein identification using the manually annotated and reviewed UniProtKB database. Manual glycopeptide searches were done using DataAnalysis 4.0 (Bruker). MS/MS spectra were used for the verification of the glycopeptides by detection of oxonium ions HexNAc (m/z = 204.1), Hex +HexNAc (m/z = 366.1), and the unique Y1 ion (peptide +HexNAc). For the relative quantification of the different glycoforms, peak areas of EICs (extracted ion chromatograms) of the first four isotopic peaks were summed. All observed charge states and adducts (ammonium) as well as the formation of formylated glycopeptides were considered. Site-specific glycosylation occupancy was calculated using the ratio of deamidated to unmodified peptide determined upon N-glycan release with PNGaseA (Europa Bioproducts).

For the digestion the remaining sample material (10 μL) was dried and resolved in 20 μL of 50 mM ammonium citrate (pH 5.0), and 0.15 mU of enzyme was added and incubated overnight at 37 °C.

RESULTS

Recombinant Production of IgA in Different Expression Hosts

To compare the capacities of plant-based and mammalian-based expression systems, the three IgA isotypes IgA1, IgA2m(1), and IgA2m(2) (Figure 1) were produced in HEK293-6E cells and in the glyco-engineered *N. benthamiana* ΔXT/FT line that almost completely lacks plant-specific β1,2-xylose and core α1,3-fucose residues. For expression of the different IgAs in plants, the leaves of *N. benthamiana* were coinfiltrated with agrobacteria containing the κ-LC and the respective α-HC. Immunoblot analysis and ELISA showed that the highest level of recombinant protein accumulated 4 days postinfiltration (data not shown). For purification of IgA from the crude plant extract, 50 g of leaf material was harvested, extracted, and subjected to affinity chromatography, followed by a SEC step. The preparative SEC profiles thereby revealed the presence of high-molecular-weight aggregates, dimeric IgA, and free heavy chain (data not shown). For further analyses, only fractions containing the monomeric structural unit of IgA were pooled. The final yield of purified monomeric IgA from *N. benthamiana* ranged from 3.5 mg/50 g of fresh weight from leaf for IgA1 and IgA2m(1) to 5 mg/50 g for IgA2m(2). For the expression of IgAs in a mammalian host, 200 mL of a HEK293-6E cell suspension culture was cotransfected with two vectors, encoding the κ-LC and the respective α-HC. The supernatant was collected and subjected to affinity chromatography, followed by SEC. As already seen in the SEC profiles of plant-produced proteins, also IgAs expressed in the HEK293 cell line showed the presence of high-molecular weight-aggregates. Again only fractions containing the monomeric IgA forms were collected. The final yield of IgA from HEK293-6E was in the range of 15 mg/L for all three isotypes.

Characterization of Purified Monomeric IgA Variants

The purified monomeric IgA variants were investigated for their overall assembly and homogeneity using SDS-PAGE and SEC coupled to MALS. Reducing SDS-PAGE of purified IgAs produced in *N. benthamiana* ΔXT/FT and in HEK293-6E cells confirmed the presence of the α-HC and the κ-LC without any degradation products (Figure 2). However, the heavy chain at 55 kDa can be observed as a double band. The distinct bands were cut from the gel and separately analyzed by mass spectrometry (Supplementary Figure S2). Thereby it was shown that the band with a higher molar mass contains more oligomannosidic glycans and has a higher glycosylation occupancy of the C-terminal N-site compared to the band with lower molar mass.

Under nonreducing conditions, IgA1 and IgA2m(2) show a predominant band at a molar mass around 160 kDa representing the fully assembled molecule. The plant -produced IgA2m(1) variant displayed additional bands at 115, 100, and 45 kDa, which likely represent heavy and light chain dimers. The HEK293-derived IgA2m(1) also shows additional bands at 115 and 20 kDa. However, SEC profiles of all IgA variants,

DOI: 10.1021/acs.jproteome.7b00121
J. Proteome Res. 2017, 16, 2560−2570

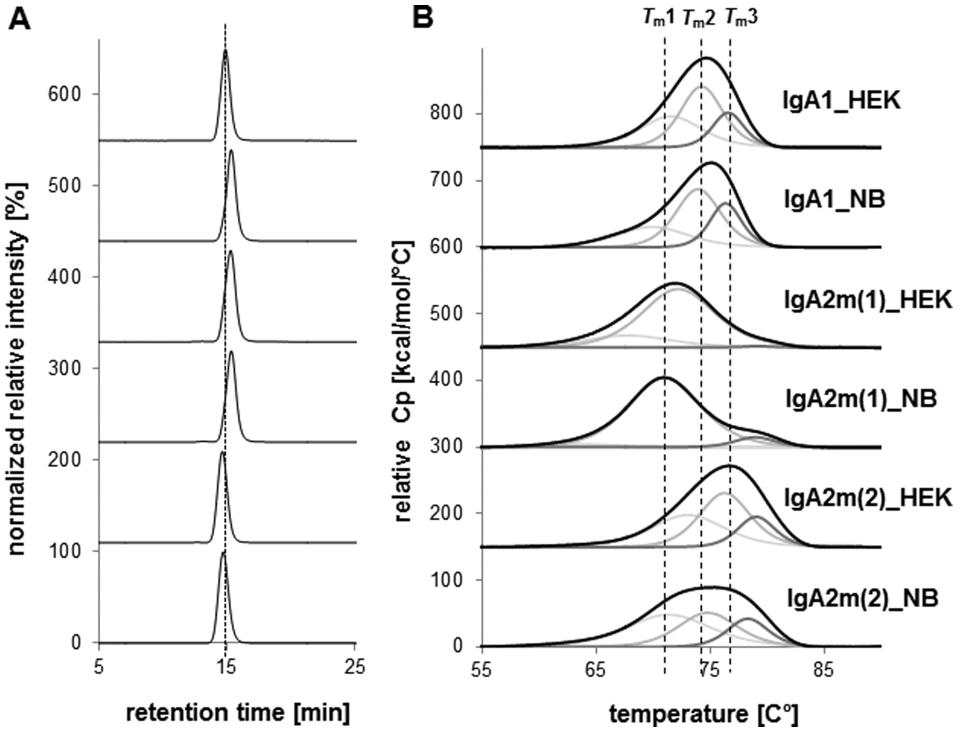

Figure 3. Homogeneity and thermal stability of the IgA isotypes IgA1, IgA2m(1), and IgA2m(2). (A) SE-HPLC measurements of the different IgA isotypes purified from HEK293-6E cells (HEK) and *N. benthamiana* (NB). To facilitate comparison between the different variants the elution time of IgA1 produced in HEK293 cells is marked with dashed lines. (B) Differential scanning calorimetry analysis of IgAs produced in *N. benthamiana* (NB) and HEK293-6E cells (HEK). The black bold lines show representative DSC thermograms, whereas the gray lines are the deconvoluted peaks of each domain transition. For comparison, the three midterm transitions of the CH2, Fab, and CH3 domain (T_m1 = 71.6 ± 0.1 °C, T_m2= 74.3 ± 0.05 °C, and T_m3 = 76.6 ± 0.1 °C) of IgA1 produced in HEK293 cells are marked with dashed lines.

including IgA2m(1) produced in both systems, gave narrow and single monodisperse peaks (Figure 3A). The masses of these peaks of ∼160 kDa were confirmed by MALS and correspond to the fully assembled monomeric forms. Furthermore, no aggregates and no aberrantly assembled IgA variants could be detected.

Next, we investigated the thermal stability of the IgA variants by DSC (Figure 3B). Unfolding of the recombinant IgAs is reflected by a broad endotherm. Analysis and fitting suggested the presence of three independent transitions allowing identification of the transition midpoint temperatures of the CH2 (T_m1), Fab (T_m2), and CH3 (T_m3) domains, as already described for IgG.[30] Immunoglobulin A1 produced in HEK293 cells exhibited melting temperatures at 71.6 ± 0.01, 74.3 ± 0.05, and 76.6 ± 0.1 °C, respectively. The plant-produced counterpart exhibited almost identical T_m2 and T_m3 values, whereas unfolding of the CH2 domain started at a slightly lower temperature.

Comparison of the two IgA2 allotypes shows significant differences in thermal stability with IgA2m(1) being less stable than IgA2m(2). Immunoglobulin A2m(1) produced in HEK293 cells exhibited melting temperatures at 67.9 ± 0.05, 72.3 ± 0.1, and 79.2 ± 0.1 °C, respectively. Similar to IgA1, the plant-produced variant showed almost identical T_m2 and T_m3 values, whereas T_m1 was decreased by ∼4 °C. In the allotype IgA2m(2) produced in HEK293 cells both the CH2 and Fab domains are more stable (T_m1 = 73.1 ± 0.05 and T_m2 = 76.3 ± 0.1 °C), whereas the calculated T_m3 value was almost similar to that of IgA2m(1). The endotherm of the plant-derived variant was broader and the respective T_m values of the three transitions were slightly decreased (Figure 3B). In general, the hierarchy of thermal stability is IgA2m(2) > IgA1 > IgA2m(1). In the plant-derived products the CH2 domain was always slightly destabilized compared with the HEK293-produced variants, whereas the differences in melting temperatures of the Fab and CH3 domains were at most ∼1 °C.

To confirm the functionality of all expressed IgAs, binding to the HER2 antigen was assessed by ELISA and the half maximal effective concentration (EC_{50}) was determined for each recombinant monomeric IgA variant. Thereby it could be shown that the antigen binding behavior of all three IgA isotypes was very similar and independent of the production host (Figure 4).

Glycan Profiles of IgAs Produced in Different Expression Platforms

The observed differences in thermal unfolding of IgA variants from different expression hosts may arise from differences in glycosylation. There are two predicted N-glycosylation sites in the α-HC of IgA1 and four to five N-glycosylation sites in IgA2m(1) and IgA2m(2), respectively. In addition, IgA1 has nine potential O-glycosylation sites in the proline-rich hinge region. To assess the glycosylation status of purified monomeric IgA isotypes produced in *N. benthamiana* or HEK293-6E, the α-HC was subjected to SDS-PAGE and stained with Coomassie Brilliant Blue. The corresponding band was excised, digested with trypsin, and analyzed by LC−ESI−MS for site-specific N-glycosylation and the presence of modifications within the IgA1 hinge region. Furthermore, all samples were additionally digested with PNGase A to release the attached N-glycans. After the PNGase A digestion, the ratios of the resulting deamidated peptides (glycosylated) to

DOI: 10.1021/acs.jproteome.7b00121
J. Proteome Res. 2017, 16, 2560−2570

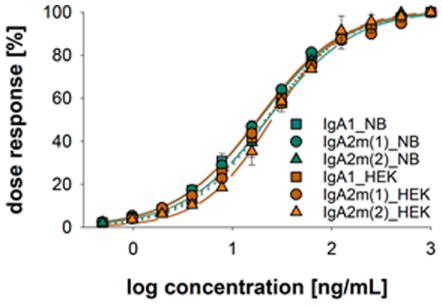

	EC_{50} [ng/mL]		
	IgA1	IgA2m(1)	IgA2m(2)
HEK293-6E	21.8 ± 0.38	22.38 ± 0.25	25.10 ± 0.24
N. benthamiana	18.87 ± 0.23	18.20 ± 0.22	22.40 ± 0.23

Figure 4. Binding of IgA variants to HER2. Determination of EC_{50} values of IgA isotypes produced in *N. benthamiana* and HEK293 cells to the extracellular domain of HER2 by ELISA. Each value is the mean ± standard deviation from three independent measurements.

unmodified (nonglycosylated) peptides were quantified to determine the glycosylation efficiency of both expression systems at each N-glycosylation site. All predicted N-glycosylation sites were found to be occupied in all IgA variants (Figure 5). Both systems were equally efficient in attachment of N-glycans and all except the C-terminal N-glycosylation site were almost fully glycosylated. The C-terminal N-glycosylation site present in the tailpiece of all IgAs was only 40−60% glycosylated. Although the two hosts do not significantly differ in their N-glycosylation efficiency, both systems differ tremendously in terms of structural composition of attached glycans. The N-glycans found on plant-produced IgA showed a comparably homogeneous profile, with biantennary complex-type structures like $GlcNAc_1Man_3GlcNAc_2$ (MGn/GnM) and $GlcNAc_2Man_3GlcNAc_2$ (GnGn) as major glycoforms (Figure 6 and Table 1). The presence of N-glycan structures with a single terminal GlcNAc residue in *N. benthamiana*-derived IgA variants is in accordance with previous data, suggesting an incomplete processing of the NLT site in the CH2 domain by *N*-acetylglucosaminyltransferase II (GnTII).[31] Furthermore, variable amounts of oligomannosidic structures were detected along with small amounts of complex N-glycans carrying the plant-specific core α1,3-fucose. This modification results from the incomplete silencing of core α1,3-fucosyltransferase in the *N. benthamiana* ΔXT/FT line.[29] HEK293-produced IgAs showed clear site-specific differences and more diverse N-glycan profiles compared with plant-produced IgAs. Several of the detected glycopeptide masses correspond to complex N-glycan compositions that could not be distinguished because of the same theoretical mass. These structures include different branched complex N-glycans with or without a bisecting GlcNAc (Table 1). However, the predominant glycoforms found attached to the NVT, NSS, NLT, and NIT sites of the respective IgA isotype are biantennary complex-type structures with high levels of galactosylation and up to 30% sialylation. The NVS glycosylation site in the C-terminal tailpiece comprises more highly branched complex N-glycans with high levels of incompletely galactosylated triantennary glycans carrying a bisecting GlcNAc or tetraantennary glycans. Only a small degree of sialylation was found at this N-glycosylation site. The N-glycans from HEK293-derived IgAs also vary in the attachment of core-fucose, which is present on all complex N-glycans except those found on the NLT site from the CH2 domain.

The most significant difference between the two expression systems *N. benthamiana* ΔXT/FT and HEK293-6E was the modification of the proline-rich hinge region of IgA1. O-glycans found on IgA1 produced in mammalian cells are a combination of mucin-type core structures with a maximal occupation of six out of nine potential O-glycosylation sites (Figure 7). On the hinge region of plant-produced recombinant IgA1 we detected the conversion of proline residues to hydroxyproline and the presence of additional pentoses, presumably representing attached arabinose chains.

Taken together, the site-specific analysis of glycosylation revealed major differences between individual N-glycosylation sites on the heavy chain of each IgA subtype. Although the glycan composition differed considerably between the plant and mammalian expression systems, the site-specific features appear conserved.

DISCUSSION

The role of glycosylation for immunoglobulins like IgA is still not well understood. In recent studies, the potential of recombinant anti-HER2 IgAs has been investigated.[13,19] These studies suggest that defined glycan modifications, such as the attachment of terminal sialic acid residues, are critical to increase the half life of IgAs in vivo. However, because of the absence of site-specific glycan analysis, important information was not revealed. Moreover, in addition to well-established mammalian cell systems, the use of plant-based production for recombinant immunoglobulins is gaining more and more attention as plants allow the production of customized

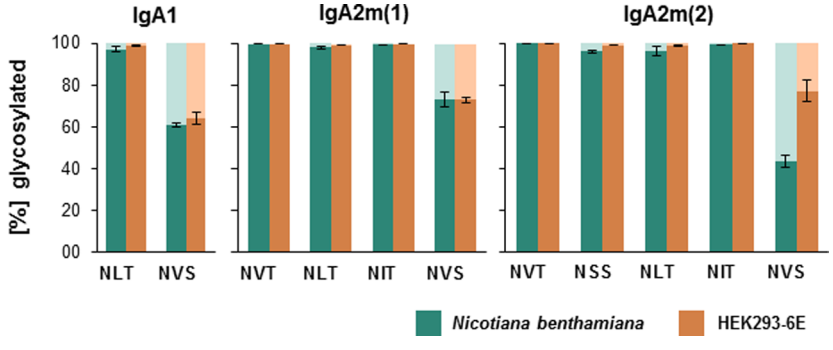

Figure 5. N-glycosylation site occupancy of IgA isotypes produced in HEK293-6E cells and in *N. benthamiana*. Each value is the mean ± standard deviation from two independent experiments.

DOI: 10.1021/acs.jproteome.7b00121
J. Proteome Res. 2017, 16, 2560−2570

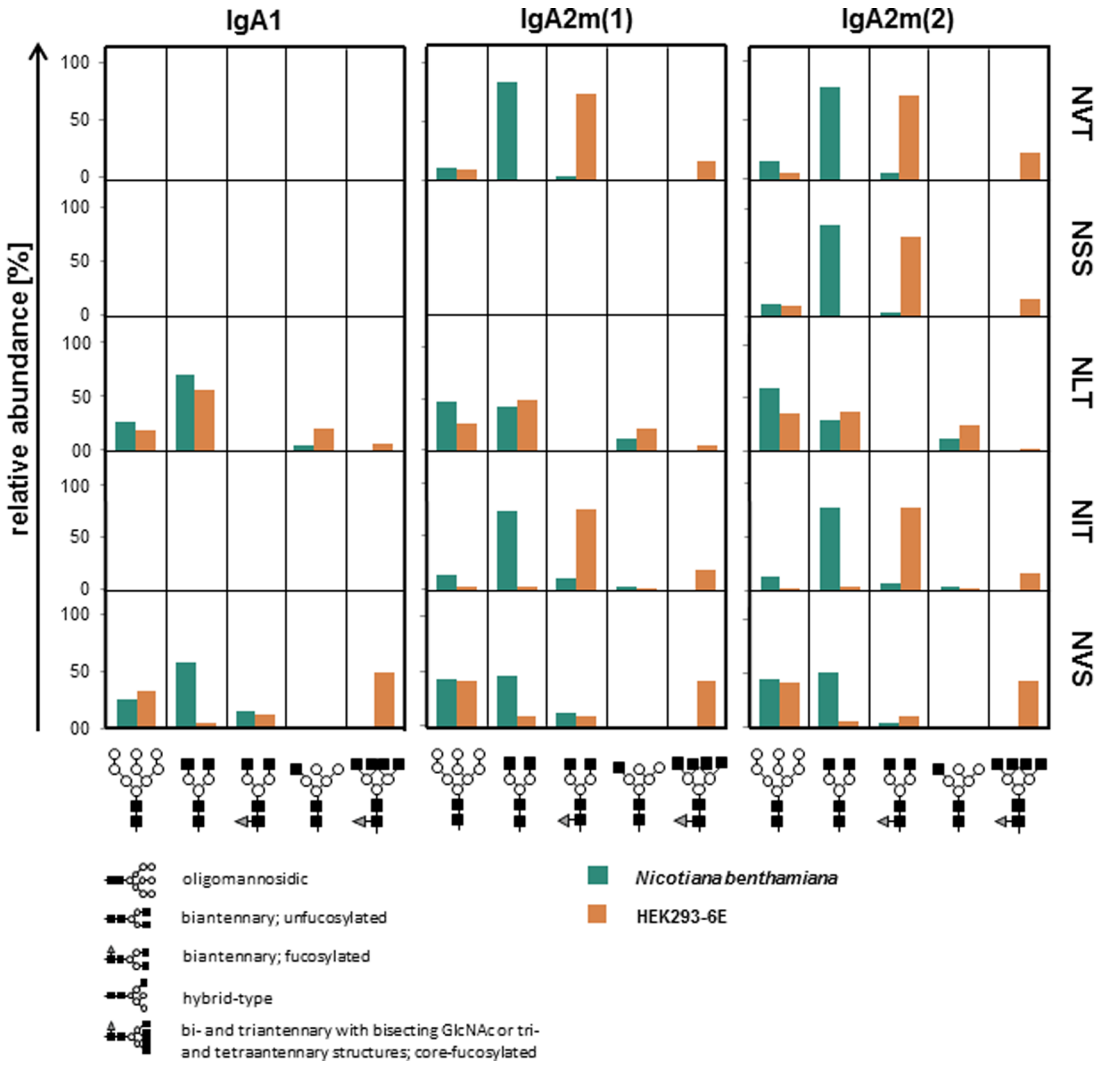

Figure 6. Relative abundance of N-glycans found on IgA isotypes produced in *N. benthamiana* and HEK293-6E cells. Glycoforms are grouped from left to right into oligomannosidic, biantennary without core-fucose, biantennary with core-fucose, hybrid-type, and bi- and triantennary with bisecting GlcNAc or triand tetranatennary structures with core-fucose.

homogeneous glycans with few engineering steps.[18,22,25,31−33] Here we compared the two different systems and performed a comprehensive analysis of the glycans at each site of three anti-HER2 IgA subtypes.

In both systems an almost complete occupancy with N-glycans was observed on all sites except the one in the C-terminal tailpiece, demonstrating that glycosylation efficiency was essentially the same. This finding is remarkable, as there are differences in the composition and function of the plant and mammalian oligosaccharyltransferase complexes that catalyze the transfer of the oligosaccharide to asparagine residues.[34] The incomplete glycosylation of the C-terminal tailpiece is likely caused by inefficient posttranslational glycosylation mediated by a specific catalytic subunit of the oligosaccharyltransferase complex.[35] All other sites are presumably cotranslationally glycosylated while the polypeptide is still synthesized.

As a consequence of the limited N-glycan processing repertoire in the Golgi, the glycan diversity found on plant-produced recombinant IgAs was clearly reduced. In particular, plant N-glycans lack tri- and tetraantennary structures, bisecting GlcNAc, β1,4-galactose, and capping with sialic acid. Those glycan modifications were all detected on the HEK293-derived IgA, resulting in increased heterogeneity. In addition, the HEK293-derived IgA may also contain smaller amounts of *N*-acetyllactosamine-repeat containing N-glycans that were not distinguished from some tri- and tetraantennary N-glycans and contribute to heterogeneity.

Despite having completely identical amino acid sequences, plant- and human-cell-derived IgA subtypes exhibited differences in thermal stability. Because the respective variants differ only in glycosylation, we propose that observed differences in T_m values are related to the presence of distinct glycoforms causing the variation in thermal stability. Comparable DSC measurements are not available for recombinant or native IgA molecules, but data from thermal unfolding of IgG showed that oligomannosidic and deglycosylated forms were less stable.[36] However, because of the different positioning (exposed for IgA, confined between the two CH2 domains for IgG) of the Fc oligosaccharide no direct comparison can be made. Nevertheless, in the plant-derived IgA variants the CH2 domain was always destabilized by about 2−4 °C compared with the HEK293 produced variants, whereas the differences in T_m values of the Fab and CH3 domains were very small. The significant difference in thermal stability of the Fab and CH2

DOI: 10.1021/acs.jproteome.7b00121
J. Proteome Res. 2017, 16, 2560−2570

Table 1. Quantification of the Relative Abundance of N-Glycans Detected on IgA Isotypes Produced in *N. benthamiana* and HEK293-6E Cells[a]

			IgA1				IgA2m(1)								IgA2m(2)									
			N.B		HEK		N.B				HEK				N.B					HEK				
			NLT	NVS	NLT	NVS	NVT	NLT	NIT	NVS	NVT	NLT	NIT	NVS	NVT	NSS	NLT	NIT	NVS	NVT	NSS	NLT	NIT	NVS
		% unglycosylated	2.9	38.9	1.1	35.9	<0.1	2.0	0.7	26.6	<0.1	0.7	<0.1	26.8	<0.1	3.9	3.7	0.6	56.5	<0.1	1.0	0.8	<0.1	22.9
oligomannosidic	Man4		0.4		0.4			0.7	0.5			0.3					0.8	0.8				0.3		
	Man5		1.2	0.3	4.4	14.0	0.5	2.0	0.5	0.8	9.4	6.1	2.0	25.1	1.2	0.4	2.8	0.8	0.3	6.1	2.6	7.3	2.0	26.1
	Man6		6.2	1.7	3.1	8.5	0.7	6.8	0.4	1.5		5.0		9.2	1.2	0.9	7.9	0.5	3.7			6.0		8.1
	Man7		4.8	9.9	5.0	4.8	2.7	11.4	1.4	14.2		7.6		2.8	3.8	2.9	13.8	1.4	13.3			10.5		2.5
	Man8		7.6	10.8	2.8	4.3	5.4	13.2	6.5	18.6		4.1		2.7	4.6	5.9	14.6	5.4	18.2			6.1		2.7
	Man9		5.4	2.7	2.4	1.8	2.5	12.6	4.1	6.7		3.2		1.4	4.9	2.3	18.0	3.9	9.0			5.7		1.8
	Man9+1Hex		0.2	0.5				0.3	0.1	0.6						0.3	0.5	0.2	0.3					
biantennary - unfucosylated	MM		6.3	1.2			10.2	4.2	12.7						18.7	10.7	2.6	14.9						
	MGn		30.8	3.7	2.8		20.0	22.8	20.0	5.4		2.4	1.1		13.3	16.6	17.4	18.4	7.5			2.1	1.3	
	GnGn		31.9	53.5	16.6	1.7	54.2	14.6	40.7	40.5		15.3	2.0	3.3	46.0	47.6	9.7	43.3	43.2			13.2	2.6	2.0
	GnA				8.7							7.6										6.3		
	AA				3.6							2.5										2.1		
	GnNa				11.0							10.8										7.3		
	ANa				11.4	2.6						8.5		5.0								4.9		3.1
	NaNa				1.4							1.6										0.7		
biantennary - fucosylated	MMF								2.1							2.6		1.6						
	MGnF								2.7				3.8			3.0		1.4			2.8		3.8	
	MAF												1.8										1.9	
	GnGnF			15.8		5.7	3.9		6.0	11.7	23.8		25.6	8.0	6.2	6.9		4.1	4.4	25.3	27.7		24.9	7.2
	GnAF										15.4		14.6							13.6	13.6		15.0	
	AAF					2.9					10.9		10.4	0.7						7.0	7.0		9.9	1.3
	GnNaF										6.2		5.2							7.0	5.2		6.8	
	ANaF					3.8					15.5		12.3	0.2						14.9	8.1		13.4	1.6
	NaNaF										2.1		1.4							3.2	1.0		1.6	
hybrid type	Man4Gn / MA		2.9		4.7			5.3	1.2			4.9					5.2	1.4				5.2		
	Man5Gn		2.4		7.7			6.0	0.8			8.1	0.8				6.5	1.3				10.7	1.0	
	Man5Gn+1Hex				2.3				0.3			2.5						0.4				3.1		
	Man4Na				3.8							3.4										3.6		
	Man5Na				1.3							1.8										2.3		
biantennary with bisecting GlcNAc and/or triantennary	GnGnbi / GnGnGn				4.4							3.0										1.8		
	GnAbi / GnGnA				2.1							1.3										0.9		
	GnGnFbi / GnGnGnF					10.9					7.7		9.1	9.2						11.4	14.3		7.2	9.2
	GnAFbi / GnGnAF					4.4					5.8		5.9	3.2						6.4	9.8		5.2	3.8
	AAFbi / GnAAF					2.1					3.3		2.9	4.9						5.0	3.5		2.6	4.0
	AAAF					1.3							1.0	1.3							0.7		0.9	1.4
	AANaF					2.4								1.4										1.3
	GnNaFbi / GnGnNaF																				1.9			
	ANaFbi / GnANaF																				1.1			
triantennary with bisecting GlcNAc and/or tetraantennary	GnGnGnFbi / GnGnGnGnF					11.2								8.8										7.5
	GnGnAFbi / GnGnGnAF					4.0								4.1										5.1
	GnAAFbi / GnGnAAF					2.1								1.9							0.6			3.0
	AAAFbi / GnAAAF					2.4								1.1										1.8
	AAAAF					1.6								1.2										1.0
	AANaFbi / GnAANaF					0.4								2.0										1.5
	AAANaF					4.2								0.6										2.0
	GnGnGnGnFbi					2.9								1.8										1.7

Hexose GlcNAc Mannose Fucose Galactose Sialic acid

[a]N-glycans are abbreviated according to the ProGlycAn system (www.proglycan.com). The symbols for the monosaccharides are drawn according to the nomenclature from the Consortium for Functional Glycomics. Please note that *N*-acetyllactosamine repeats may also be present on HEK293-6E cell-derived IgA N-glycans, which cannot be distinguished from some tri- and tetraantennary N-glycans by the used MS analysis.

DOI: 10.1021/acs.jproteome.7b00121
J. Proteome Res. 2017, 16, 2560−2570

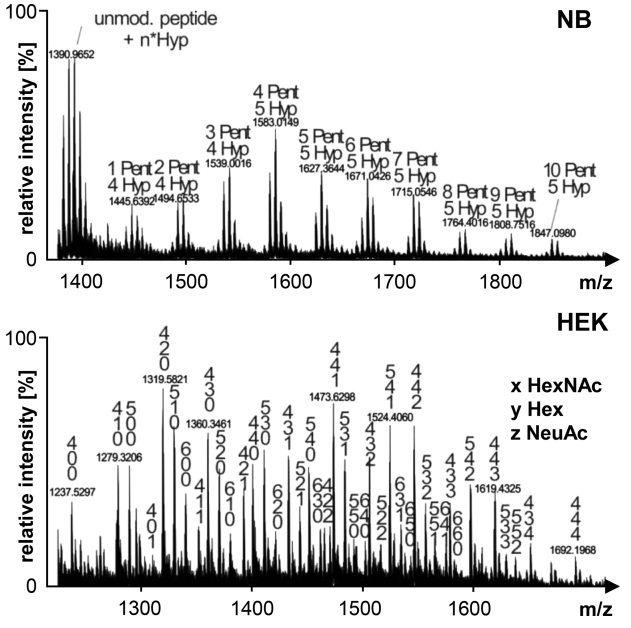

Figure 7. O-glycosylation profiles of *N. benthamiana* (NB) and HEK293-6E (HEK)-derived recombinant IgA1. Mass spectra of the hinge region peptide (HYTNPSQDVTVPCPVPSTPPTPSPSTPPTP-SPSCCHPR) are shown ($[M+3H]^{3+}$ for NB and $[M+4H]^{4+}$ for HEK). Glycosylated peaks are indicated: pentoses (Pent), hydroxyproline (Hyp), putative *N*-acetylgalactosamine (HexNAc), hexoses (Hex), and sialic acid residues (NeuAc).

domains between the two IgA2 isoforms seems to be related to the presence of the IgA2m(2)-typical disulfide bridge between the CL and CH1 domains (Figure 1).

Plants do not have a functional mucin-type O-glycosylation pathway[37,38] but perform plant-specific modifications. Thereby proline is converted to hydroxyproline, followed by the addition of arabinoses to the hydroxyproline-residues. Apart from *N. benthamiana,* these plant-type modifications have been previously described for human IgA1 derived from maize seeds.[39] While it will be of interest to determine the effect of the plant-type O-glycosylation on the biophysical properties and stability of IgA1, the hydroxyproline residues and attached glycan moieties may elicit an unwanted immune response when present on recombinant IgA1[40] and hamper O-glycan engineering approaches. The importance of hinge region modifications is well documented for IgA nephropathy, a kidney disease where autoantibodies against O-glycans from the IgA1 hinge region lead to glomerular immune complex deposits.[41] Strategies to eliminate the unwanted prolyl-4-hydroxylase activity have been successfully applied to a moss-based expression system[42] and need to be adopted for the commonly used *N. benthamiana*-based system.

Recombinant IgA subtypes from the human cell line displayed a considerable number of diverse complex N-glycans and clear site-specific differences like the lack of core α1,6-fucose on the conserved N-glycan located in the CH2 domain. The absence of this modification has also been reported for serum or CHO-produced IgA and presumably results from steric hindrance of processing in the Golgi.[43−45] Interestingly, this difference in processing is not only limited to mammalian core α1,6-fucosyltransferase but also found in plants that modify complex N-glycans with core α1,3-fucose. The absence of plant-specific fucosylation has been observed on the CH2 N-glycan of IgAs expressed in wild-type *N. benthamiana* plants[18,31] and was also found in the present study on recombinant anti-HER2 IgAs when expressed in wild-type plants (data not shown). The local interaction of the complex N-glycan with amino acids from the CH2 domain likely prevents the modification with α1,6- or α1,3-linked fucose. Site-specific N-glycan processing has been observed for several glycoproteins, but the structural polypeptide features that affect these modifications are currently not understood. In this respect, it will be of great interest to perform mutational analysis of the local amino acid environment surrounding the N-glycosylation site and examine the effect on the N-glycan structures. Combined with molecular -modeling experiments this could help us to better understand glycan-processing reactions.

Moreover, in the light of the dramatic effect of the nonfucosylated IgG1 Fc N-glycan on cytotoxicity, it is tempting to speculate that the absence of core fucose on complex N-glycans at this particular position of IgA1 is biologically relevant. A critical role of core fucose for N-glycan processing of immunoglobulins has been recently shown for cetuximab, which carries an N-glycan in the Fab domain in addition to the one in the CH2 domain.[46] While processing of the oligosaccharide in the Fab domain is unaffected by fucosylation, the presence of core fucose leads to increased levels of sialylated Fc glycans. Notably, there is mounting evidence of the antigen-specific generation of immunoglobulin glycoforms during diseases;[47] for example, increased amounts of afucosylated IgGs have been detected on naturally occurring antivirus antibodies of infected patients.[48,49] In summary, these data suggest that the fucosylation of N-glycans on distinct sites of different immunoglobulins is a key determinant of their immunomodulatory functions. The role of this particular nonfucosylated N-glycan in the IgA CH2 domain needs to be further investigated in the future.

Compared with the role of the Fc glycosylation, the importance of N-glycans for interaction of IgM, IgEs, or IgAs with their cellular receptors is less understood.[47] An oligomannosidic glycan at a particular position of the IgE heavy chain has recently been shown to affect IgE binding to the Fcε receptor.[50] Although the N-glycosylation site of the IgA CH2 domain is close to the Fcα receptor binding site and approaches the receptor, there is no contact.[14,44,51] Consequently, it has been proposed that the IgA N-glycans do not contribute to immune effector functions mediated by the Fcα receptor. However, variations in glycosylation may induce subtle conformational changes affecting the overall protein stability or interaction with other receptors, like those involved in protein turnover.[13] Further studies will aim to generate defined IgA glycoforms to unravel the contribution of the glycan composition to protein stability and diverse receptor interactions.

■ ASSOCIATED CONTENT

Supporting Information

The Supporting Information is available free of charge on the ACS Publications website at DOI: 10.1021/acs.jproteome.7b00121.

DOI: 10.1021/acs.jproteome.7b00121
J. Proteome Res. 2017, 16, 2560−2570

Supplementary Figure S1. MS spectra of the tryptic glycopeptides derived from the alpha chain of the purified IgA subtypes. Supplementary Figure S2. MS spectra showing different N-glycan profiles in the two bands derived from the 55 kDa heavy chain. (PDF)

AUTHOR INFORMATION

Corresponding Author

*E-mail: richard.strasser@boku.ac.at. Tel: +43-1-47654-94145.

ORCID

Richard Strasser: 0000-0001-8764-6530

Notes

The authors declare no competing financial interest.

ACKNOWLEDGMENTS

We thank Professor George Lomonosoff (John Innes Centre, Norwich, U.K.) and Plant Bioscience Limited (PBL) (Norwich, U.K.) for supplying the pEAQ-HT expression vector. This work was performed with support of the PhD program BioToP-Biomolecular Technology of Proteins funded by the Austrian Science Fund (FWF Project W1224) and by a grant from the Austrian Federal Ministry of Transport, Innovation and Technology (bmvit) and Austrian Science Fund (FWF): TRP 242-B20.

ABBREVIATIONS

DSC, differential scanning calorimetry; α-HC, alpha heavy chain; HEK, human embryonic kidney; HER2, human epidermal growth factor receptor 2; Ig, immunoglobulin; κ-LC, kappa light chain; LC−ESI−MS, liquid chromatography electrospray ionization mass spectrometry; MALS, multiangle light scattering; MWCO, molecular weight cutoff; SEC, size exclusion chromatography

REFERENCES

(1) Dechant, M.; Beyer, T.; Schneider-Merck, T.; Weisner, W.; Peipp, M.; van de Winkel, J. G.; Valerius, T. Effector mechanisms of recombinant IgA antibodies against epidermal growth factor receptor. *J. Immunol.* **2007**, *179* (5), 2936−43.

(2) Pascal, V.; Laffleur, B.; Debin, A.; Cuvillier, A.; van Egmond, M.; Drocourt, D.; Imbertie, L.; Pangault, C.; Tarte, K.; Tiraby, G.; Cogne, M. Anti-CD20 IgA can protect mice against lymphoma development: evaluation of the direct impact of IgA and cytotoxic effector recruitment on CD20 target cells. *Haematologica* **2012**, *97* (11), 1686−94.

(3) Boross, P.; Lohse, S.; Nederend, M.; Jansen, J. H.; van Tetering, G.; Dechant, M.; Peipp, M.; Royle, L.; Liew, L. P.; Boon, L.; van Rooijen, N.; Bleeker, W. K.; Parren, P. W.; van de Winkel, J. G.; Valerius, T.; Leusen, J. H. IgA EGFR antibodies mediate tumour killing in vivo. *EMBO Mol. Med.* **2013**, *5* (8), 1213−26.

(4) Shields, R. L.; Lai, J.; Keck, R.; O'Connell, L. Y.; Hong, K.; Meng, Y. G.; Weikert, S. H.; Presta, L. G. Lack of fucose on human IgG1 N-linked oligosaccharide improves binding to human Fcgamma RIII and antibody-dependent cellular toxicity. *J. Biol. Chem.* **2002**, *277* (30), 26733−40.

(5) Shinkawa, T.; Nakamura, K.; Yamane, N.; Shoji-Hosaka, E.; Kanda, Y.; Sakurada, M.; Uchida, K.; Anazawa, H.; Satoh, M.; Yamasaki, M.; Hanai, N.; Shitara, K. The absence of fucose but not the presence of galactose or bisecting N-acetylglucosamine of human IgG1 complex-type oligosaccharides shows the critical role of enhancing antibody-dependent cellular cytotoxicity. *J. Biol. Chem.* **2003**, *278* (5), 3466−73.

(6) Nimmerjahn, F.; Ravetch, J. V. Translating basic mechanisms of IgG effector activity into next generation cancer therapies. *Cancer Immun.* **2012**, *12*, 13.

(7) Reusch, D.; Tejada, M. L. Fc glycans of therapeutic antibodies as critical quality attributes. *Glycobiology* **2015**, *25* (12), 1325−34.

(8) Subedi, G. P.; Hanson, Q. M.; Barb, A. W. Restricted motion of the conserved immunoglobulin G1 N-glycan is essential for efficient FcgammaRIIIa binding. *Structure* **2014**, *22* (10), 1478−88.

(9) Rifai, A.; Fadden, K.; Morrison, S. L.; Chintalacharuvu, K. R. The N-glycans determine the differential blood clearance and hepatic uptake of human immunoglobulin (Ig)A1 and IgA2 isotypes. *J. Exp. Med.* **2000**, *191* (12), 2171−82.

(10) Stockert, R. J.; Kressner, M. S.; Collins, J. C.; Sternlieb, I.; Morell, A. G. IgA interaction with the asialoglycoprotein receptor. *Proc. Natl. Acad. Sci. U. S. A.* **1982**, *79* (20), 6229−31.

(11) Yang, W. H.; Aziz, P. V.; Heithoff, D. M.; Mahan, M. J.; Smith, J. W.; Marth, J. D. An intrinsic mechanism of secreted protein aging and turnover. *Proc. Natl. Acad. Sci. U. S. A.* **2015**, *112* (44), 13657−62.

(12) Basset, C.; Devauchelle, V.; Durand, V.; Jamin, C.; Pennec, Y. L.; Youinou, P.; Dueymes, M. Glycosylation of immunoglobulin A influences its receptor binding. *Scand. J. Immunol.* **1999**, *50* (6), 572−9.

(13) Rouwendal, G. J.; van der Lee, M. M.; Meyer, S.; Reiding, K. R.; Schouten, J.; de Roo, G.; Egging, D. F.; Leusen, J. H.; Boross, P.; Wuhrer, M.; Verheijden, G. F.; Dokter, W. H.; Timmers, M.; Ubink, R. A comparison of anti-HER2 IgA and IgG1 in vivo efficacy is facilitated by high N-glycan sialylation of the IgA. *MAbs* **2016**, *8* (1), 74−86.

(14) Herr, A. B.; Ballister, E. R.; Bjorkman, P. J. Insights into IgA-mediated immune responses from the crystal structures of human FcalphaRI and its complex with IgA1-Fc. *Nature* **2003**, *423* (6940), 614−20.

(15) Narimatsu, Y.; Kubota, T.; Furukawa, S.; Morii, H.; Narimatsu, H.; Yamasaki, K. Effect of glycosylation on cis/trans isomerization of prolines in IgA1-hinge peptide. *J. Am. Chem. Soc.* **2010**, *132* (16), 5548−9.

(16) Royle, L.; Roos, A.; Harvey, D. J.; Wormald, M. R.; van Gijlswijk-Janssen, D.; Redwan, E.-R. M.; Wilson, I. A.; Daha, M. R.; Dwek, R. A.; Rudd, P. M. Secretory IgA N- and O-glycans provide a link between the innate and adaptive immune systems. *J. Biol. Chem.* **2003**, *278* (22), 20140−53.

(17) Woof, J. M.; Russell, M. W. Structure and function relationships in IgA. *Mucosal Immunol.* **2011**, *4* (6), 590−597.

(18) Westerhof, L. B.; Wilbers, R. H.; van Raaij, D. R.; Nguyen, D. L.; Goverse, A.; Henquet, M. G.; Hokke, C. H.; Bosch, D.; Bakker, J.; Schots, A. Monomeric IgA can be produced in planta as efficient as IgG, yet receives different N-glycans. *Plant Biotechnol J.* **2014**, *12* (9), 1333−42.

(19) Meyer, S.; Nederend, M.; Jansen, J. H.; Reiding, K. R.; Jacobino, S. R.; Meeldijk, J.; Bovenschen, N.; Wuhrer, M.; Valerius, T.; Ubink, R.; Boross, P.; Rouwendal, G.; Leusen, J. H. Improved in vivo anti-tumor effects of IgA-Her2 antibodies through half-life extension and serum exposure enhancement by FcRn targeting. *MAbs* **2016**, *8* (1), 87−98.

(20) Lohse, S.; Meyer, S.; Meulenbroek, L. A.; Jansen, J. H.; Nederend, M.; Kretschmer, A.; Klausz, K.; Moginger, U.; Derer, S.; Rosner, T.; Kellner, C.; Schewe, D.; Sondermann, P.; Tiwari, S.; Kolarich, D.; Peipp, M.; Leusen, J. H.; Valerius, T. An Anti-EGFR IgA That Displays Improved Pharmacokinetics and Myeloid Effector Cell Engagement In Vivo. *Cancer Res.* **2016**, *76* (2), 403−17.

(21) Plomp, R.; Hensbergen, P. J.; Rombouts, Y.; Zauner, G.; Dragan, I.; Koeleman, C. A.; Deelder, A. M.; Wuhrer, M. Site-specific N-glycosylation analysis of human immunoglobulin e. *J. Proteome Res.* **2014**, *13* (2), 536−46.

(22) Loos, A.; Gruber, C.; Altmann, F.; Mehofer, U.; Hensel, F.; Grandits, M.; Oostenbrink, C.; Stadlmayr, G.; Furtmuller, P. G.; Steinkellner, H. Expression and glycoengineering of functionally active heteromultimeric IgM in plants. *Proc. Natl. Acad. Sci. U. S. A.* **2014**, *111* (17), 6263−8.

DOI: 10.1021/acs.jproteome.7b00121
J. Proteome Res. 2017, 16, 2560−2570

(23) Deshpande, N.; Jensen, P. H.; Packer, N. H.; Kolarich, D. GlycoSpectrumScan: fishing glycopeptides from MS spectra of protease digests of human colostrum sIgA. *J. Proteome Res.* **2010**, *9* (2), 1063−75.
(24) Huang, J.; Guerrero, A.; Parker, E.; Strum, J. S.; Smilowitz, J. T.; German, J. B.; Lebrilla, C. B. Site-specific glycosylation of secretory immunoglobulin A from human colostrum. *J. Proteome Res.* **2015**, *14* (3), 1335−49.
(25) Qiu, X.; Wong, G.; Audet, J.; Bello, A.; Fernando, L.; Alimonti, J. B.; Fausther-Bovendo, H.; Wei, H.; Aviles, J.; Hiatt, E.; Johnson, A.; Morton, J.; Swope, K.; Bohorov, O.; Bohorova, N.; Goodman, C.; Kim, D.; Pauly, M. H.; Velasco, J.; Pettitt, J.; Olinger, G. G.; Whaley, K.; Xu, B.; Strong, J. E.; Zeitlin, L.; Kobinger, G. P. Reversion of advanced Ebola virus disease in nonhuman primates with ZMapp. *Nature* **2014**, *514* (7520), 47−53.
(26) Cho, H.-S.; Mason, K.; Ramyar, K. X.; Stanley, A. M.; Gabelli, S. B.; Denney, D. W.; Leahy, D. J. Structure of the extracellular region of HER2 alone and in complex with the Herceptin Fab. *Nature* **2003**, *421* (6924), 756−760.
(27) Sainsbury, F.; Thuenemann, E. C.; Lomonossoff, G. P. pEAQ: versatile expression vectors for easy and quick transient expression of heterologous proteins in plants. *Plant Biotechnol. J.* **2009**, *7* (7), 682−93.
(28) Durocher, Y.; Perret, S.; Kamen, A. High-level and high-throughput recombinant protein production by transient transfection of suspension-growing human 293-EBNA1 cells. *Nucleic Acids Res.* **2002**, *30* (2), E9.
(29) Strasser, R.; Stadlmann, J.; Schahs, M.; Stiegler, G.; Quendler, H.; Mach, L.; Glossl, J.; Weterings, K.; Pabst, M.; Steinkellner, H. Generation of glyco-engineered Nicotiana benthamiana for the production of monoclonal antibodies with a homogeneous human-like N-glycan structure. *Plant Biotechnol J.* **2008**, *6* (4), 392−402.
(30) Garber, E.; Demarest, S. J. A broad range of Fab stabilities within a host of therapeutic IgGs. *Biochem. Biophys. Res. Commun.* **2007**, *355* (3), 751−7.
(31) Dicker, M.; Tschofen, M.; Maresch, D.; Konig, J.; Juarez, P.; Orzaez, D.; Altmann, F.; Steinkellner, H.; Strasser, R. Transient Glyco-Engineering to Produce Recombinant IgA1 with Defined N- and O-Glycans in Plants. *Front. Plant Sci.* **2016**, *7*, 18.
(32) Paul, M.; Reljic, R.; Klein, K.; Drake, P. M.; van Dolleweerd, C.; Pabst, M.; Windwarder, M.; Arcalis, E.; Stoger, E.; Altmann, F.; Cosgrove, C.; Bartolf, A.; Baden, S.; Ma, J. K. Characterization of a plant-produced recombinant human secretory IgA with broad neutralizing activity against HIV. *MAbs* **2014**, *6* (6), 1585−97.
(33) Strasser, R.; Altmann, F.; Steinkellner, H. Controlled glycosylation of plant-produced recombinant proteins. *Curr. Opin. Biotechnol.* **2014**, *30*, 95−100.
(34) Strasser, R. Plant protein glycosylation. *Glycobiology* **2016**, *26* (9), 926−939.
(35) Shrimal, S.; Trueman, S. F.; Gilmore, R. Extreme C-terminal sites are posttranslocationally glycosylated by the STT3B isoform of the OST. *J. Cell Biol.* **2013**, *201* (1), 81−95.
(36) Zheng, K.; Yarmarkovich, M.; Bantog, C.; Bayer, R.; Patapoff, T. W. Influence of glycosylation pattern on the molecular properties of monoclonal antibodies. *MAbs* **2014**, *6* (3), 649−58.
(37) Yang, Z.; Drew, D. P.; Jorgensen, B.; Mandel, U.; Bach, S. S.; Ulvskov, P.; Levery, S. B.; Bennett, E. P.; Clausen, H.; Petersen, B. L. Engineering mammalian mucin-type O-glycosylation in plants. *J. Biol. Chem.* **2012**, *287* (15), 11911−23.
(38) Castilho, A.; Neumann, L.; Daskalova, S.; Mason, H. S.; Steinkellner, H.; Altmann, F.; Strasser, R. Engineering of sialylated mucin-type O-glycosylation in plants. *J. Biol. Chem.* **2012**, *287* (43), 36518−26.
(39) Karnoup, A. S.; Turkelson, V.; Anderson, W. H. O-linked glycosylation in maize-expressed human IgA1. *Glycobiology* **2005**, *15* (10), 965−81.
(40) Pinkhasov, J.; Alvarez, M. L.; Rigano, M. M.; Piensook, K.; Larios, D.; Pabst, M.; Grass, J.; Mukherjee, P.; Gendler, S. J.; Walmsley, A. M.; Mason, H. S. Recombinant plant-expressed tumour-associated MUC1 peptide is immunogenic and capable of breaking tolerance in MUC1.Tg mice. *Plant Biotechnol J.* **2011**, *9* (9), 991−1001.
(41) Knoppova, B.; Reily, C.; Maillard, N.; Rizk, D. V.; Moldoveanu, Z.; Mestecky, J.; Raska, M.; Renfrow, M. B.; Julian, B. A.; Novak, J. The Origin and Activities of IgA1-Containing Immune Complexes in IgA Nephropathy. *Front. Immunol.* **2016**, *7*, 117.
(42) Parsons, J.; Altmann, F.; Graf, M.; Stadlmann, J.; Reski, R.; Decker, E. L. A gene responsible for prolyl-hydroxylation of moss-produced recombinant human erythropoietin. *Sci. Rep.* **2013**, *3*, 3019.
(43) Tanaka, A.; Iwase, H.; Hiki, Y.; Kokubo, T.; Ishii-Karakasa, I.; Toma, K.; Kobayashi, Y.; Hotta, K. Evidence for a site-specific fucosylation of N-linked oligosaccharide of immunoglobulin A1 from normal human serum. *Glycoconjugate J.* **1998**, *15* (10), 995−1000.
(44) Gomes, M. M.; Wall, S. B.; Takahashi, K.; Novak, J.; Renfrow, M. B.; Herr, A. B. Analysis of IgA1 N-glycosylation and its contribution to FcalphaRI binding. *Biochemistry* **2008**, *47* (43), 11285−99.
(45) Yoo, E. M.; Yu, L. J.; Wims, L. A.; Goldberg, D.; Morrison, S. L. Differences in N-glycan structures found on recombinant IgA1 and IgA2 produced in murine myeloma and CHO cell lines. *MAbs* **2010**, *2* (3), 320−34.
(46) Castilho, A.; Gruber, C.; Thader, A.; Oostenbrink, C.; Pechlaner, M.; Steinkellner, H.; Altmann, F. Processing of complex N-glycans in IgG Fc-region is affected by core fucosylation. *MAbs* **2015**, *7* (5), 863−70.
(47) Plomp, R.; Bondt, A.; de Haan, N.; Rombouts, Y.; Wuhrer, M. Recent Advances in Clinical Glycoproteomics of Immunoglobulins (Igs). *Mol. Cell. Proteomics* **2016**, *15* (7), 2217−28.
(48) Ackerman, M. E.; Crispin, M.; Yu, X.; Baruah, K.; Boesch, A. W.; Harvey, D. J.; Dugast, A. S.; Heizen, E. L.; Ercan, A.; Choi, I.; Streeck, H.; Nigrovic, P. A.; Bailey-Kellogg, C.; Scanlan, C.; Alter, G. Natural variation in Fc glycosylation of HIV-specific antibodies impacts antiviral activity. *J. Clin. Invest.* **2013**, *123* (5), 2183−92.
(49) Wang, T. T.; Sewatanon, J.; Memoli, M. J.; Wrammert, J.; Bournazos, S.; Bhaumik, S. K.; Pinsky, B. A.; Chokephaibulkit, K.; Onlamoon, N.; Pattanapanyasat, K.; Taubenberger, J. K.; Ahmed, R.; Ravetch, J. V. IgG antibodies to dengue enhanced for FcgammaRIIIA binding determine disease severity. *Science* **2017**, *355* (6323), 395−398.
(50) Shade, K. T.; Platzer, B.; Washburn, N.; Mani, V.; Bartsch, Y. C.; Conroy, M.; Pagan, J. D.; Bosques, C.; Mempel, T. R.; Fiebiger, E.; Anthony, R. M. A single glycan on IgE is indispensable for initiation of anaphylaxis. *J. Exp. Med.* **2015**, *212* (4), 457−67.
(51) Mattu, T. S.; Pleass, R. J.; Willis, A. C.; Kilian, M.; Wormald, M. R.; Lellouch, A. C.; Rudd, P. M.; Woof, J. M.; Dwek, R. A. The glycosylation and structure of human serum IgA1, Fab, and Fc regions and the role of N-glycosylation on Fcalpha receptor interactions. *J. Biol. Chem.* **1998**, *273* (4), 2260−72.

DOI: 10.1021/acs.jproteome.7b00121
J. Proteome Res. 2017, 16, 2560−2570

SUPPORTING INFORMATION

Exploring site-specific N-glycosylation of HEK293 and plant-produced human IgA isotypes

Kathrin Göritzer[a], *Daniel Maresch*[b], *Friedrich Altmann*[b], *Christian Obinger*[b], *Richard Strasser*[a]*

[a]Department of Applied Genetics and Cell Biology, University of Natural Resources and Life Sciences, Muthgasse 18, A-1190 Vienna

[b]Department of Chemistry, Division of Biochemistry, University of Natural Resources and Life Sciences, Muthgasse 18, A-1190 Vienna

*corresponding author: Richard Strasser, email: richard.strasser@boku.ac.at, phone: +43-1-47654-94145

Table of Content

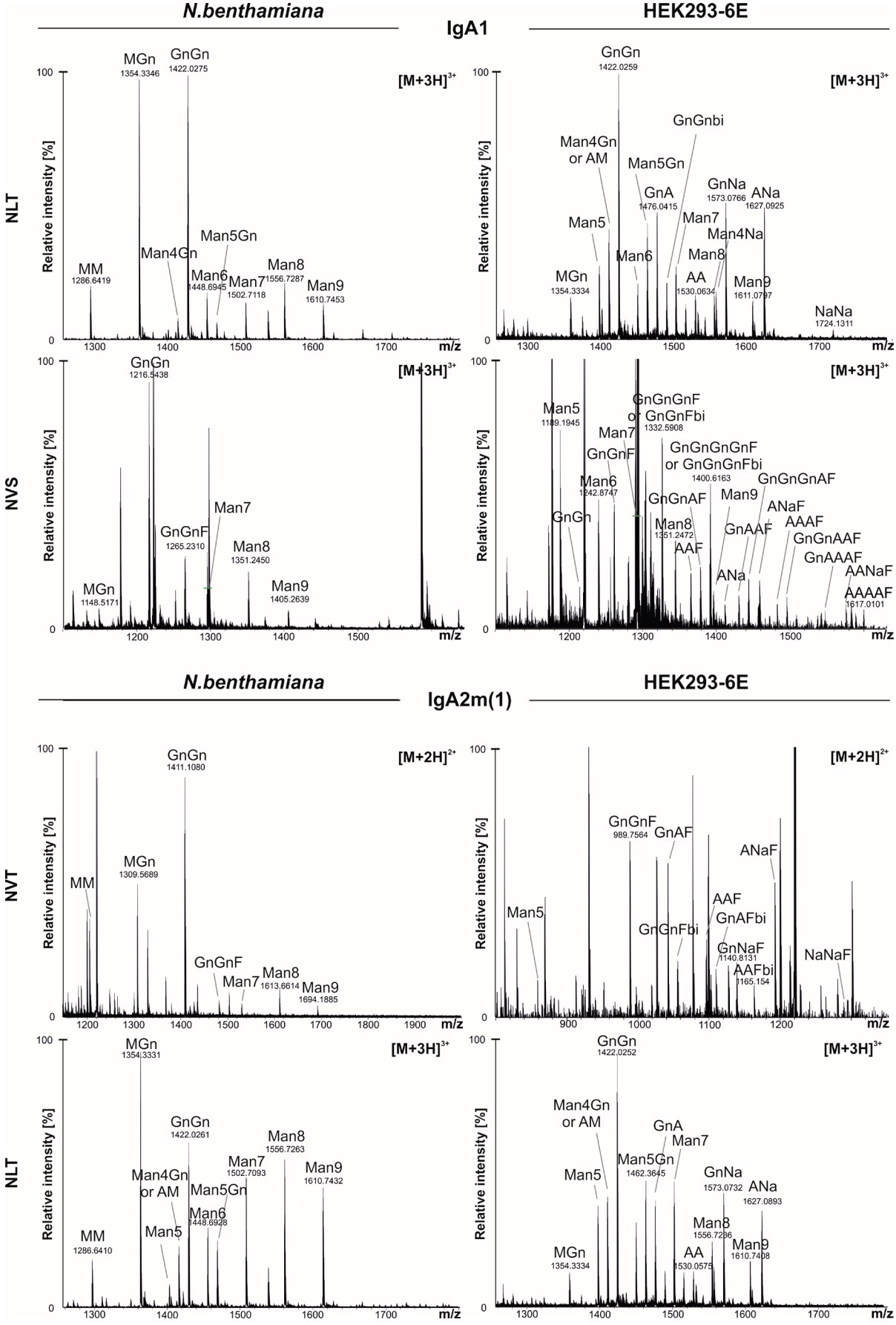
N.benthamiana
IgA1
HEK293-6E
NLT
NVS
Relative intensity [%]
m/z
[M+3H]3+
MGn 1354.3346
GnGn 1422.0275
MM 1286.6419
Man4Gn
Man5Gn
Man6 1448.6945
Man7 1502.7118
Man8 1556.7287
Man9 1610.7453
GnGn 1422.0259
GnGnbi
Man4Gn or AM
Man5Gn
GnA 1476.0415
GnNa 1573.0766
ANa 1627.0925
Man5
Man7
Man4Na
Man6
Man8
MGn 1354.3334
AA 1530.0634
Man9 1611.0797
NaNa 1724.1311
GnGn 1216.5438
GnGnF 1265.2310
Man7
Man8 1351.2450
MGn 1148.5171
Man9 1405.2639
Man5 1189.1945
GnGnGnF or GnGnFbi 1332.5908
Man7
GnGnF
GnGnGnGnF or GnGnGnFbi 1400.6163
GnGnGnAF
Man6 1242.8747
GnGnAF
Man9
ANaF
GnGn
Man8 1351.2472
AAF
GnAAF
AAAF
GnGnAAF
GnAAAF
ANa
AANaF
AAAAF 1617.0101
N.benthamiana
IgA2m(1)
HEK293-6E
NVT
NLT
[M+2H]2+
[M+3H]3+
GnGn 1411.1080
MM
MGn 1309.5689
GnGnF
Man7
Man8 1613.6614
Man9 1694.1885
GnGnF 989.7564
GnAF
ANaF
Man5
AAF
GnAFbi
GnGnFbi
GnNaF 1140.8131
AAFbi 1165.154
NaNaF
MGn 1354.3331
GnGn 1422.0261
Man8 1556.7263
Man7 1502.7093
Man9 1610.7432
Man4Gn or AM
Man5Gn
Man6 1448.6928
Man5
MM 1286.6410
GnGn 1422.0252
Man4Gn or AM
GnA
Man7
Man5Gn 1462.3645
Man5
GnNa 1573.0732
ANa 1627.0893
Man8 1556.7286
Man9 1610.7408
MGn 1354.3334
AA 1530.0575

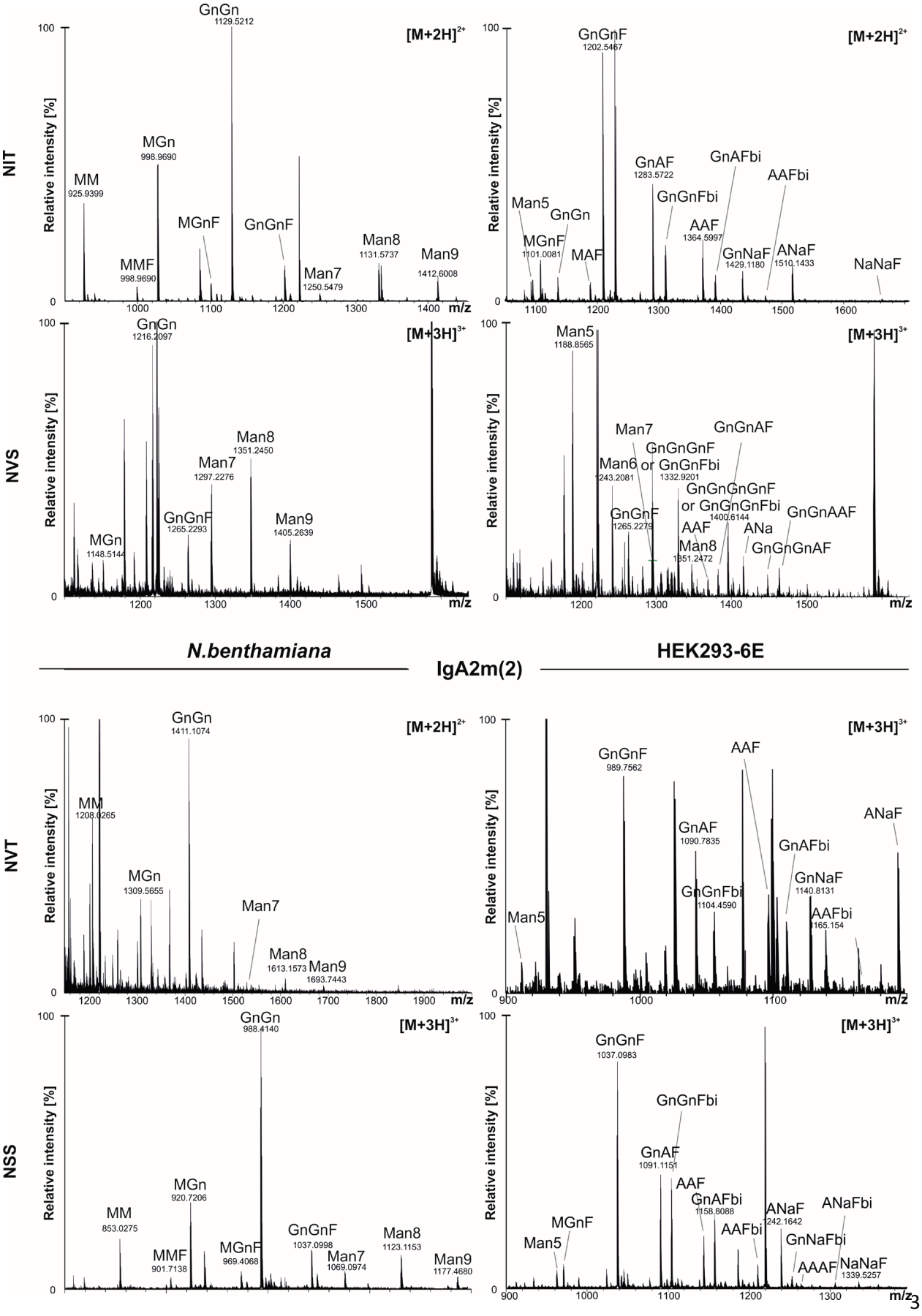
NIT
NVS
NVT
NSS
Relative intensity [%]
m/z
[M+2H]2+
[M+3H]3+
GnGn 1129.5212
MM 925.9399
MGn 998.9690
MMF 998.9690
MGnF
GnGnF
Man7 1250.5479
Man8 1131.5737
Man9 1412.6008
GnGnF 1202.5467
GnAF 1283.5722
GnAFbi
AAFbi
GnGnFbi
Man5
GnGn
AAF 1364.5997
MGnF 1101.0081
MAF
GnNaF 1429.1180
ANaF 1510.1433
NaNaF
GnGn 1216.2097
Man8 1351.2450
Man7 1297.2276
GnGnF 1265.2293
Man9 1405.2639
MGn 1148.5144
Man5 1188.8565
Man7
GnGnAF
GnGnGnF
Man6 or GnGnFbi 1243.2081
1332.9201
GnGnGnGnF
or GnGnGnFbi 1400.6144
GnGnAAF
GnGnF 1265.2279
AAF
ANa
Man8 1351.2472
GnGnGnAF
N.benthamiana
IgA2m(2)
HEK293-6E
GnGn 1411.1074
MM 1208.0265
MGn 1309.5655
Man7
Man8 1613.1573
Man9 1693.7443
GnGnF 989.7562
AAF
ANaF
GnAF 1090.7835
GnAFbi
GnNaF 1140.8131
GnGnFbi 1104.4590
Man5
AAFbi 1165.154
GnGn 988.4140
MGn 920.7206
MM 853.0275
MMF 901.7138
MGnF 969.4068
GnGnF 1037.0998
Man7 1069.0974
Man8 1123.1153
Man9 1177.4680
GnGnF 1037.0983
GnGnFbi
GnAF 1091.1151
AAF
GnAFbi 1158.8088
ANaF 1242.1642
ANaFbi
MGnF
Man5
AAFbi
GnNaFbi
AAAF
NaNaF 1339.5257

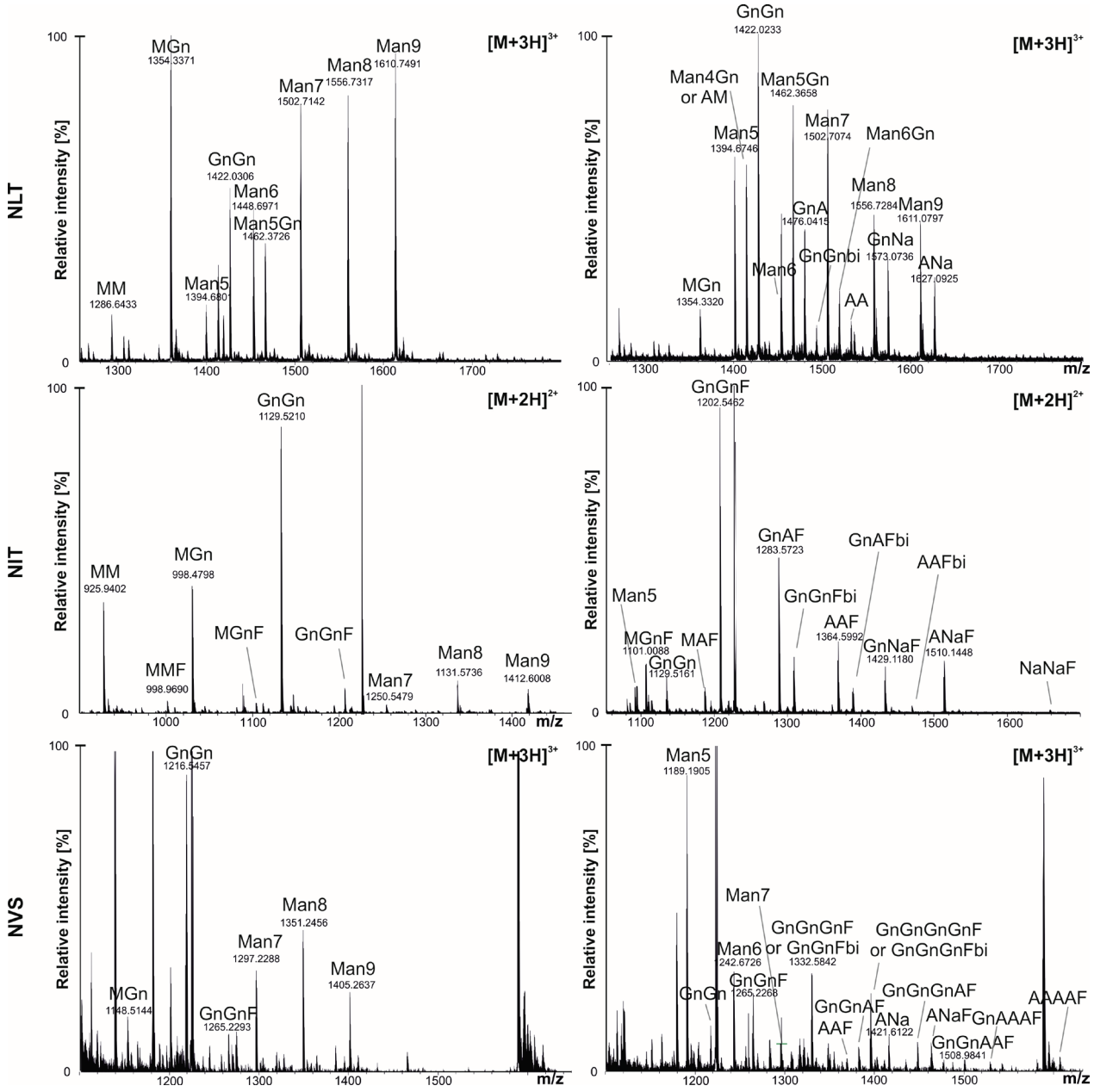

Supplemental Figure 1. MS-spectra of the tryptic glycopeptides derived from the alpha chain of the purified IgA subtypes.

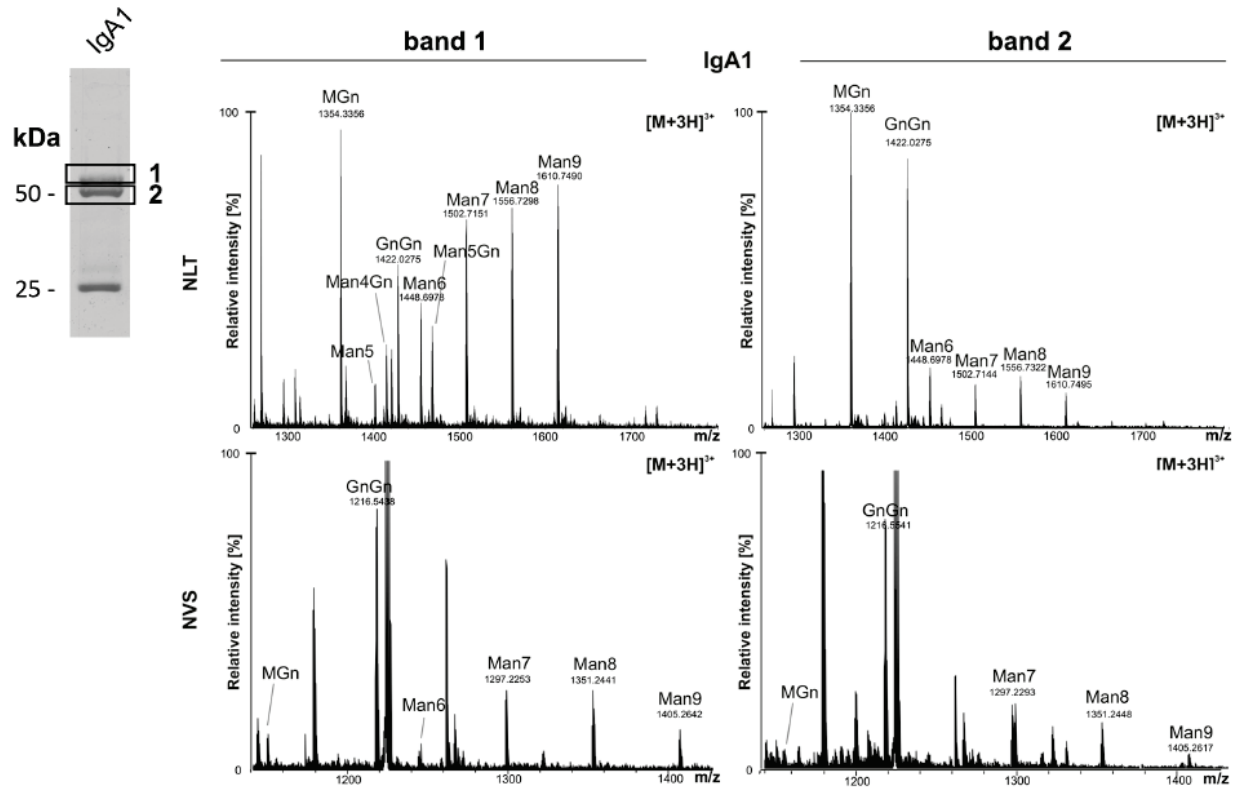

Supplemental Figure 2. MS-spectra showing different N-glycan profiles in the two bands derived from the 55 kDa heavy chain

Distinct Fc alpha receptor N-glycans modulate the binding affinity to immunoglobulin A (IgA) antibodies

Göritzer K., Turupcu A., Maresch D., Novak J., Altmann F., Oostenbrink C., Obinger C., Strasser R.

Research article

J Biol Chem. 2019 Jul 30. pii: jbc.RA119.009954. doi: 10.1074/jbc.RA119.009954.

JBC Papers in Press. Published on July 30, 2019 as Manuscript RA119.009954
The latest version is at http://www.jbc.org/cgi/doi/10.1074/jbc.RA119.009954

Distinct Fc alpha receptor N-glycans modulate the binding affinity to immunoglobulin A (IgA) antibodies

Kathrin Göritzer[1], Aysegül Turupcu[2], Daniel Maresch[3], Jan Novak[4], Friedrich Altmann[3], Chris Oostenbrink[2], Christian Obinger[3], and Richard Strasser[1]*

From the [1]Department of Applied Genetics and Cell Biology, University of Natural Resources and Life Sciences, Muthgasse 18, A-1190 Vienna; [2]Department of Material Sciences and Process Engineering, University of Natural Resources and Life Sciences, Muthgasse 18, A-1190 Vienna; [3]Department of Chemistry, Division of Biochemistry, University of Natural Resources and Life Sciences, Muthgasse 18, A-1190 Vienna; [4]Department of Microbiology, University of Alabama at Birmingham, 845 19th Street, Birmingham, AL 35294

Running Title: *Role of IgA and FcαRI N-glycans*

*To whom correspondence should be addressed: Richard Strasser, Department of Applied Genetics and Cell Biology, University of Natural Resources and Life Sciences, Muthgasse 18, A-1190 Vienna; richard.strasser@boku.ac.at; Tel. +43-1-47654-94145; Fax. +43-1-47654-94009

Keywords: antibody, Fc receptor, glycobiology, glycoprotein structure, glycosylation, immunoglobulin A, molecular dynamics, recombinant protein expression, adaptive immunity, posttranslational modification

ABSTRACT

Human immunoglobulin A (IgA) is the most prevalent antibody class at mucosal sites with an important role in mucosal defense. Little is known about the impact of *N*-glycan modifications of IgA1 and IgA2 on binding to the Fc alpha receptor (FcαRI) which is also heavily glycosylated at its extracellular domain. Here, we transiently expressed human epidermal growth factor receptor 2 (HER2)-binding monomeric IgA1, IgA2m(1) and IgA2m(2) variants in *Nicotiana benthamiana* ΔXT/FT plants lacking the enzymes responsible for generating non-human *N*-glycan structures. By co-infiltrating IgA with the respective glycan modifying enzymes, we generated IgA carrying distinct homogenous *N*-glycans. We demonstrate that distinctly different *N*-glycan profiles do not influence antigen binding or the overall structure and integrity of the IgA antibodies, but did affect their thermal stability. Using size-exclusion chromatography, differential scanning and isothermal titration calorimetry, surface plasmon resonance spectroscopy, and molecular modeling, we probed distinct IgA1 and IgA2 glycoforms for binding to four different FcαRI glycoforms and investigated the thermodynamics and kinetics of complex formation. Our results suggest that different *N*-glycans on the receptor significantly contribute to binding affinities for its cognate ligand. We also noted that full-length IgA and FcαRI form a mix of 1:1 and 1:2 complexes tending toward a 1:1 stoichiometry due to different IgA tailpiece conformations that make it less likely that both binding sites are simultaneously occupied. In conclusion, *N*-glycans of human IgA do not affect its structure and integrity, but its thermal stability, and FcαRI *N*-glycans significantly modulate binding affinity to IgA.

Glycosylation is an important co- and posttranslational modification that affects many properties of proteins including folding, stability, subcellular localization and interaction with other proteins. A very prominent example for the important role of glycosylation is the single *N*-glycan in the CH2 domain of the Fc region of immunoglobulin (Ig) G. The presence of this *N*-glycan is crucial to maintain an open conformation of the Fc domain (1) and influences properties like conformational and thermal stabilities (2). Furthermore, it was found that specific *N*-glycan modifications such as removal of the core fucosylation lead to increased binding affinity to the Fcγ receptor IIIa (3-6) due to

increased carbohydrate-carbohydrate interactions with the *N*-glycans of the Fcγ receptor promoting substantially increased antibody dependent cellular cytotoxicity (7).

While the impact of IgG Fc *N*-glycans on Fcγ receptor binding is well studied, the role of *N*-glycans on recombinant and endogenous human receptor has been characterized only recently (8,9). These studies revealed cell-type dependent differences in *N*-glycan composition and showed for example that oligomannosidic *N*-glycans lead to a 12-fold increase in affinity of the Fcγ receptor IIIa to IgG1 Fc (10). These data suggest that both the IgG Fc *N*-glycan modifications and the presence of distinct *N*-glycans on the corresponding receptor contribute to the modulation of the immune response.

Surprisingly, despite the great importance of IgG glycosylation, little is known about the role of glycans for other Ig isotypes. Human IgA, the predominant antibody at mucosal sites occurs in two subclasses, IgA1 and IgA2, and for IgA2 there are two major allotypes (IgA2m(1) and IgA2m(2)). All these IgA variants are extensively glycosylated. IgA1 has two *N*-glycans, one in the CH2 domain and on in the tailpiece and several *O*-glycosylation sites in the extended hinge region. IgA2 variants lack *O*-glycans but carry four to five *N*-glycans on the heavy chain (11).

Instead of stabilizing intramolecular interactions between the two heavy chains of IgG, the *N*-glycan in the IgA1 CH2 domain is located at the surface of the protein and may influence the conformation of the protein and its binding to different receptors (12). Available data about the interaction of IgA with the FcαRI did not give a clear answer whether distinct IgA glycans play a role in the receptor interaction (13-17). The use of IgA isolated from human serum or recombinant IgA produced in mammalian cells bearing rather heterogeneous *N*-glycans have complicated the interpretation of the results. This also applies to FcαRI, which is heavily glycosylated with 6 predicted *N*-glycosylation and 9 putative *O*-glycosylation sites at its extracellular domain.

Here, we used a plant-based glyco-engineering approach to generate IgA1, IgA2m(1) and IgA2m(2) carrying distinct homogeneous *N*-glycans. Additionally, we produced four distinct glycoforms of the extracellular domain of FcαRI in HEK293F cells. This approach allowed a detailed investigation of the impact of the *N*-glycosylation of the two IgA subclasses and of the extracellular domain of FcαRI on the thermodynamics and kinetics of complex formation by using a broad array of biochemical and biophysical methods including size-exclusion chromatography coupled to multi-angle light scattering (SE-HPLC-MALS), differential scanning (DSC), isothermal titration calorimetry (ITC), surface plasmon resonance spectroscopy (SPR) as well as molecular modeling and simulation.

Results

Production of IgA isotypes with defined N-glycans

To assess the impact of *N*-glycosylation on structure-function relationships, different IgA variants bearing homogenous *N*-glycans were generated. IgA1 produced in HEK293F cells has very heterogeneous complex *N*-glycans with high amounts of branched and incompletely sialylated structures (18) (**Fig. 1A**, $IgA1_{complex}$). A more homogenous *N*-glycosylation profile was obtained by expressing IgA1 in HEK293F cells in the presence of the class I α-mannosidase inhibitor kifunensine resulting in IgA1 with exclusively oligomannosidic *N*-glycans (**Fig. 1A**, $IgA1_{Man9}$). To produce additional glycoforms, we expressed IgA1 transiently in glyco-engineered *N. benthamiana* which are capable of producing glycoproteins with homogenous human-like *N*-glycans (19,20). IgA1 carrying mostly biantennary $GlcNAc_2Man_3GlcNAc_2$ (GnGn) complex *N*-glycans was produced in the ΔXT/FT line (21) by over-expressing a *trans*-Golgi targeted human *N*-acetylglucosaminyltransferase II (GnTII). Co-expression of two different *N. benthamiana* β-hexosaminidases targeted to the *trans*-Golgi and to the apoplast resulted in the formation of truncated $Man_3GlcNAc_2$ (MM) and $GlcNAc_1Man_3GlcNAc_2$ *N*-glycan structures (**Fig. 1A**, $IgA1_{MM}$). IgA1 with predominately terminally galactosylated glycans (**Fig. 1A**, $IgA1_{AA}$) was obtained by co-expression of GnTII and β1,4-galactosyltransferase (22). Finally, IgA1 with terminally sialylated *N*-glycans (**Fig. 1A**, $IgA1_{NaNa}$) was produced by further co-expressing the entire CMP-N-acetylneuraminic acid (CMP-Neu5Ac) biosynthesis pathway, the

transporter that delivers CMP-sialic acid to the Golgi and the α2,6-sialyltransferase to transfer CMP-sialic acid to terminal galactose on the glycoprotein (20).

The transient co-expression of IgA2m(1) and IgA2m(2) isotypes with the respective *N*-glycan processing enzymes enabled the modification of their oligosaccharides in a similar manner as described for IgA1 (**Fig. S1**). However, the efficiency of *N*-glycan modifications varied between different *N*-glycosylation sites and IgA isotypes. While the CH2-resident site (NLT) could be modified very efficiently in IgA1 (**Fig. 1A**), the extension to terminally sialylated *N*-glycans was less efficient on the corresponding site in the IgA2 isotypes (**Fig. S1**). In the latter, this *N*-glycosylation site is in close proximity to another CH2-resident site (NIT), which displays high amounts of sialylated (NaNa) *N*-glycans. Furthermore, also the underglycosylated NVS site in the tailpiece of IgA1 and IgA2 isotypes displayed reduced amounts of modified *N*-glycans compared to other IgA *N*-glycosylation sites (18,23). Taken together, using expression in HEK293F cells and in glyco-engineered plants the production of IgA variants with tailored *N*-glycans (glycoforms) was achieved.

Characterization of different IgA glycoforms

The purified monomeric IgA glycoforms were investigated for their overall assembly and homogeneity using SDS-PAGE and SE-HPLC coupled to MALS. The non-reducing SDS-PAGE of the purified IgA1 glycoforms shows a predominant band at a molar mass around 160 kDa for each variant (**Fig. 1B**), representing the fully assembled antibody without the presence of any degradation products or impurities. The SEC profiles gave narrow single and monodisperse peaks. The retention time shifts due to different *N*-glycan composition (**Fig. 1C)**. HEK293F produced $IgA1_{complex}$ and $IgA1_{Man9}$ displayed the shortest retention time, followed by the plant-produced $IgA1_{NaNa,}$ $IgA1_{AA}$, $IgA1_{GnGn}$ and $IgA1_{MM}$ glycoforms. This hierarchy also applied to the IgA2m(1) and IgA2m(2) isotypes (**Fig. S2**). The shift towards longer retention times in plant-produced IgA variants compared to HEK-derived IgAs results from their lower molecular masses confirmed by MALS due to a higher degree of underglycosylation of the tailpiece *N*-glycosylation site (**Fig. S3**) (18,23).

Next, the thermal stability of the IgA variants was investigated by differential scanning calorimetry (DSC). As described previously, the thermal unfolding of IgA is represented by a broad endotherm which suggests the presence of three independent transitions [1]. This allows the identification of the transition midpoint temperatures of the CH2 (T_m1), Fab (T_m2) and CH3 (T_m3) domains as already described for IgG (18,24). $IgA1_{complex}$ produced in HEK293F cells exhibited melting temperatures at 71.5 ± 0.06 (T_m1), 74.2 ± 0.04 (T_m2) and 76.3 ± 0.05 (T_m3) °C (**Fig. 1D**), respectively, that are in accordance with previously reported endotherms of IgA1 produced in HEK293-6E cells that were measured on a different DSC machine (18). While the HEK293F-produced $IgA1_{Man9}$ showed slightly decreased thermal unfolding temperatures of the CH2 domain, this effect was more pronounced in plant-derived variants. However, the stability of the CH2 domain of plant-produced IgA1 slightly increased with more extended *N*-glycans with the hierarchy of thermal stability being $IgA1_{NaNa}$>$IgA1_{AA}$>$IgA1_{GnGn}$>$IgA1_{MM}$. This correlation has been observed for the IgA2m(1) and IgA2m(2) subclasses as well (**Table S1**).

Overall, our findings indicate an effect of *N*-glycan modifications on thermal stability. However, the difference in thermal stability of HEK293F and plant-derived IgA1 and IgA2 variants could additionally be attributed to a higher degree of underglycosylation of the tailpiece *N*-glycosylation site of plant-produced IgA. Furthermore, the different *O*-glycan modifications in the hinge region of plant- and HEK293F-derived IgA1 might contribute to thermal stability as well. IgA1 has 9 potential *O*-glycosylation sites in its extended proline-rich hinge region of which 6 are found to be occupied with a combination of mucin-type core structures in HEK293F-derived IgA1. On the hinge region of plant-produced IgA1, on the other hand, conversion of proline residues to hydroxyproline and the presence of additional pentoses are observed that might destabilize plant-derived IgA1 (18,25,26). Together with *N*-glycan modifications these different hinge region *O*-glycans could also contribute to the observed

differences in thermal unfolding of the CH2 domain.

Finally, binding to the antigen HER2 was assessed by ELISA and the half maximal effective concentration was determined for the different IgA1 glycoforms. As expected, antigen binding behavior of all IgA1 glycoforms are very similar and independent of glycosylation or production host (**Fig. S4**).

Analysis of FcαRI glycosylation

Previous reports indicated the contribution of distinct Fcγ receptor *N*-glycans to IgG binding (10). It is possible that the *N*-glycan composition of FcαRI plays a similar role for IgA1 interaction. In the crystal structure of the IgA1-Fc in complex with a FcαRI produced in insect cells, distinct *N*-glycans of the receptor are in close proximity to the interaction surface and are suspected to influence receptor binding (12). Compared to humans, insect cell *N*-glycans are significantly smaller and thus the receptor with human-type complex *N*-glycans might be even closer to the interaction surface than it appears in the crystal structure (27). Although a role of FcαRI *N*-glycosylation for IgA binding has been described (28), no site-specific information about the *N*-glycan composition of FcαRI sites is available yet. There are 6 predicted *N*-glycosylation and 9 putative *O*-glycosylation sites in the extracellular domain of human FcαRI (CD89). To assess the *N*-glycosylation status of recombinant FcαRI, the extracellular domain was expressed in HEK293F cells. Purified FcαRI was digested with trypsin as well as Asp-N and analyzed by LC-ESI-MS to determine the *N*-glycosylation status and site-specific *N*-glycan composition (**Fig. 2A**). Not all predicted *N*-glycosylation sites were found to be occupied. While the first three *N*-terminal glycosylation sites N44, N58 and N120 are fully occupied, the sites N56 and N165 on the tryptic peptide 4 are incompletely glycosylated and the C-terminal *N*-glycosylation site N177 was only found unglycosylated. The *N*-glycans found on the recombinant receptor are very heterogenous and display site-specific variations in terms of level of branching, galactosylation and sialylation (**Fig. 2B**). Generally, the peaks correspond to complex-type biantennary or branched *N*-glycans with high levels of fucosylation as well as incomplete galactosylation and sialylation. Several of the detected glycopeptide masses could not be assigned to a distinct glycan composition because of the possible presence of multiple isobaric structures including different branched complex *N*-glycans with or without a bisecting GlcNAc and modification on the non-reducing end. MS2 spectra of the N-terminal glycopeptide indicate the presence of fucosylation on the non-reducing end rather than core-fucosylation. Furthermore, investigation of the tryptic peptides of a recombinant FcαRI that only has single GlcNAc residues at each *N*-glycosylation site (see next section) did not indicate the presence of any additional *O*-glycan modifications.

Production and characterization of different FcαRI glycoforms

Next, the influence of different *N*-glycan modifications on the structure and function of FcαRI was investigated. Therefore, receptor variants with either complex sialylated (FcαRI), complex desialylated ($FcαRI_{desia}$) or oligomannosidic ($FcαRI_{Man9}$) *N*-glycans, as well as a variant with single GlcNAc residues attached to Asn ($FcαRI_{GlcNAc}$) were generated (**Fig. 3A**) and subjected to thorough biochemical and biophysical investigation. Upon SDS-PAGE, 40 kDa bands of the purified receptor variants were detected, except for the variant with single GlcNAc residues which appeared as 25 kDa band (**Fig. 3B**). SE-HPLC runs gave single monodisperse peaks for all glycosylated variants with molecular masses of 42 kDa for the FcαRI, 40 kDa for $FcαRI_{desia}$, 37 kDa for $FcαRI_{Man9}$ confirmed by MALS (**Fig. 3C and Fig. S3**). The $FcαRI_{GlcNAc}$ variant having a molecular mass of 25.5 kDa displays two additional small peaks suggesting disturbed conformational integrity.

To further investigate the effect of different *N*-glycan modifications on the overall conformation of the receptor, circular dichroism spectroscopy (CD) experiments were carried out. Therefore, far-UV spectra between 260 nm to 200 nm were recorded for the FcαRI, $FcαRI_{Man9}$ and $FcαRI_{GlcNAc}$ variants (**Fig. 3D**). The CD-spectrum of the FcαRI exhibits a minimum at 214 nm representing the predominant presence of β-sheets and low abundance of α-helical structures, which is in accordance to the crystal-structure of FcαRI (12). The spectrum of $FcαRI_{Man9}$ is very

similar while $FcαRI_{GlcNAc}$ displays a shift of the minima suggesting an alteration in the secondary structure. It has to be noted, that also the lack of sugar moieties in the $FcαRI_{GlcNAc}$ can cause a slight shift in absorbance since also carbohydrates themselves represent a small CD signal (29).

Next, the influence of this alteration in the secondary structure on the thermal stability of the $FcαRI_{GlcNAc}$ variant was analyzed using differential scanning calorimetry. All FcαRI glycoforms showed nearly identical endotherms with $FcαRI_{GlcNAc}$ being slightly destabilized by approximately 1.5°C (**Fig. 3E**). Furthermore, rescans revealed the capability of FcαRI to re-fold, while this feature is lost in the variant with single GlcNAc residues (**Fig. S5**).

The impact of IgA and FcαRI glycans on the kinetics and thermodynamics of complex formation

To examine the role of the *N*-glycans for the IgA and FcαRI binding, surface plasmon resonance (SPR) spectroscopy with different IgA and FcαRI glycoforms were conducted. Thereby the different IgA1, IgA2m(1) and IgA2m(2) glycoforms were immobilized on a Protein L chip in an oriented manner with the Fc-domain pointing towards the solution. Next, single-cycle kinetic experiments were carried out by injecting five increasing concentrations of the different FcαRI variants. Although the crystal structure of the IgA1-FcαRI complex suggests a 1:2 stoichiometry (12,30), the obtained response units of the binding curves in SPR experiments proposed a 1:1 binding model, and the sensorgram was fitted accordingly. Using this set up medium binding affinities to the FcαRI with K_D values between 150 and 250 nM were obtained for HEK293F- and plant-produced IgA with a general hierarchy of affinity of IgA1 > IgA2m(1) > IgA2m(2) (**Fig. 4**). Characteristic for the interaction of all IgA-FcαRI complexes was a rapid association and dissociation, which has also been described in previous studies (30-32). IgA2 isotypes showed decreased association and dissociation rates compared to IgA1. Moreover, the differences in binding affinity observed for all different IgA as well as FcαRI glycoforms were mediated by the association rate (**Table S2**). The influence of the IgA *N*-glycans on the binding affinity, was reproducible but small with the sialylated glycoform $IgA1_{NaNa}$ being the best binder, an effect that cannot be observed to the same extent in the IgA2 isotypes (**Fig. 4**). This could be due to the less complete modification of the NVS site glycans in these variants or a different conformational orientation of the IgA2-glycans.

The IgA1 *O*-glycosylation sites in the hinge regions are located 20-30 Å away from the FcαRI-IgA1 interacting region. They are therefore not expected to interact with the receptor and would at most contribute by minor long-range electrostatic effects or by causing conformational changes of IgA1 (33). Moreover, *O*-glycans are different in plant and HEK293F-produced IgA1 (18), but the measured affinities towards FcαRI of plant- and HEK293F-derived IgA1 are comparable.

In contrast to the IgA *N*-glycans, FcαRI *N*-glycans contributed significantly to the binding interaction (**Fig. 4**). While a slight increase of binding affinity of the desialylated $FcαRI_{desia}$ could be observed, modification of the *N*-glycans towards oligomannosidic structures as well as single GlcNAc residues had more dramatic effects. The $FcαRI_{Man9}$ variant was able to bind all glycoforms of the three different IgA isotypes 2 to 3 times better than the variants with complex *N*-glycans. The single GlcNAc-containing variant, even displayed a 10-fold increase in binding affinity. This correlation is also found in all glycoforms of the IgA2 isotypes (**Fig. 4**) and is consistent with a previous study (28).

Next, in order to investigate if the instability due to the removal of most of the *N*-glycans can be compensated through stabilization of the complex, DSC of FcαRI or $FcαRI_{GlcNAc}$ in a 1:1 complex with IgA1 were carried out. In complex with IgA1 the FcαRI undergoes a significant increase in thermal stability which is even more pronounced in the IgA1-$FcαRI_{GlcNAc}$ complex. Furthermore, also the CH2 domain of IgA1 shows an increase of the transition midpoint temperature from 71.5 to 72.8 °C in both complexes (**Fig. 3F**).

Stoichiometry of the IgA-FcαRI interaction

Unexpectedly, SPR experiments suggested a 1:1 binding model of the IgA-FcαRI complex which is in discrepancy to the suggested 1:2

stoichiometry found in the crystal structure and ultra-centrifugation experiments in previous studies (12,30,34). To investigate this further, mixtures of the different IgA variants with the various FcαRI variants were applied to SE-HPLC coupled to MALS to determine the molecular mass of the complex. $IgA1_{GnGn}$ and FcαRI applied in a molar ratio of 1:4 formed a complex at around 165 kDa (**Fig. 5A**) which is below the theoretical mass of a 1:1 complex (187 kDa). Similar masses close to 1:1 complexes were revealed for all other IgA-FcαRI combinations (**Fig. S6**). Furthermore, a HEK293F-produced IgA1-Fc deletion protein lacking the Fab domain was analyzed in the same manner to exclude the possibility that the Fab arms interfere with the complex formation. The SEC profiles of the mixture of IgA1-Fc and FcαRI showed the formation of a stable complex at 97 kDa that corresponds closely to the theoretical mass of a 1:1 complex (105 kDa) (**Fig. 5B**).

The discrepancy in binding stoichiometry between the crystal structure (1:2) and our SPR and SEC-analysis (1:1) could be caused by a cooperative binding behavior in which the binding of free IgA1 to FcαRI might show a significant higher affinity than the interaction of the IgA1-FcαRI complex with the second FcαRI (35). To investigate this hypothesis, isothermal titration calorimetry (ITC) was performed. IgA protein samples were used at high concentrations in a sample cell to which highly concentrated receptor was titrated. In this set up the ligand cannot be separated spatially from its receptor after dissociation, which, however, is possible during SEC. ITC binding experiments of $IgA1_{complex}$ and $IgA2m(2)_{complex}$ with either FcαRI or $FcαRI_{Man9}$ exhibited a single transition giving a 1:1.3 binding stoichiometry for each IgA-receptor combination (**Fig. 6** and **Fig. S7**). This suggests the same affinity of the first and second binding event of FcαRI while only 30% of the time a 1:2 complex was present. The obtained binding affinities of IgA1 to FcαRI and $FcαRI_{Man9}$ were approximatley 2.5-fold lower compared to the conducted SPR experiments, but similar for IgA2m(2) binding to FcαRI and $FcαRI_{Man9}$. This difference could be attributed to the IgA immobilization on a surface in SPR experiments, while ligand and analyte are in solution during ITC (**Fig. S7**).

Molecular modeling of the IgA1 and FcαRI interaction

To obtain more insights into the role of *N*-glycosylation as well as the mechanisms that govern the IgA-FcαRI interaction, a molecular model was generated based on the IgA1-Fc-FcαRI crystal structure, the in-solution structure of the full-length IgA1 determined by small-angle X-ray scattering (SAXS) and addition of the IgA1 and FcαRI *N*-glycans. Therefore, iterative alignment of an *N*-glycan library was applied to the used *N*-glycosylation sites and the obtained structures were minimized. One of the lowest energetic conformations was selected (**Fig. 7A**). A possible explanation for the discrepancy in the binding stoichiometry as observed in the crystal structure (PDB-ID 1ow0) as well as ultra-centrifugation studies (12,30) and as determined in this work might be the absence of the IgA1's tailpiece in previous binding stoichiometry determinations (12,13,30,34). Solution structures based on SAXS data sets (provided by David W. Wright)(36) suggested five alternative tailpiece conformations (**Fig. 7B**). These different tailpiece conformations of IgA1 exist in a mixture causing the complex formation to follow a conformational selection. Thus, FcαRI binding will only occur when the IgA1-Fc tailpiece has a suitable binding conformation resulting in a mixture of 1:1 and 1:2 complexes.

Furthermore, the model offers an explanation for the unoccupied site N177 and the partially glycosylated site N165 discovered by site-specific glycopeptide analysis of FcαRI. Therefore, an oligomannosidic (Man9 structure) motion library was used on the glycosylated regions and the accessibility of the experimentally unoccupied sites was investigated (**Fig. 7C**). The interference of *N*-glycans at sites N44 and N156 with N177 and in a similar way the interference of the *N*-glycan at N120 with N165 make them likely inaccessible for the oligosaccharyltransferase complex catalyzing the *N*-glycosylation reaction. The solvent-accessible surface area (SASA) is ~ 67 $Å^2$ for N165 and N177 and ranges from 90 to 120 $Å^2$ for the rest of the *N*-glycosylation sites. Since protein *N*-glycosylation occurs mainly co-translationally in higher eukaryotes (37), the transfer of *N*-glycans to preceding *N*-glycosylation sites may sterically

hinder the transfer of other *N*-glycans or modulate the folding of the receptor to reduce the SASA at specific sites.

Discussion

The detailed biophysical and biochemical characterization of the different IgA glycoforms showed that modification of the *N*-glycans does not affect the overall structure and integrity but the thermal stability of the protein. This is in accordance with our previous study where we showed that plant- and HEK-derived IgA variants exhibit differences in thermal stability, despite having identical amino acid sequences (18). The observed shifts of the transition midpoint temperatures of the CH2 domain of different IgA glycoforms produced in plants as well as different glycoforms produced in HEK293F cells suggest that complex *N*-glycans are beneficial for the thermal stability of IgA. Besides the various *N*-glycans found on IgA, IgA1 additionally has nine potential *O*-glycosylation sites in its extended proline-rich hinge region of which six are found to be occupied with mucin-type *O*-glycans in HEK293F-produced IgA1. On the hinge region of plant-produced IgA1, on the other hand, conversion of proline residues to hydroxyproline and the presence of additional pentoses are observed (18,25,26). Thus, the destabilization of the CH2 domain of the different plant-derived IgA1 glycoforms compared to HEK293F-produced ones could not only result from different *N*-glycan composition but also from the plant-specific hinge region modifications.

The crystal structure of the Fc domain of IgA1 in complex with two FcαRI suggests not only a role of the IgA *N*-glycans for structural properties of the protein but also a possible direct interaction with the FcαRI (12). Although the Fc domain of IgA generally resembles the Fc of IgG, the position of the CH2 domain *N*-glycan differs dramatically. In contrast to the IgG *N*-glycan, which is found between the upper Fc domains, the CH2-resident IgA *N*-glycan is located on the external surface and approaches within 8 Å of the FcαRI in the crystal structure (12). However, not the complete *N*-glycan is resolved and thus the *N*-glycan could directly contact FcαRI. Previous studies reported contradictory results on the importance of the CH2 resident *N*-glycan (13-17). With our set of IgA variants with tailored *N*-glycans we conducted quantitative SPR analysis to solve this controversy. These experiments showed that different glycoforms of all IgA isotypes do not significantly influence FcαRI binding. Apart from FcαRI it has been proposed that IgA binds to multiple cellular receptors (38). While terminal sialylation likely reduces the binding to asialoglycoprotein receptors and thus slows down the fast clearance of IgA (39), the contribution of *N*-glycans to the interaction with other receptors remains to be shown.

The role of glycosylation in antibody-receptor interaction has been traditionally focused on the function of the *N*-glycans of the antibody rather than the receptor. However, recent studies have led to renewed interests and focused on the role of the Fcα receptor *N*-glycans in IgG interaction and subsequent immune responses (10). As seen in the molecular model, the elongated complex-type human *N*-glycan is right at the interface and could directly influence the interaction of IgA with the Fcα receptor. Only little information exists as to the exact nature of the *N*-glycans found on FcαRI in humans. This is attributable to the limited possibilities to access sufficient quantity of the native receptor from neutrophils, monocytes or eosinophils and represents a significant barrier for structure-function studies. Due to glycosylation with several potential *N*- and *O*-glycans the mass of the 32 kDa protein can range from 55 to 100 kDa in the cells of the myeloid linage. These differences suggest extensive and cell-type-specific glycosylation (40-42) that have also been reported for other Fc receptors (10).

Site-specific *N*-glycan analysis of the recombinant FcαRI revealed that not all six *N*-glycosylation sites are fully occupied. The underglycosylation of the C-terminal *N*-glycosylation sites might be explained by restricted accessibility of the oligosaccharyltransferase complex due to protein folding or low solvent-accessible surface area as seen in our molecular model. However, the *N*-glycosylation site N58 that is closest to the IgA interaction surface is fully occupied and exhibits branched complex *N*-glycans with or without a bisecting GlcNAc, sialic acid and fucose on the non-reducing end. Mutation of the asparagine at N58 increases binding of IgA to FcαRI and a similar effect is observed for desialylated FcαRI

(10,43). Consistent with these findings, the desialylated recombinant FcαRI bound slightly better to all tested IgA glycoforms. The effect of desialylation on binding was more pronounced in previous reports where the receptor was produced in CHO cells. In addition to more efficient sialylation, CHO cells attach sialic acid in α2,3-linkage instead of the α2,6-linked sialic acid that is the predominant form in HEK293F. A three-fold increase in binding affinity could be obtained by modifying the receptor glycans towards oligomannosidic *N*-glycans. Of all tested glycoforms, the receptor variant having single GlcNAc residues bound best with a 10-fold increase of affinity. This is interesting, since CD spectroscopy revealed structural alterations in this variant while desialylation or oligomannosidic *N*-glycans did not affect the overall structural conformation or thermal stability of the receptor. However, complex formation did not only stabilize the CH2 domain of IgA1 but also compensated for the loss of stability in the $FcαRI_{GlcNAc}$ variant. This is in accordance with previously reported loss of IgA-Fc intra- and interdomain flexibility upon binding of the FcαRI which might cause higher melting temperatures (34). Supported by our molecular model of the IgA1-FcαRI complex that includes all *N*-glycosylation sites, we propose that differential binding of the receptor glycoforms could either result from changes in surface charge, by steric hindrance or in case of the $FcαRI_{GlcNAc}$ variant also from conformational changes. Thus, the *N*-glycosylation state of the receptor may not be essential for the formation of the ligand binding site per se but affects the affinity to the ligand. This is particularly interesting since different cell-types seem to glycosylate the receptor in a cell-type specific manner (40-42) and thus might modulate the potency of receptor signaling.

An unexpected finding is the discrepancy of the stoichiometry of full-length monomeric IgA variants in complex with FcαRI compared to previous studies. Co-crystallization of an IgA1-Fc construct lacking the tailpiece with FcαRI identified a clear 1:2 binding stoichiometry (12). Further ultra-centrifugation studies and SPR experiments confirmed this observation (13,30). Here, SPR and SEC-HPLC-MALS measurements revealed a 1:1 stoichiometry. For SEC-HPLC-MALS, IgAs were mixed with FcαRI in a 1:4 molar ratio with an adequately high concentration that exceeds the low affinity K_D of the second binding event postulated in previous studies more than 10-fold. This concentration theoretically should allow the occupation of both identical FcαRI binding sites of IgA. A deletion of IgA lacking the Fab domain led to the same conclusion. SEC is a separation technology where the two interaction partners migrate differently after dissociation. By contrast, during ITC analysis the binding partners are in equilibrium in a closed reaction chamber similar to the conditions during crystallization processes and dilution and separation effects found in SEC experiments are not present. Therefore, the high concentrations of the interaction partners should allow binding to a low affinity site as well. ITC results clearly showed a 1:1.3 binding stoichiometry with a single transition, suggesting the presence of a mixture of 1:1 and 1:2 complexes, with both binding events of FcαRI being very similar. A likely explanation for the discrepancy might be the absence of the IgA1's tailpiece in the protein used for crystallization and ultra-centrifugation studies. Previously, differences in binding affinities of the receptor to monomeric IgA1 from serum and recombinant IgA1-Fc lacking the tailpiece and the hinge region could be observed in SPR experiments when a 1:2 model was applied (13). Since the hinge region is 20-30 Å away from the interaction surface it was hypothesized that the tailpiece plays a role in the differences in affinity (13). Based on our observation in ITC experiments and our molecular model that was obtained by superposition of the complex crystal structure and SAXS data of full-length IgA, we propose that the tailpiece does not necessarily change the interaction surface but that it exists in different conformations allowing binding of a second FcαRI only if a suitable condition is met. Understanding the mode of IgA-FcαRI binding is important as a higher stoichiometry has recently been linked to enhanced ITAM (Immunoreceptor Tyrosine-based Activating Motif) signaling that lead to potent neutrophil effector functions (44). A predominant 1:1 binding would therefore suggest that the postulated avidity effects are not necessarily responsible for the superiority of IgA-

elicited tumor killing by neutrophils compared to poor IgG-mediated killing.

Experimental Procedures

Construct design and cloning – All constructs used for the expression of anti-HER2 binding IgA1, IgA2m(1) and IgA2m(2) isotypes in *N. benthamiana* and HEK293 cells have been described in detail recently (18). The vectors for the transient expression of the different anti-HER2 IgA isotypes in HEK293F cells were constructed by flanking the previously described codon-optimized DNA sequences of the heavy chains (α-HC) and the kappa light chain (κ-LC) with DNA sequences encoding the signal peptides 'MELGLSWIFLLAILKGVQC' and 'MDMRVPAQLLGLLLLWLSGARC', respectively and the restriction sites BamHI and SalI. The synthesized DNA was then amplified by PCR with the primers "gWiz_1F" (TCTGAGCAGTACTCGTTGCTG)/"gWiz_1R "(AACAACAGATGGCTGGCAAC). The corresponding coding regions for the heavy chains and the kappa light chain were then separately cloned into the BamHI/SalI sites of the mammalian expression vector gWIZ (Genlantis, San Diego, CA). The codon-optimized sequence for the expression of the Fc domain of IgA1 in HEK293F including the signal peptide of the α-HC and BamHI/SalI restriction sites was synthesized by GeneArt (Thermo Fisher Scientific, USA) and cloned into the gWIZ vector as described above.

The codon-optimized DNA sequence for the expression of the extra-cellular domain of the human FcαRI (P24071.1) with a C-terminal Penta-His tag and the same N-terminal signal peptide for secretion of the κ-LC in HEK293F was synthesized by GeneArt. The sequence was amplified with the primers "String_10F" (CTTCCGGCTCGTTTGGTCGAC)/ "String_2R (AAAACCCTGGCGGGATCC), digested with SalI/BamHI and cloned into SalI/BamHI digested gWIZ vector.

The sequence coding for the catalytic domain of human N-acetylglucosaminyltransferase II (GnTII) was amplified by PCR from the vector pPT2M-GnTII with the primes "Hs-GnTII-9F" (GGATCCGAGGCGGACAACCTGACGCTG CG)/ "Hs-GnTII-10R" (CTCGAGTCACTGCAGTCTTCTATAACTTT TAC) (26). The PCR product was digested with BamHI/XhoI and cloned into the BamHI/SalI digested p20-RST-CTS-Fc vector, thereby removing the Fc-GFP insert and generating pPT2-RST-HsGnTII vector containing the CTS region from rat α2,6-sialyltransferase (RST) for *trans*-Golgi targeting (45).

The sequence and cloning of *N. benthamiana* β-hexosaminidases (NbHEXO) has been described previously (46). To obtain constructs expressing the catalytic domain of NbHEXO3 with an N-terminal *N. benthamiana* chitinase signal peptide (23), the NbHEXO3 sequence was amplified from the p31-NbHEXO3 vector using the primers "Nb-Hexo3-F7" (TATAGGATCCAAGTACCCTGATACCTCT GGAATT)/ "Nb-Hexo3-R7" (TATAAGATCTTTGCTGATAGCAAGAACC TGGATC). The PCR product was digested with BamHI/BglII and cloned into the BamHI digested p31 vector to obtain p31-NbHEXO3(CD). The signal peptide was obtained by PCR amplification from *N. benthamiana* cDNA with the "Nb-Chi_F1" (TATATCTAGAATGAGGCTTAGAGAATTC ACAG) and "Nb-Chi_R1" (TATAGGATCCTGCCGAGGCAGAGAGTA GGAGAGA) primers, digestion of the PCR product with XbaI/BamHI and cloning into XbaI/BamHI digested p31-NbHEXO3(CD) to generate p31-SP-NbHEXO3(CD) for targeting of NbHEXO3 to the apoplast. A construct with the catalytic domain 2 of NbHEXO3 fused to the RST-CTS region was obtained by amplification of p31-NbHEXO3 with the primers "Nb-Hexo3-F9" (TATAGGATCCTTGAAGATATGGCCGATG CCACTA)/"Nb-Hexo3-R7" (TATAAGATCTTTGCTGATAGCAAGAACC TGGATC), digestion with BamHI/BglII and cloning into BamHI digested p31 to obtain p31-NbHEXO3(CD2). The RST-CTS sequence was excised from p20-RST-CST-Fc with XbaI/BamHI and cloned into XbaI/BamHI sites of p31-NbHEXO3(CD2) to generate p31-RST-NbHEXO3(CD2) for targeting to the *trans*-Golgi. Binary vectors for the expression of proteins involved in galactosylation, CMP-sialic acid biosynthesis, Golgi transport and sialic acid transfer were available from previous studies (20).

Expression and purification of IgA glycoforms – For the expression of different recombinant IgA glycoforms in 5 to 6 weeks old *N. benthamiana* ΔXT/FT plants, syringe-mediated agro-infiltration was used (18,21). The recombinant IgAs were either expressed alone or co-infiltrated with the vectors coding for the respective proteins for *N*-glycan modifications. Thereby, an OD600 of 0.15 was used for the κ-LC, the α-HC and GnTII. All remaining constructs involved in glycan modification were added with a final OD600 of 0.05. After 4 days, infiltrated leaf material was harvested and the clarified crude extract was prepared for IgA purification as described before (18).

For the transient expression of the different IgA isotypes in HEK293F cells, cultures were maintained and transfected according to the manufacturer's manual in FreeStyle™ expression medium (Thermo Fisher Scientific, US). High quality plasmid preparations were obtained with the PureYield™ plasmid midiprep system (Promega, USA). For the transfection of a 200 mL culture with a cell density of $1.0x10^6$ cells/mL a total of 200 µg plasmid-DNA, consisting of 100 µg κ-LC and 100 µg of the respective α-HC, were mixed in 4 mL OptiPro™ SFM medium (Thermo Fisher Scientific, US). Another 4 mL of OptiPro™ SFM medium containing 2.5 µg/mL linear polyethylenimine (PEI) (Polysciences Inc., Germany) were added to the DNA solution and incubated for 15 minutes before the mixture was slowly titrated to the cell culture. To obtain IgA isotypes with oligomannosidic *N*-glycans the class I α-mannosidase inhibitor kifunensine (Santa Cruz Biotechnology, US) was added to the cell culture in a final concentration of 10 µM. The cultures were incubated for 7 days at 37°C in a humidified atmosphere with 8% CO_2 on an orbital shaker rotating at 135 rpm. The supernatant containing the secreted soluble protein was harvested by centrifugation at 25000 g for 30 minutes at 4°C and was additionally filtrated through a 0.45 µm Durapore membrane filter (Merck Millipore, Germany). IgA from clarified *N. benthamiana* ΔXT/FT leaf extract and supernatant of HEK293F cells was purified with IgA CaptureSelect affinity resin (Thermo Fisher Scientific, US), followed by a size-exclusion chromatography (SEC) step as described (18).

Expression and purification of FcαRI glycoforms – For the recombinant production of different glycoforms of the extra-cellular domain of the FcαRI, HEK293F cells were cultured and transfected as described in the previous section. To obtain FcαRI with oligomannosidic N-glycans ($FcαRI_{Man9}$) the cultures were transfected in the presence of 10 µM kifunensine. The cell culture supernatants were harvested after 6 days, prepared for purification as described above and diluted 1:2 in loading buffer (20 mM TRIS, 500 mM NaCl and 10 mM imidazole). The solution was loaded onto a 5 mL HisTrap HP column (GE Healthcare, USA) equilibrated with 5 column volumes loading buffer and bound protein was eluted by applying 250 mM imidazole. Eluted fractions containing the protein of interest were pooled and dialyzed over night against Dulbecco's Phosphate Buffered Saline (PBS) (Sigma-Aldrich, USA) supplemented with 200 mM NaCl at 4 °C using a SnakeSkin dialysis tubing with a 10 kDa molecular weight cut-off (Thermo Fisher Scientific, USA). Protein samples were then further concentrated using a 10 kDa Amicon Ultra centrifugal filter (Merck Millipore, Germany). To obtain desialylated FcαRI ($FcαRI_{desia}$) 100 µg of FcαRI were digested with 1000 U neuraminidase (NEB) according to the manufacturer's protocol. To generate a variant of FcαRI with a single N-acetylglucosamine (GlcNAc) at each N-glycosylation site ($FcαRI_{GlcNAc}$) 500 µg of $FcαRI_{Man9}$ were digested with 4000 units endoglycosidase H (Endo H, New England Biolabs, US), followed by Endo H removal with an amylose resin (New England Biolabs, US). The different FcαRI glycoforms were then subjected to size-exclusion chromatography (SEC) on a HiLoad 16/600 Superdex 200 pg column (GE Healthcare, USA) equilibrated with the same buffer used for dialysis.

SDS-PAGE – For reducing or non-reducing SDS-PAGE a total of 5 µg of purified protein were either loaded on a 4-15% Mini-PROTEAN® TGX™ gel (Bio-Rad laboratories, USA) or a 10% polyacrylamide gel. Separated proteins were detected by Coomassie Brilliant Blue staining.

Size-exclusion chromatography coupled to multi-angle light scattering (SE-HPLC-MALS) – To verify the conformational integrity and molecular weight of purified IgAs, FcαRI and IgA-FcαRI complexes, high performance-liquid-chromatography (HPLC) coupled to a size-exclusion chromatography column (Superdex 200 10/300 GL column ,GE Healthcare, USA) combined with multi-angle light scattering were carried out as described previously (18). HPLC (Shimadzu prominence LC20) was equipped with MALS (WYATT Heleos Dawn8+ QELS; software ASTRA6), refractive index detector (RID-10A, Shimadzu) and a diode array detector (SPD-M20A, Shimadzu). Single protein measurements were performed by injection of a total amount of 25 µg protein. For the determination of the mass of IgA-FcαRI complexes, the different IgA variants were mixed with the receptor in a molar ratio of 1:4 starting from 25 µg of the respective IgA.

Differential scanning calorimetry (DSC) – The thermal stability of the IgA variants, FcαRI and different IgA-FcαRI complexes was analyzed by differential scanning calorimetry (DSC) using a MicroCal PEAQ-DSC (Malvern, UK). SEC-purified IgA samples were diluted to a concentration of 5 µM, FcαRI was diluted to 10 µM and IgA-FcαRI complex were mixed in a 1:1 ratio to form a complex with a 10 µM concentration in PBS buffer. Samples were filtrated through a 0.1 µm Ultrafree-MC filter (Merck Millipore, Germany) before measurements in the temperature range of 30 °C to 100 °C with a heating rate of 1 °C/min were carried out. Buffer baselines were subtracted, normalized for protein concentration and fitted with a non-two-state thermal unfolding model using the MicroCal PEAQ-DSC software.

Circular dichroism spectroscopy (CD) – CD was performed using a Chirascan™ CD spectrometer (Applied Photophysics, UK). The instrument was flushed with a nitrogen flow of 5 L/min. The different FcαRI glycoforms were brought to an absorbance at 280 nm of 0.8 in 5 mM phosphate buffer pH 7.4. Samples were measured in a cuvette with a path length of 1 mm in the far-UV region ranging from 190 to 260 nm, a 5 nm/s scan speed and a 3 nm band width.

N- and O-glycan analysis – A total of 20 µg purified protein was reduced, S-alkylated and digested with trypsin (Promega, USA). If required samples were additionally digested with the endoprotease Asp-N (Sigma Aldrich, US). Glycopeptides were then analyzed by capillary reversed-phase chromatography and electron-spray mass spectrometry using a Bruker Maxis 4G Q-TOF instrument as described previously (18). Site-specific glycosylation occupancy was calculated using the ratio of deamidated to unmodified peptide determined upon *N*-glycan release with PNGase A (Europa Bioproducts).

Surface plasmon resonance spectroscopy (SPR) – Binding experiments of IgA glycoforms to different FcαRI variants were performed using a Biacore T200 (GE Healthcare Life Sciences, Sweden). All measurements were conducted with a Protein L sensor chip (GE Healthcare Life Sciences, Sweden) and all sample dilutions were prepared in 1xPBS, 0.05% Tween and 0.1% BSA. Capture of the different IgA variants on the Protein L surface was performed for 60 sec with a concentration of 2 µg/mL and a flow rate of 10 µL/sec. Flow cell 2 remained unmodified to serve as a reference cell for the subtraction of systematic instrument noise and drift. FcαRI binding curves were generated in single-cycle kinetic experiments at five different concentration ranging from 31.5 nM to 500 nM with 60 sec association and 60 sec dissociation time at a flow rate of 10 µL/min. After each run, surface regeneration was accomplished using of 10 mM glycine pH 1.7 for 120 sec at a flow rate of 30 µL/min. Binding affinities (K_D) were calculated with the Biacore T2 Evaluation software using a 1:1 binding model. All experiments were repeated as four independent kinetic runs from two different IgA and FcαRI preparations.

Isothermal titration calorimetry (ITC) – ITC measurements were performed on a MicroCal Automated PEAQ-ITC (Malvern Instruments, UK) to investigate the binding stoichiometry of IgA-FcαRI complexes in solution. All samples were prepared in PBS buffer (pH 7.4),

centrifuged at 20000 g for 10 min at room temperature and filtered through a 0.1 µm Ultrafree-MC filter (Merck Millipore, Germany) prior to measurement. The sample cell was filled with 10 µM IgA solution and titrated with a 160 µM stock solution of the respective FcαRI. Titrations were conducted at 25°C using an initial injection of 0.1 µL followed by 19 successive injections of 1.5 µL with a 150 seconds injection interval. Binding stoichiometry (N) was determined using the Microcal PEAQ-ITC analysis software.

Molecular modeling and simulation – The molecular model of the IgA1-Fc in complex with FcαRI was made using the complex crystal structure with the PDB-ID 1ow0 (12). The model of IgA1-Fc including the CH2-resident and tailpiece *N*-glycosylation site was based on data from SAXS studies and were obtained upon request (36). The variable regions of IgA1 were modeled with the PIGSPro web server, which is a predictive modeling tool specialized for immunoglobulins (47). Complex ($GlcNAc_2Man_3GlcNAc_2$, GnGn type) and oligomannosidic ($Man_9GlcNAc_2$) *N*-glycans were attached to IgA1 and FcαRI, respectively. For the generation of the 3D models of the glycan structures an enhanced sampling method, consisting of two steps, was used. First, the biased potentials for the glycosidic linkages of disaccharides are built up, followed by a sampling step to cover the conformational space of the larger glycans (48,49). This approach enables the creation of motion libraries of GnGn type and $Man_9GlcNAc_2$ glycans. An example of the latter is shown in the supplementary section (**Fig. S8**). After step-wise alignment of glycan motion libraries at each *N*-glycosylation site a short minimization with conjugate gradient (50) using the GROMOS11 biomolecular simulation package (http://www.gromos.net) was applied (51). Molecular interactions were described according to the 53A6glyc parameter set (52,53) of the GROMOS force field for carbohydrates and the 54A8 parameter set (54) for the protein. After each alignment of the glycan, the conformation with the lowest energy was selected. The solvent-accessible surface area (SASA) for the *N*-glycosylation sites were calculated using the PDBePISA web server (55).

Acknowledgements: We thank Professor George Lomonosoff (John Innes Centre, Norwich, UK) and Plant Bioscience Limited (PBL) (Norwich, UK) for supplying the pEAQ-HT expression vector, as well as David W. Wright (Vanderbilt University Medical Center, Nashville, US) for providing the IgA SAXS data sets. Plant based glycan engineering tools were generated in the frame of Laura Bassi Centres of Expertise PlantBioP (Grant 822757, appointed to Herta Steinkellner, BOKU, Vienna, AUT). This project was further supported by EQ-BOKU VIBT GmbH and the BOKU Core Facility *Biomolecular & Cellular Analysis*.

Conflict of interest: The authors declare that they have no conflicts of interest with the contents of this article.

References

1. Borrok, M. J., Jung, S. T., Kang, T. H., Monzingo, A. F., and Georgiou, G. (2012) Revisiting the role of glycosylation in the structure of human IgG Fc. *ACS Chem. Biol.* **7**, 1596-1602
2. Mimura, Y., Church, S., Ghirlando, R., Ashton, P. R., Dong, S., Goodall, M., Lund, J., and Jefferis, R. (2000) The influence of glycosylation on the thermal stability and effector function expression of human IgG1-Fc: properties of a series of truncated glycoforms. *Mol. Immunol.* **37**, 697-706
3. Okazaki, A., Shoji-Hosaka, E., Nakamura, K., Wakitani, M., Uchida, K., Kakita, S., Tsumoto, K., Kumagai, I., and Shitara, K. (2004) Fucose depletion from human IgG1 oligosaccharide enhances binding enthalpy and association rate between IgG1 and FcγRIIIa. *J. Mol. Biol.* **336**, 1239-1249
4. Shields, R. L., Lai, J., Keck, R., O'Connell, L. Y., Hong, K., Meng, Y. G., Weikert, S. H., and Presta, L. G. (2002) Lack of fucose on human IgG1 N-linked oligosaccharide improves binding to human Fcγ RIII and antibody-dependent cellular toxicity. *J. Biol. Chem.* **277**, 26733-26740

5. Shinkawa, T., Nakamura, K., Yamane, N., Shoji-Hosaka, E., Kanda, Y., Sakurada, M., Uchida, K., Anazawa, H., Satoh, M., Yamasaki, M., Hanai, N., and Shitara, K. (2003) The absence of fucose but not the presence of galactose or bisecting N-acetylglucosamine of human IgG1 complex-type oligosaccharides shows the critical role of enhancing antibody-dependent cellular cytotoxicity. *J. Biol. Chem.* **278**, 3466-3473
6. Dekkers, G., Treffers, L., Plomp, R., Bentlage, A. E. H., de Boer, M., Koeleman, C. A. M., Lissenberg-Thunnissen, S. N., Visser, R., Brouwer, M., Mok, J. Y., Matlung, H., van den Berg, T. K., van Esch, W. J. E., Kuijpers, T. W., Wouters, D., Rispens, T., Wuhrer, M., and Vidarsson, G. (2017) Decoding the human immunoglobulin G-glycan repertoire reveals a spectrum of Fc-receptor- and complement-mediated-effector activities. *Front. Immunol.* **8**, 877
7. Ferrara, C., Grau, S., Jager, C., Sondermann, P., Brunker, P., Waldhauer, I., Hennig, M., Ruf, A., Rufer, A. C., Stihle, M., Umana, P., and Benz, J. (2011) Unique carbohydrate-carbohydrate interactions are required for high affinity binding between FcγRIII and antibodies lacking core fucose. *Proc. Natl. Acad. Sci. U.S.A.* **108**, 12669-12674
8. Hayes, J. M., Frostell, A., Cosgrave, E. F., Struwe, W. B., Potter, O., Davey, G. P., Karlsson, R., Anneren, C., and Rudd, P. M. (2014) Fc γ receptor glycosylation modulates the binding of IgG glycoforms: a requirement for stable antibody interactions. *J. Proteome Res.* **13**, 5471-5485
9. Hayes, J. M., Frostell, A., Karlsson, R., Muller, S., Martin, S. M., Pauers, M., Reuss, F., Cosgrave, E. F., Anneren, C., Davey, G. P., and Rudd, P. M. (2017) Identification of Fc γ receptor glycoforms that produce differential binding kinetics for rituximab. *Mol. Cell Proteomics* **16**, 1770-1788
10. Patel, K. R., Roberts, J. T., Subedi, G. P., and Barb, A. W. (2018) Restricted processing of CD16a/Fc γ receptor IIIa N-glycans from primary human NK cells impacts structure and function. *J. Biol. Chem.* **293**, 3477-3489
11. Woof, J. M., and Russell, M. W. (2011) Structure and function relationships in IgA. *Mucosal Immunol.* **4**, 590-597
12. Herr, A. B., Ballister, E. R., and Bjorkman, P. J. (2003) Insights into IgA-mediated immune responses from the crystal structures of human FcαRI and its complex with IgA1-Fc. *Nature* **423**, 614-620
13. Gomes, M. M., Wall, S. B., Takahashi, K., Novak, J., Renfrow, M. B., and Herr, A. B. (2008) Analysis of IgA1 N-glycosylation and its contribution to FcαRI binding. *Biochemistry* **47**, 11285-11299
14. Mattu, T. S., Pleass, R. J., Willis, A. C., Kilian, M., Wormald, M. R., Lellouch, A. C., Rudd, P. M., Woof, J. M., and Dwek, R. A. (1998) The glycosylation and structure of human serum IgA1, Fab, and Fc regions and the role of N-glycosylation on Fcα receptor interactions. *J. Biol. Chem.* **273**, 2260-2272
15. Basset, C., Devauchelle, V., Durand, V., Jamin, C., Pennec, Y. L., Youinou, P., and Dueymes, M. (1999) Glycosylation of immunoglobulin A influences its receptor binding. *Scand. J. Immunol.* **50**, 572-579
16. Carayannopoulos, L., Max, E. E., and Capra, J. D. (1994) Recombinant human IgA expressed in insect cells. *Proc. Natl. Acad. Sci. U.S.A.* **91**, 8348-8352
17. Pleass, R. J., Dunlop, J. I., Anderson, C. M., and Woof, J. M. (1999) Identification of residues in the CH2/CH3 domain interface of IgA essential for interaction with the human Fcα receptor (FcαR) CD89. *J. Biol. Chem.* **274**, 23508-23514
18. Göritzer, K., Maresch, D., Altmann, F., Obinger, C., and Strasser, R. (2017) Exploring site-specific N-glycosylation of HEK293 and plant-produced human IgA isotypes. *J. Proteome Res.* **16**, 2560-2570
19. Strasser, R. (2014) Biological significance of complex N-glycans in plants and their impact on plant physiology. *Front. Plant Sci.* **5**, 363

20. Castilho, A., Strasser, R., Stadlmann, J., Grass, J., Jez, J., Gattinger, P., Kunert, R., Quendler, H., Pabst, M., Leonard, R., Altmann, F., and Steinkellner, H. (2010) In planta protein sialylation through overexpression of the respective mammalian pathway. *J. Biol. Chem.* **285**, 15923-15930
21. Strasser, R., Stadlmann, J., Schähs, M., Stiegler, G., Quendler, H., Mach, L., Glössl, J., Weterings, K., Pabst, M., and Steinkellner, H. (2008) Generation of glyco-engineered *Nicotiana benthamiana* for the production of monoclonal antibodies with a homogeneous human-like N-glycan structure. *Plant Biotechnol. J.* **6**, 392-402
22. Strasser, R., Castilho, A., Stadlmann, J., Kunert, R., Quendler, H., Gattinger, P., Jez, J., Rademacher, T., Altmann, F., Mach, L., and Steinkellner, H. (2009) Improved virus neutralization by plant-produced anti-HIV antibodies with a homogeneous β1,4-galactosylated N-glycan profile. *J. Biol. Chem.* **284**, 20479-20485
23. Castilho, A., Beihammer, G., Pfeiffer, C., Göritzer, K., Montero-Morales, L., Vavra, U., Maresch, D., Grünwald-Gruber, C., Altmann, F., Steinkellner, H., and Strasser, R. (2018) An oligosaccharyltransferase from *Leishmania major* increases the N-glycan occupancy on recombinant glycoproteins produced in *Nicotiana benthamiana*. *Plant Biotechnol. J.* **16**, 1700-1709
24. Garber, E., and Demarest, S. J. (2007) A broad range of Fab stabilities within a host of therapeutic IgGs. *Biochem. Biophys. Res. Commun.* **355**, 751-757
25. Karnoup, A. S., Turkelson, V., and Anderson, W. H. (2005) O-linked glycosylation in maize-expressed human IgA1. *Glycobiology* **15**, 965-981
26. Dicker, M., Maresch, D., and Strasser, R. (2016) Glyco-engineering for the production of recombinant IgA1 with distinct mucin-type O-glycans in plants. *Bioengineered* **7**, 484-489
27. Harrison, R. L., and Jarvis, D. L. (2006) Protein N-glycosylation in the baculovirus-insect cell expression system and engineering of insect cells to produce "mammalianized" recombinant glycoproteins. *Adv. Vir. Res.* **68**, 159-191
28. Xue, J., Zhao, Q., Zhu, L., and Zhang, W. (2010) Deglycosylation of FcαR at N58 increases its binding to IgA. *Glycobiology* **20**, 905-915
29. Coduti, P. L., Gordon, E. C., and Bush, C. A. (1977) Circular dichroism of oligosaccharides containing N-acetyl amino sugars. *Anal. Biochem.* **78**, 9-20
30. Herr, A. B., White, C. L., Milburn, C., Wu, C., and Bjorkman, P. J. (2003) Bivalent binding of IgA1 to FcαRI suggests a mechanism for cytokine activation of IgA phagocytosis. *J. Mol. Biol.* **327**, 645-657
31. Wines, B. D., Hulett, M. D., Jamieson, G. P., Trist, H. M., Spratt, J. M., and Hogarth, P. M. (1999) Identification of residues in the first domain of human Fc α receptor essential for interaction with IgA. *J. Immunol.* **162**, 2146-2153
32. Oortwijn, B. D., Roos, A., van der Boog, P. J., Klar-Mohamad, N., van Remoortere, A., Deelder, A. M., Daha, M. R., and van Kooten, C. (2007) Monomeric and polymeric IgA show a similar association with the myeloid FcαRI/CD89. *Mol. Immunol.* **44**, 966-973
33. Boehm, M. K., Woof, J. M., Kerr, M. A., and Perkins, S. J. (1999) The Fab and Fc fragments of IgA1 exhibit a different arrangement from that in IgG: a study by X-ray and neutron solution scattering and homology modelling. *J. Mol. Biol.* **286**, 1421-1447
34. Posgai, M. T., Tonddast-Navaei, S., Jayasinghe, M., Ibrahim, G. M., Stan, G., and Herr, A. B. (2018) FcαRI binding at the IgA1 CH2-CH3 interface induces long-range conformational changes that are transmitted to the hinge region. *Proc. Natl. Acad. Sci. U.S.A.* **115**, E8882-E8891
35. Lobner, E., Humm, A. S., Göritzer, K., Mlynek, G., Puchinger, M. G., Hasenhindl, C., Rüker, F., Traxlmayr, M. W., Djinovic-Carugo, K., and Obinger, C. (2017) Fcab-HER2 interaction: a menage a trois. Lessons from X-Ray and solution studies. *Structure* **25**, 878-889.e5
36. Hui, G. K., Wright, D. W., Vennard, O. L., Rayner, L. E., Pang, M., Yeo, S. C., Gor, J., Molyneux, K., Barratt, J., and Perkins, S. J. (2015) The solution structures of native and patient monomeric human IgA1 reveal asymmetric extended structures: implications for function and IgAN disease. *Biochem. J.* **471**, 167-185

37. Aebi, M. (2013) N-linked protein glycosylation in the ER. *Biochim. Biophys. Acta* **1833**, 2430-2437
38. Heineke, M. H., and van Egmond, M. (2017) Immunoglobulin A: magic bullet or Trojan horse? *Eur. J. Clin. Invest.* **47**, 184-192
39. Rouwendal, G. J., van der Lee, M. M., Meyer, S., Reiding, K. R., Schouten, J., de Roo, G., Egging, D. F., Leusen, J. H., Boross, P., Wuhrer, M., Verheijden, G. F., Dokter, W. H., Timmers, M., and Ubink, R. (2016) A comparison of anti-HER2 IgA and IgG1 in vivo efficacy is facilitated by high N-glycan sialylation of the IgA. *mAbs* **8**, 74-86
40. Geissmann, F., Launay, P., Pasquier, B., Lepelletier, Y., Leborgne, M., Lehuen, A., Brousse, N., and Monteiro, R. C. (2001) A subset of human dendritic cells expresses IgA Fc receptor (CD89), which mediates internalization and activation upon cross-linking by IgA complexes. *J. Immunol.* **166**, 346-352
41. van Egmond, M., Damen, C. A., van Spriel, A. B., Vidarsson, G., van Garderen, E., and van de Winkel, J. G. J. (2001) IgA and the IgA Fc receptor. *Trends Immunol.* **22**, 205-211
42. Morton, H. C., Schiel, A. E., Janssen, S. W., and van de Winkel, J. G. (1996) Alternatively spliced forms of the human myeloid Fc α receptor (CD89) in neutrophils. *Immunogenetics* **43**, 246-247
43. Monteiro, R. C., Kubagawa, H., and Cooper, M. D. (1990) Cellular distribution, regulation, and biochemical nature of an Fc α receptor in humans. *J. Exp. Med.* **171**, 597-613
44. Brandsma, A. M., Bondza, S., Evers, M., Koutstaal, R., Nederend, M., Jansen, J. H. M., Rosner, T., Valerius, T., Leusen, J. H. W., and Ten Broeke, T. (2019) Potent Fc receptor signaling by IgA leads to superior killing of cancer cells by neutrophils compared to IgG. *Front. Immunol.* **10**, 704
45. Schoberer, J., Liebminger, E., Botchway, S. W., Strasser, R., and Hawes, C. (2013) Time-resolved fluorescence imaging reveals differential interactions of N-glycan processing enzymes across the Golgi stack in planta. *Plant Physiol.* **161**, 1737-1754
46. Shin, Y. J., Castilho, A., Dicker, M., Sadio, F., Vavra, U., Grünwald-Gruber, C., Kwon, T. H., Altmann, F., Steinkellner, H., and Strasser, R. (2016) Reduced paucimannosidic N-glycan formation by suppression of a specific β-hexosaminidase from *Nicotiana benthamiana*. *Plant Biotechnol. J.* **15**, 197-206
47. Lepore, R., Olimpieri, P. P., Messih, M. A., and Tramontano, A. (2017) PIGSPro: prediction of immunoGlobulin structures v2. *Nucleic Acids Res.* **45**, W17-W23
48. Hansen, H. S., and Hunenberger, P. H. (2010) Using the local elevation method to construct optimized umbrella sampling potentials: calculation of the relative free energies and interconversion barriers of glucopyranose ring conformers in water. *J. Comput. Chem.* **31**, 1-23
49. Turupcu, A., and Oostenbrink, C. (2017) Modeling of oligosaccharides within glycoproteins from free-energy landscapes. *J. Chem. Inf. Model.* **57**, 2222-2236
50. Fletcher, R., and Reeves, C. M. (1964) Function minimization by conjugate gradients. *Comput. J.* **7**, 149-154
51. Schmid, N., D. Christ, C., Christen, M., P. Eichenberger, A., and van Gunsteren, W. (2012) Architecture, implementation and parallelisation of the GROMOS software for biomolecular simulation. *Comput. Phys. Commun.* **183**, 890-903
52. Pol-Fachin, L., Rusu, V. H., Verli, H., and Lins, R. D. (2012) GROMOS 53A6GLYC, an improved GROMOS force field for hexopyranose-based carbohydrates. *J. Chem. Theory Comput.* **8**, 4681-4690
53. Pol-Fachin, L., Verli, H., and Lins, R. D. (2014) Extension and validation of the GROMOS 53A6(GLYC) parameter set for glycoproteins. *J. Comput. Chem.* **35**, 2087-2095
54. Reif, M. M., Hünenberger, P. H., and Oostenbrink, C. (2012) New interaction parameters for charged amino acid side chains in the GROMOS force field. *J. Chem. Theory Comput.* **8**, 3705-3723
55. Krissinel, E., and Henrick, K. (2007) Inference of macromolecular assemblies from crystalline state. *J. Mol. Biol.* **372**, 774-797

FOOTNOTES

This work was supported by the Austrian Science Fund, FWF (Doctoral Program BioToP–Biomolecular Technology of Proteins (W1224)) and by the FWF Project P31920-B32.

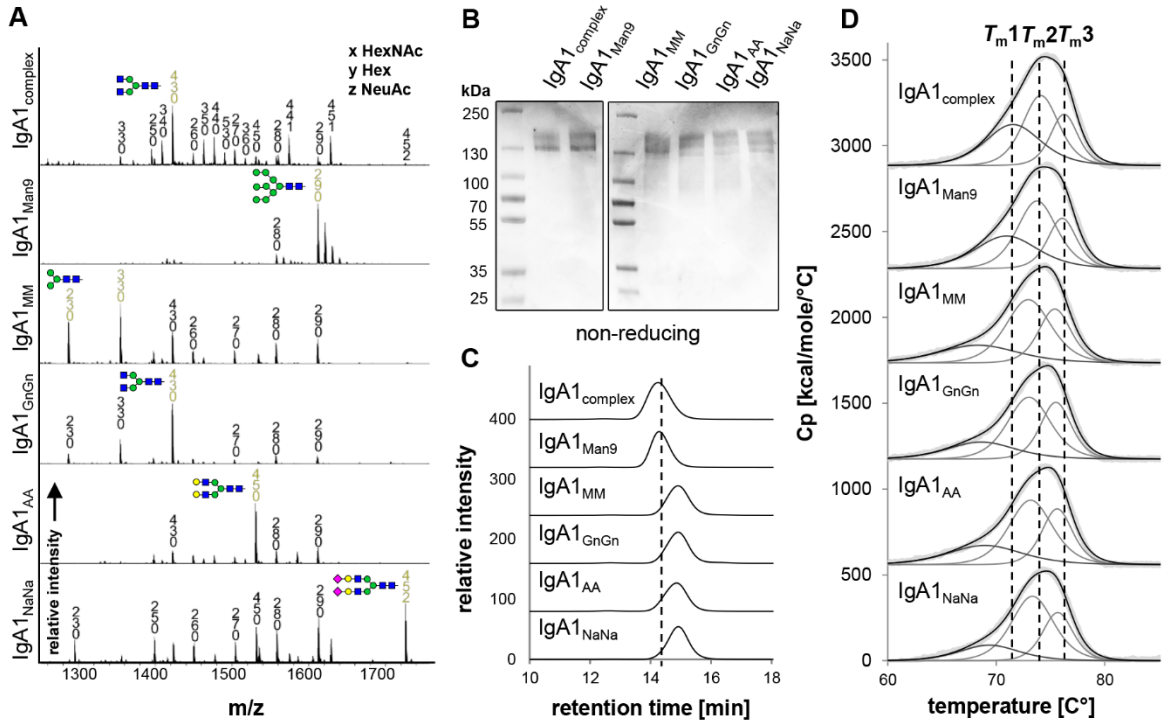

Figure 1. *N*-glycan composition and thermal stability of IgA1 glycoforms. *A*, representative MS-spectra ($[M+3H]^{3+}$) of the tryptic glycopeptide "LSLHRPALEDLLLGSEANLTCTLTGLR" containing the CH2 resident NLT-glycosylation site derived from the alpha chain of the different purified IgA1 glycoforms are shown. $IgA1_{complex}$ and $IgA1_{Man9}$ are HEK293F-derived, all other variants are plant-produced. *N*-glycans are abbreviated according to the ProGlycAn system (www.proglycan.com). The symbols for the monosaccharides are drawn according to the nomenclature from the Consortium for Functional Glycomics (http://www.functionalglycomics.org/). Illustrations of selected major peaks are shown. *B*, SDS-PAGE of purified IgA1 glycoforms under non-reducing conditions followed by Coomassie Brilliant Blue staining. *C*, SE-HPLC measurements of the different IgA1 glycoforms. In order to facilitate comparison between the different variants the elution time of $IgA1_{complex}$ is marked with a dashed line. *D*, DSC analysis of the IgA1 glycoforms. The black lines show fitted representative thermograms, whereas the grey lines are the deconvoluted peaks of each domain transition and the light grey line are the raw data. For comparison, the three midterm transitions of the CH2, Fab and CH3 domain of $IgA1_{complex}$ produced in HEK293F cells are marked with dashed lines.

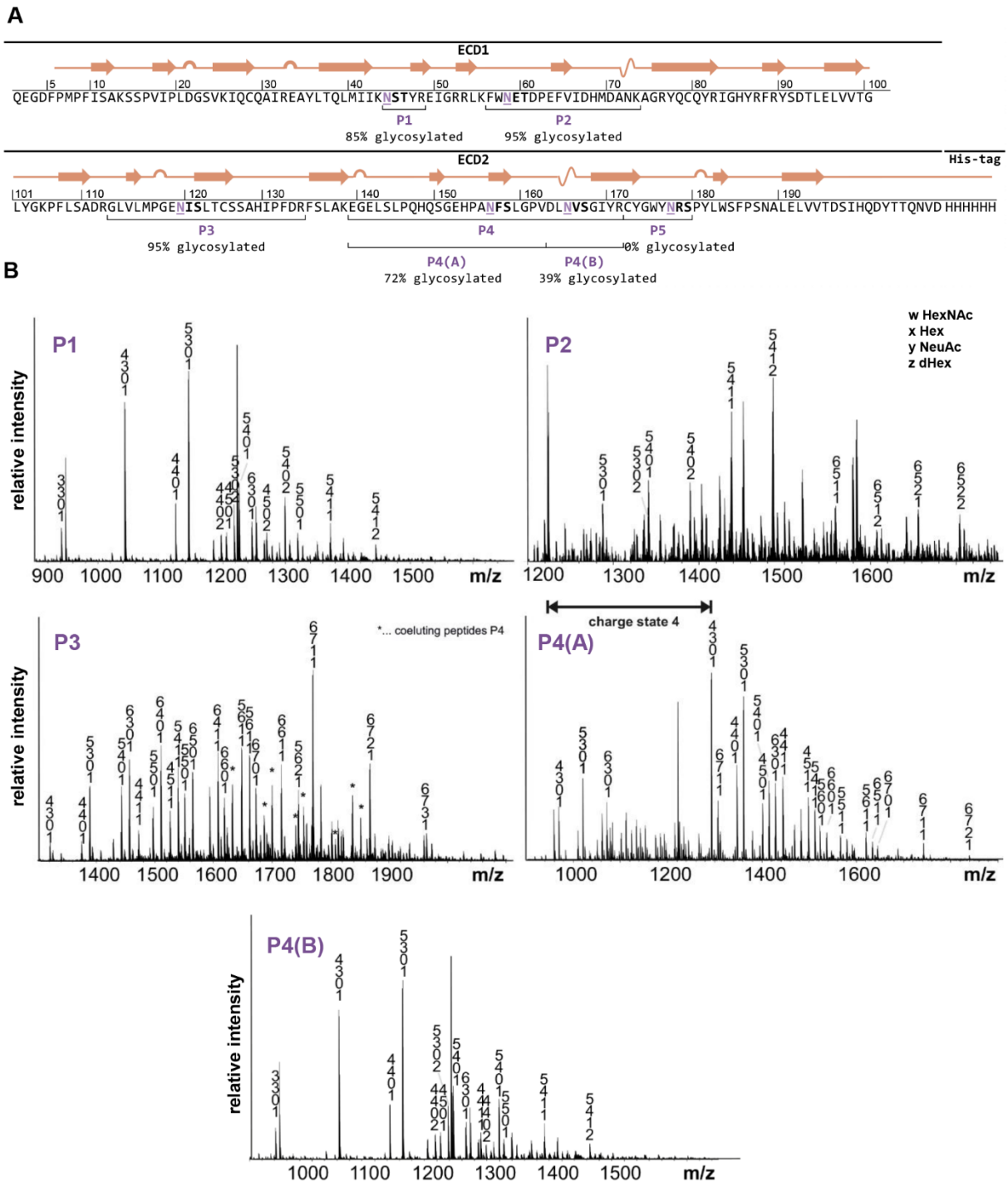

Figure 2. *N*-glycan characteristics of the recombinant extracellular domain of FcαRI. *A*, schematic representation of the secondary structure of the HEK293F-produced extracellular domain. Putative *N*-glycosylation sites are marked in purple and are underlined. The degree of *N*-glycan site occupancy (% of glycosylation) is indicated for each site and the obtained peptides are highlighted and marked P1 to P5. *B*, representative MS-spectra ($[M+3H]^{3+}$) of the glycopeptides P1 to P4(B) obtained from digested recombinant FcαRI.

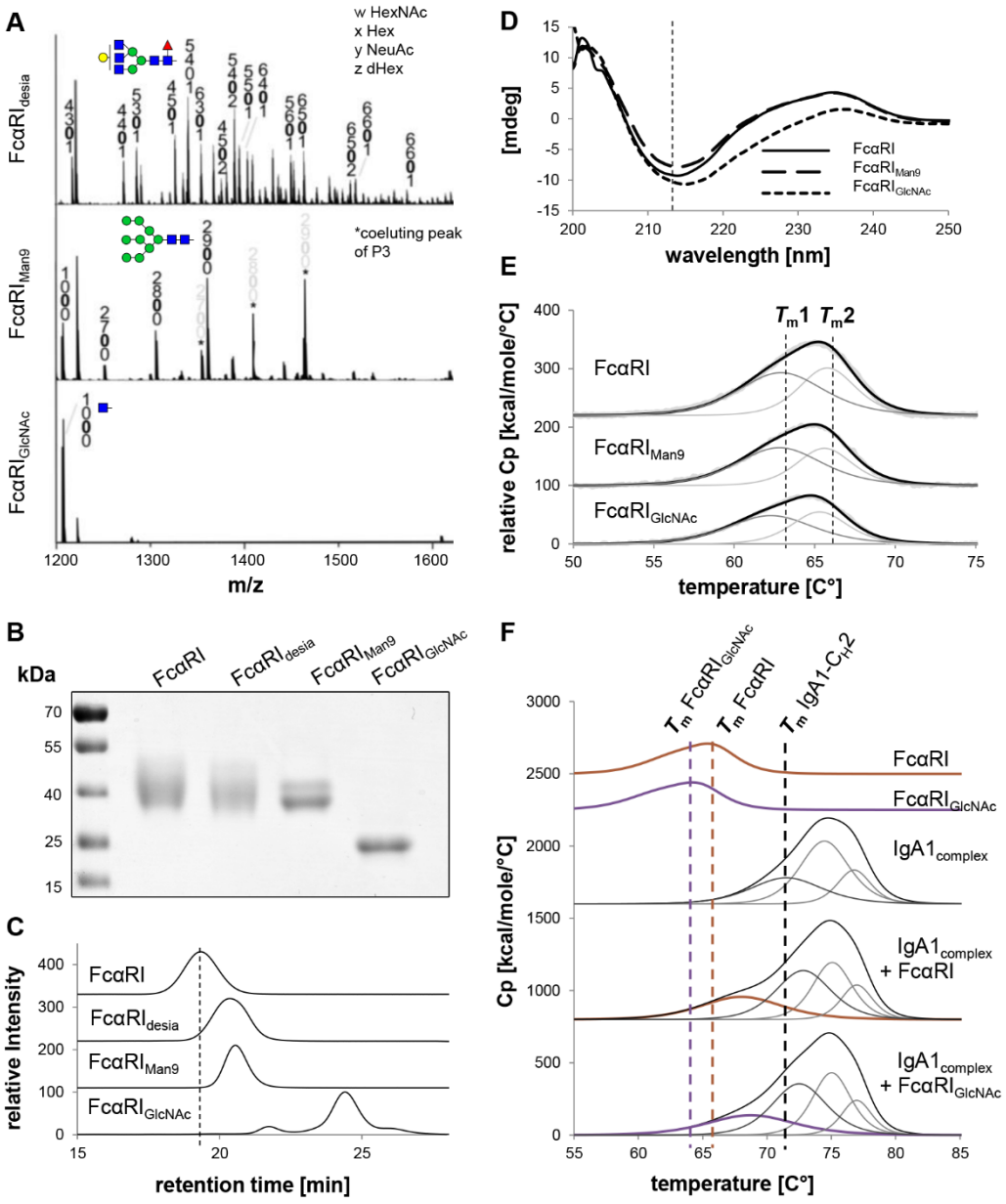

Figure 3. Homogeneity and thermal stability of different FcαRI glycoforms. *A*, representative MS-spectra of the tryptic glycopeptide P2 obtained from digested FcαRI$_{desia}$ ([M+3H]$^{3+}$), FcαRI$_{Man9}$ ([M+3H]$^{3+}$) and FcαRI$_{GlcNAc}$ ([M+3H]$^{2+}$). *B*, SDS-PAGE of the different purified FcαRI glycoforms under reducing conditions. Proteins were detected by Coomassie Brilliant Blue staining. *C*, SE-HPLC measurements of the FcαRI glycoforms. In order to facilitate comparison between the different variants the elution time of the FcαRI with complex sialylated *N*-glycosylation is marked with dashed lines. *D*, CD analysis of different FcαRI glycoforms. The CD-spectra minimum of FcαRI at 214 nm is marked in dashed lines for comparison. *E*, DSC analysis of different FcαRI glycoforms. The black lines show fitted representative DSC thermograms, whereas the grey lines are the deconvoluted peaks of each domain transition and the light grey line are the raw data. For comparison, the two midterm transitions of each FcαRI domain are marked with dashed lines. *F*, DSC analysis of different FcαRI glycoforms and IgA1-FcαRI complexes mixed in a molar ratio of 1 to 1. Bold lines show fitted representative DSC thermograms, whereas the thin lines are the deconvoluted peaks of each domain transition. For comparison the midterm transition of FcαRI, FcαRI$_{GlcNAc}$ and the CH2 domain of IgA1 are marked with dashed lines.

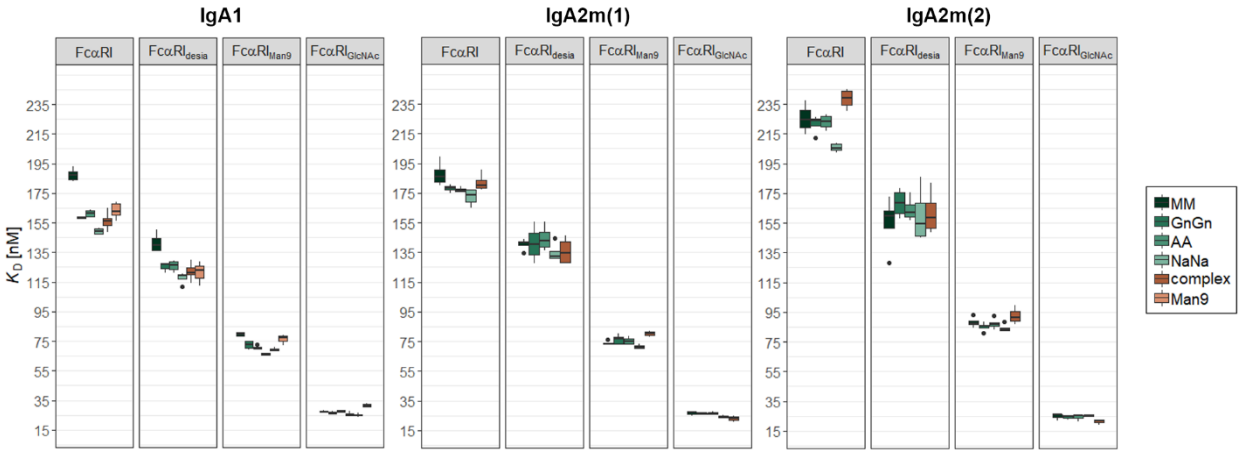

Figure 4. The effect of *N*-glycans on binding affinities of IgA1, IgA2m(1) and IgA2m(2) to FcαRI. K_D values were obtained by SPR spectroscopy in single-cycle kinetic experiments from 4 independent measurements of two different receptor preparations. IgA1 glycoforms were captured on a protein L chip and increasing concentrations of the respective FcαRI glycoforms were injected. The obtained curves were fitted with a 1:1 binding model.

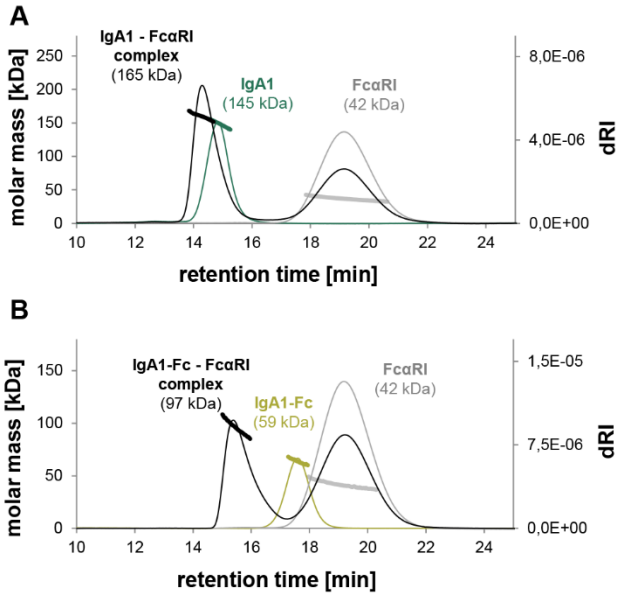

Figure 5. SE-HPLC-MALS reveals molar masses of IgA1 and FcαRI complexes that correspond to a 1:1 stoichiometry. *A*, overlay of the elution profile of IgA1 (green), FcαRI (gray) and a mixture of IgA1 and FcαRI in a ratio of 1:4 (black). *B*, overlay of the elution profile of IgA1-Fc (light green), FcαRI (gray) and a mixture of IgA1_Fc and FcαRI in a ratio of 1:4 (black). Note that the depicted molar masses are derived from MALS measurements and thus do not exactly match the exact molar masses.

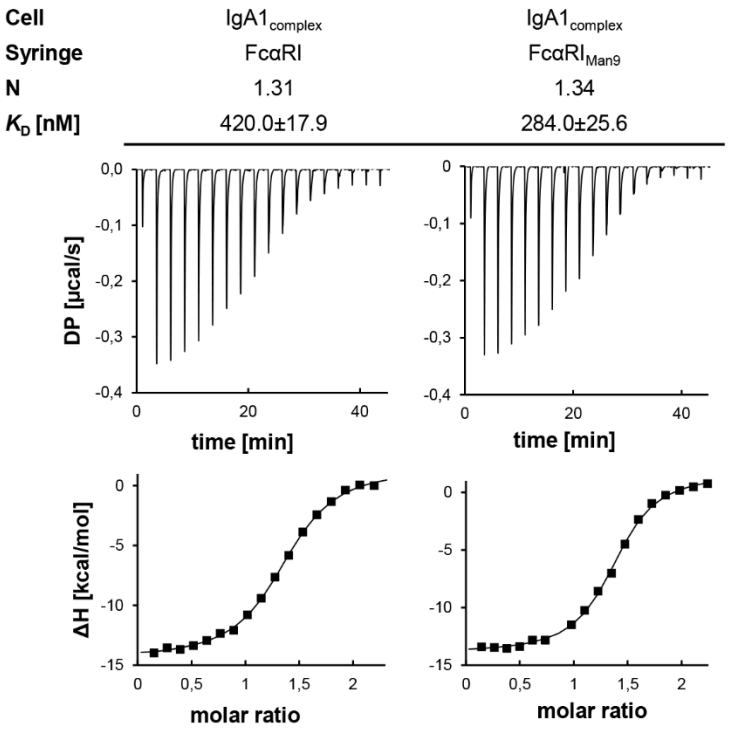

Figure 6. Isothermal titration calorimetry indicates the same affinity for the first and second binding event of IgA1 to FcαRI. The upper panels show the raw data representing the response to 19 injections at 25°C and the lower panels the integrated data.

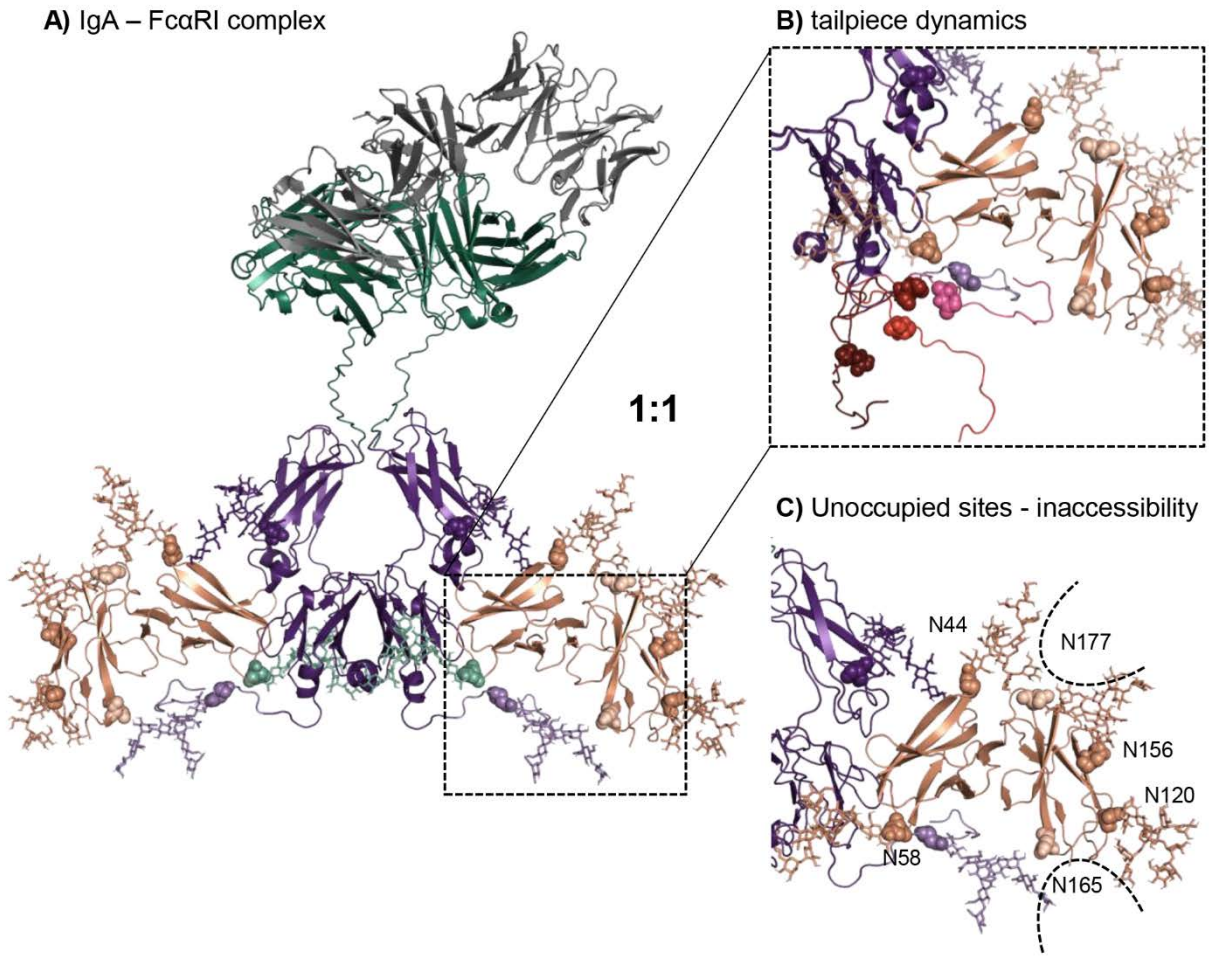

Figure 7. The molecular model of *N*-glycosylated IgA1-Fc in complex with FcαRI suggests a 1:1 binding stoichiometry. *A*, IgA1-Fc region colored in purple, constant heavy and light chain colored in green, variable region colored in gray and FcαRI colored in salmon. IgA1-Fc has a CH2-resident and a tailpiece *N*-glycan (shown in lighter purple, *N*-glycosylation sites depicted in spheres, *N*-glycans as sticks). FcαRI has 6 potential *N*-glycosylation sites at N44, N58, N120, N156, N165 and N177 shown in spheres. The two *N*-glycosylation sites N165 and N177 which are hardly or not occupied are colored in lighter color. Complex (GnGn) *N*-glycans of IgA1-Fc and oligomannosidic (Man9) *N*-glycans of FcαRI are shown as sticks. *B*, five different tailpiece conformations (each shown in a different color) were aligned to the model where the backbone is shown as cartoon, the tailpiece *N*-glycosylation site is marked in spheres and glycans are shown as sticks. *C*, *N*-glycosylation sites N165 and N177 show the lowest solvent-accessible surface area (SASA) with ~ 67 $Å^2$, rendering the site inaccessible for *N*-glycosylation.

Distinct Fc alpha receptor N-glycans modulate the binding affinity to immunoglobulin A (IgA) antibodies

Kathrin Göritzer, Aysegül Turupcu, Daniel Maresch, Jan Novak, Friedrich Altmann, Chris Oostenbrink, Christian Obinger and Richard Strasser

J. Biol. Chem. published online July 30, 2019

SUPPORTING INFORMATION

Distinct Fc alpha receptor N-glycans modulate the binding affinity to immunoglobulin A (IgA) antibodies

Kathrin Göritzer[1], Aysegül Turupcu[2], Daniel Maresch[3], Jan Novak[4], Friedrich Altmann[3], Chris Oostenbrink[2], Christian Obinger[3], and Richard Strasser[1]*

From the [1]Department of Applied Genetics and Cell Biology, University of Natural Resources and Life Sciences, Muthgasse 18, A-1190 Vienna; [2]Department of Material Sciences and Process Engineering, University of Natural Resources and Life Sciences, Muthgasse 18, A-1190 Vienna; [3]Department of Chemistry, Division of Biochemistry, University of Natural Resources and Life Sciences, Muthgasse 18, A-1190 Vienna; [4]Department of Microbiology, University of Alabama at Birmingham, 845 19th Street, Birmingham, AL 35294

Running Title: *Role of IgA and FcαRI N-glycans*

*To whom correspondence should be addressed: Richard Strasser, Department of Applied Genetics and Cell Biology, University of Natural Resources and Life Sciences, Muthgasse 18, A-1190 Vienna; richard.strasser@boku.ac.at; Tel. +43-1-47654-94145; Fax. +43-1-47654-94009

Keywords: antibody, Fc receptor, glycobiology, glycoprotein structure, glycosylation, immunoglobulin A, molecular dynamics, recombinant protein expression, adaptive immunity, posttranslational modification

---

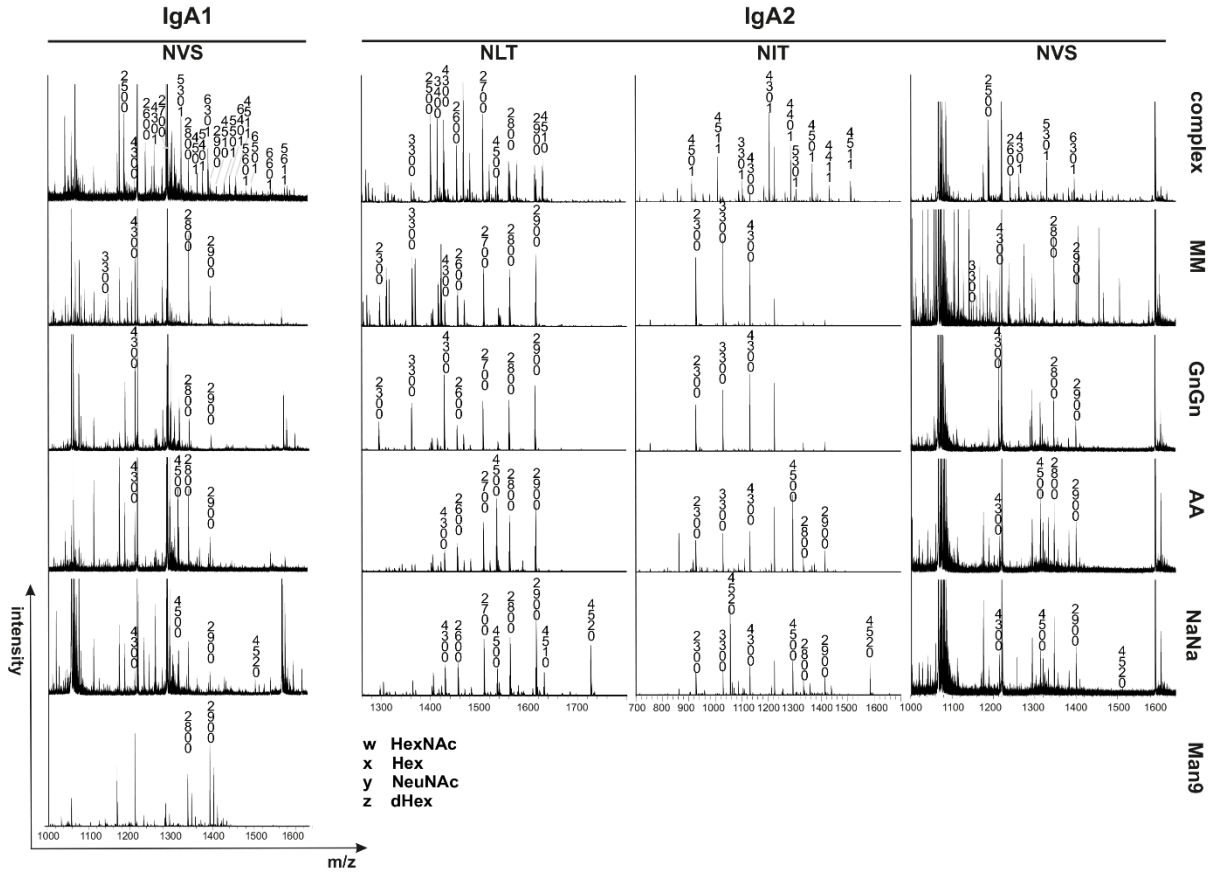

Figure S1. MS-analysis of different IgA1 and IgA2 glycoforms. Representative MS-spectra ($[M+3H]^{3+}$) of the tryptic glycopeptides "LAGKPTHVNVSVVMAEVDGTCY" of IgA1 as well as "LSLHRPALEDLLLGSEANLTCTLTGLR", "TPLTANITK" and "LAGKPTHVNVSVVMAEVDGTCY" of IgA2m(2) containing the Fc-glycosylation sites derived from the alpha chain of the different purified IgA1 and IgA2m(2) glycoforms. MS-spectra of IgA2m(1) are not shown, but resemble very accurately MS-spectra of IgA2m(2).

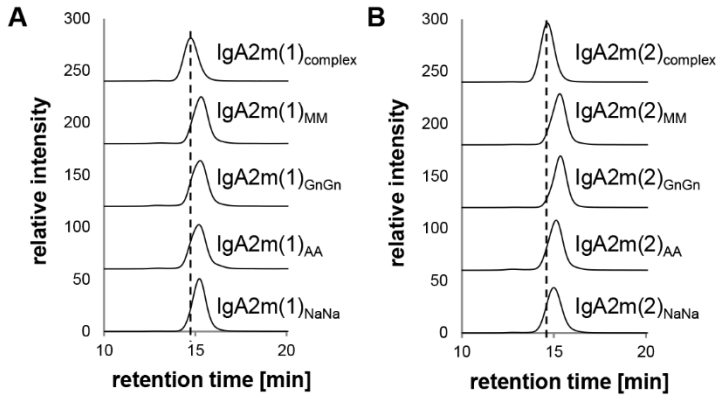

Figure S2. SE-HPLC measurements of the different IgA2m(1) (A) and IgA2m(2) (B) glycoforms. In order to facilitate comparison between the different variants the elution time of $IgA2m(1)_{complex}$ and $IgA2m(2)_{complex}$ are marked with dashed lines.

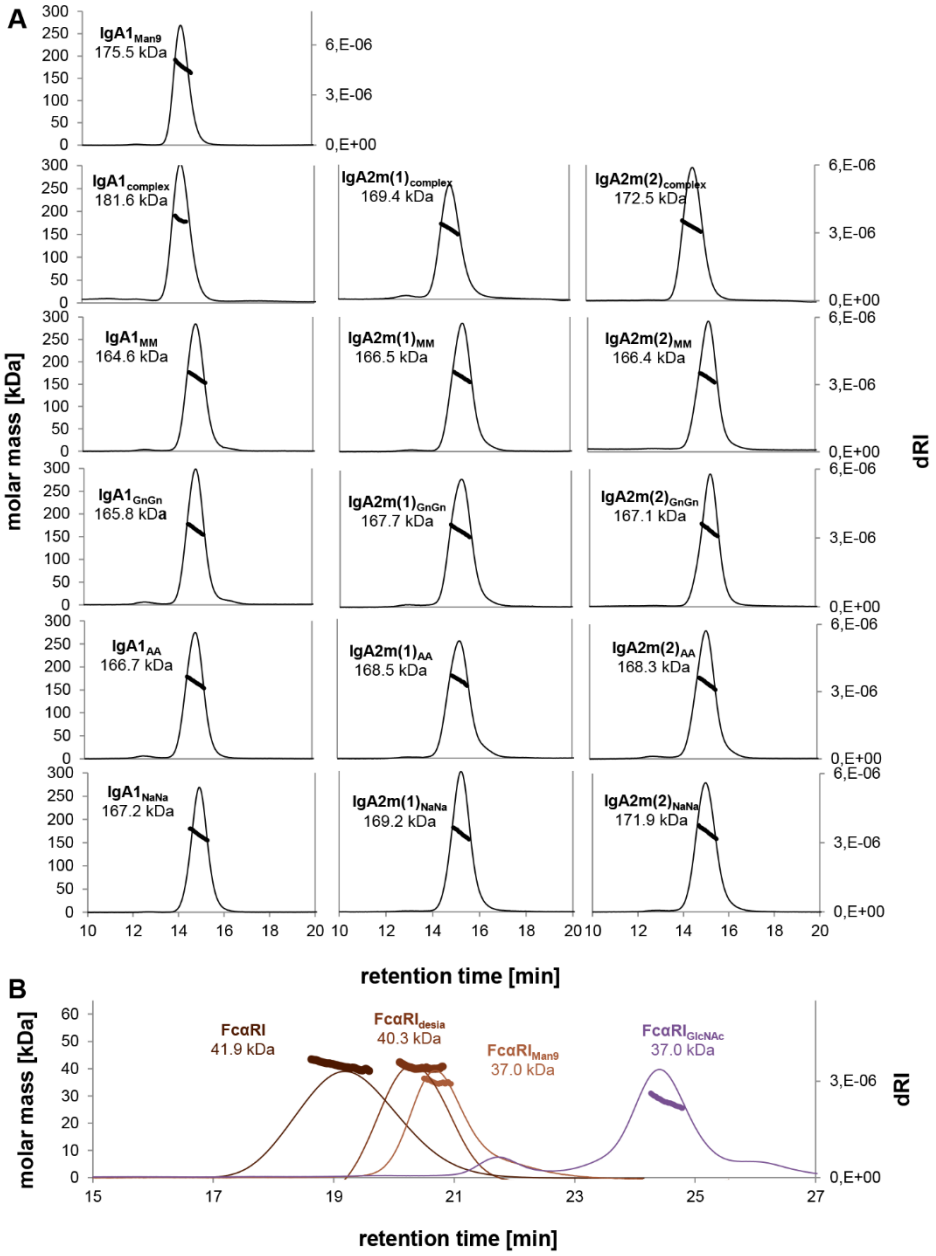

Figure S3. Representative SE-HPLC-MALS measurements of each IgA (A) and FcαRI (B) variant to determine the molar mass in solution.

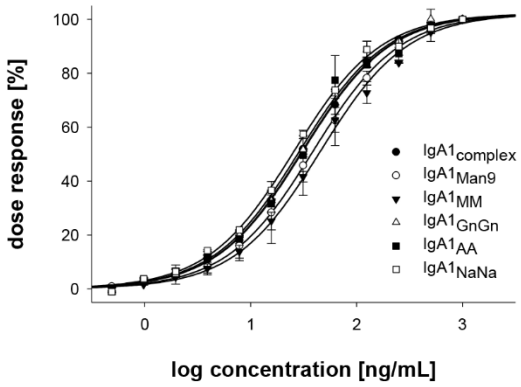

	$IgA1_{complex}$	$IgA1_{Man9}$	$IgA1_{MM}$	$IgA1_{GnGn}$	$IgA1_{AA}$	$IgA1_{NaNa}$
EC_{50} [ng/mL]	30.9	38.9	45.7	28.8	30.2	25.11

Figure S4. Binding of different IgA1 glycoforms to HER2. Determination of EC_{50} values of IgA1glycoforms was determined by ELISA as reported in a previous study [18] and were calculated as global fit of three repetitions.

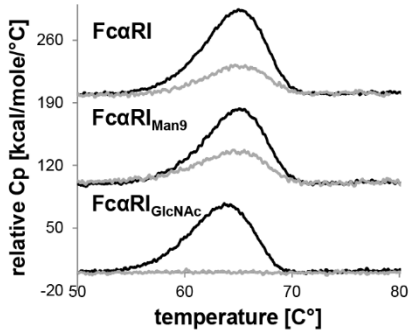

Figure S5. DSC (re-)scans of different FcαRI glycoforms. Bold lines show the raw date of DSC thermograms, whereas the thin lines are the rescan of each measurement.

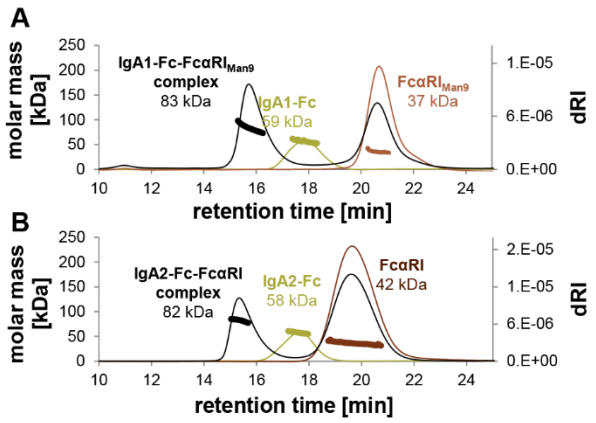

Figure S6. SE-HPLC-MALS to determine the mass of IgA-Fc-FcαRI complexes. (A) Overlay of the elution profile of IgA1-Fc (green), FcαRI$_{Man9}$ (light brown) and a mixture of IgA1-Fc and FcαRI$_{Man9}$ in a ratio of 1:4 (black). (B) Overlay of the elution profile of IgA2-Fc (green), FcαRI (brown) and a mixture of IgA1-Fc and FcαRI in a ratio of 1:4 (black). Note that the depicted molar masses are derived from MALS measurements and thus do not exactly match the exact molar masses.

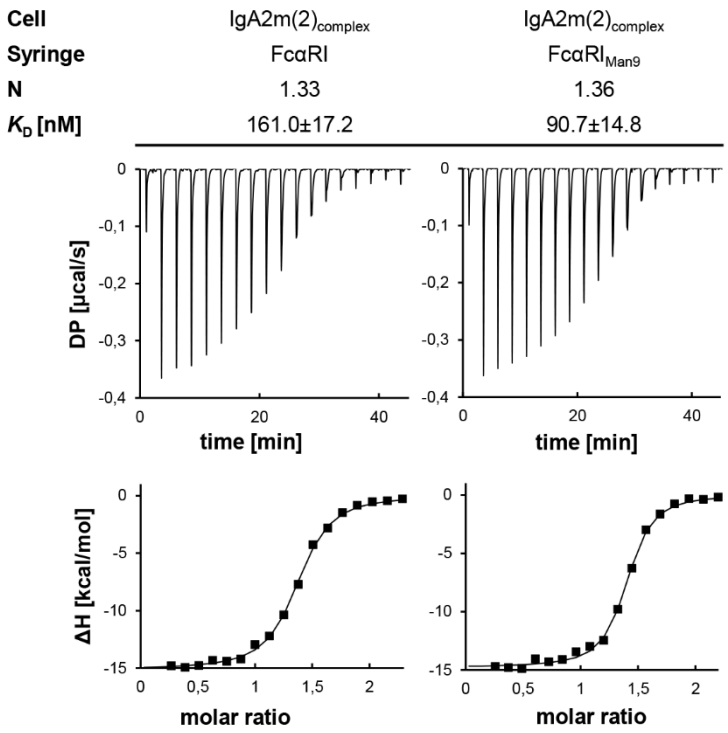

Figure S7. ITC measurements of IgA2m(2)$_{complex}$ with FcαRI and FcαRI$_{Man9}$. The upper panels show the raw data representing the response to 19 injections at 25°C and the lower panels the integrated data.

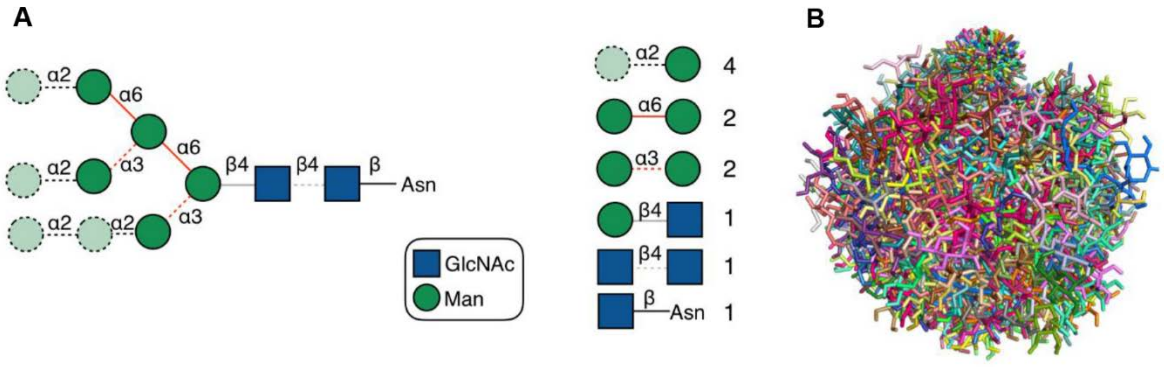

Figure S8. Generation of M9 distinct rotamer library. Using previously built local elevation potentials for each linkage, local elevation with umbrella sampling simulations (LEUS) were performed. For the M9 oligomannosidic (total 10+N linkages) N-glycan 6 different potentials were used; α-D-Man-(1→2)- α-D-Man (at 4 linkages); α-D-Man-(1→6)- α-D-Man (at 2 linkages); α-D-Man-(1→3)- α-D-Man(at 2 linkages); α-D-Man-(1→4)-β-D-GlcNAc (at 1 linkage); β-D-GlcNAc-(1→4)-β-D-GlcNAc (at 1 linkage) and β-D-GlcNAc→N (at 1 linkage). The adaptiveness of the LEUS method allows the use of already built potentials to different locations, which have the same linkage composition. (A) Composition of the M9 N-glycan is drawn with emphasized distinct linkages. On the right, distinct disaccharide linkages which were used in the generation of the local elevation potentials are depicted with number of their occurrence in the M9 glycan used in this study. (B) M9 high-mannose motion library is represented by different colors for each conformation (only 300 snapshots out of 1 million are shown here).

Table S1. Transition midpoint temperatures of the CH2 (T_m1), Fab (T_m2) and CH3 (T_m3) domains of IgA1, IgA2m(1) and IgA2m(2) glycoforms obtained from differential scanning calorimetry (DSC).

	T_m1 [°C]			T_m2 [°C]			T_m3 [°C]		
IgA1$_{complex}$	71.51	±	0.06	74.15	±	0.04	76.31	±	0.05
IgA1$_{Man}$	70.82	±	0.16	73.64	±	0.13	76.00	±	0.09
IgA1$_{MM}$	68.38	±	0.00	72.98	±	0.01	75.43	±	0.02
IgA1$_{GnGn}$	68.83	±	0.16	73.10	±	0.06	75.55	±	0.05
IgA1$_{AA}$	69.27	±	0.25	73.26	±	0.07	75.67	±	0.04
IgA1$_{NaNa}$	69.48	±	0.10	73.33	±	0.02	75.66	±	0.03
IgA2m(1)$_{complex}$	67.91	±	0.16	71.95	±	0.02	78.28	±	0.07
IgA2m(1)$_{MM}$	63.50	±	0.12	70.63	±	0.00	78.44	±	0.02
IgA2m(1)$_{GnGn}$	63.72	±	0.17	70.58	±	0.01	78.36	±	0.02
IgA2m(1)$_{AA}$	64.60	±	0.09	70.68	±	0.00	78.46	±	0.01
IgA2m(1)$_{NaNa}$	64.37	±	0.12	70.73	±	0.00	78.65	±	0.02
IgA2m(2)$_{complex}$	73.30	±	0.11	76.30	±	0.06	78.90	±	0.05
IgA2m(2)$_{MM}$	69.90	±	0.01	74.00	±	0.07	77.70	±	0.04
IgA2m(2)$_{GnGn}$	70.00	±	0.11	74.20	±	0.05	78.00	±	0.04
IgA2m(2)$_{AA}$	71.60	±	0.20	74.70	±	0.08	77.90	±	0.06
IgA2m(2)$_{NaNa}$	71.90	±	0.16	75.30	±	0.07	78.30	±	0.06

Table S2. Kinetic parameters for selected FcαRI IgA pairs. Rate constants are an average of four independent SPR experiments at 5 different concentrations.

ligand	analyte	k_{on} [(M s)$^{-1}$]			k_{off} [s^{-1}]			K_D [nM]		
IgA1$_{MM}$	FcαRI	3.5 x 10^5	±	1.0 x 10^5	0.07	±	0.01	187.43	±	3.41
IgA1$_{NaNa}$	FcαRI	5.2. x 10^5	±	4.2 x 10^4	0.07	±	0.01	149.26	±	1.68
IgA2m(1)$_{MM}$	FcαRI	4.0 x 10^5	±	7.6 x 10^4	0.07	±	0.01	187.76	±	7.24
IgA2m(1)$_{NaNa}$	FcαRI	3.9 x 10^5	±	2.5 x 10^4	0.06	±	0.01	172.53	±	5.07
IgA2m(2)$_{MM}$	FcαRI	2.8 x 10^5	±	9.9 x 103	0.06	±	0.00	225.29	±	8.54
IgA2m(2)$_{NaNa}$	FcαRI	3.0 x 10^5	±	3.8 x 10^4	0.06	±	0.00	205.74	±	2.56
IgA1$_{MM}$	FcαRI$_{GlcNAc}$	1.9 x 10^6	±	2.7 x 10^5	0.05	±	0.00	25.24	±	0.97
IgA1$_{NaNa}$	FcαRI$_{GlcNAc}$	2.3 x 10^6	±	6.1 x 10^5	0.06	±	0.01	25.76	±	1.22
IgA2m(1)$_{MM}$	FcαRI$_{GlcNAc}$	1.6 x 10^6	±	2.2 x 10^5	0.04	±	0.00	26.31	±	0.95
IgA2m(1)$_{NaNa}$	FcαRI$_{GlcNAc}$	1.7 x 10^6	±	2.2 x 10^5	0.04	±	0.00	24.20	±	0.93
IgA2m(2)$_{MM}$	FcαRI$_{GlcNAc}$	1.2 x 10^6	±	7.9 x 10^4	0.03	±	0.00	26.20	±	0.26
IgA2m(2)$_{NaNa}$	FcαRI$_{GlcNAc}$	1.3 x 10^6	±	1.4 x 10^5	0.03	±	0.00	25.22	±	0.76

CONCLUSION AND OUTLOOK

This work focused on the establishment of a robust plant-based expression system for distinct IgA glycoforms in order to systematically evaluate the impact of glycosylation on structure-function relationships of monomeric IgA1 and IgA2 antibodies and to elucidate the role of glycosylation in the IgA-FcαRI interaction. To study the influence of distinct glycosylation modifications on the biophysical and immunological properties, homogeneously glycosylated IgA is required. However, conventional mammalian expression systems typically do not address the problem of producing a vast mixture of glycoforms and are difficult to engineer towards desired glycosylation [88]. In that terms, plants such as *N. benthamiana* emerged as a promising platform to produce recombinant glycoproteins with tailored *N*- and *O*-glycans [87, 89]. Like animal cell lines, they are able to efficiently produce complex proteins and have a comparably simple *N*-glycosylation pathway, but a typical mammalian *O*-glycosylation pathway is not present at all [90, 91]. However, plants are relatively tolerant to glyco-engineering towards human-like structures. The capacity of plants to tolerate the deletion of plant-specific and the introduction of whole mammalian glycosylation pathways to obtain proteins with distinct homogeneous *N*- and *O*-glycans in sufficient amounts made this system desirable over chemical and enzymatic approaches, which are cost and labor intensive and have small yields [92-95].

In a first step, robust expression and purification of monomeric IgA1, IgA2m(1) and IgA2m(2) variants of the clinical antibody trastuzumab in *N. benthamiana* ΔXT/FT was established and the ability of plants to produce functional, well-folded, high-quality protein was assessed. Therefore, all IgA isotypes were additionally produced in human embryonic kidney 293 cells (HEK293) to compare the plant-based with a well-established mammalian-based system. Thereby, both production systems provided comparable yields of recombinant IgAs in a very short time scale. Thorough biochemical, biophysical and functional investigation showed no differences in assembly, integrity and functionality in terms of antigen binding. Thus, it can be assumed that plants are a suitable production platform for glycoproteins that are subjected to structure-function analysis and that any plant-derived effects can be excluded.

Next, the glycosylation status of the different IgA isotypes from plants and HEK293 cells was determined. For glycan structure-function studies as well as for glyco-engineering the information about site-specific *N*-glycosylation is absolutely essential, since site-specific variances can play important functional roles. Therefore, the IgA variants were digested with

trypsin and subjected to LC-ESI-MS for glycopeptide analysis. Surprisingly, the glycosylation efficiency was essentially the same in both systems with an almost complete occupancy with *N*-glycans on all sites of IgA except the one in the C-terminal tailpiece. This finding was astonishing, as there are differences in the composition of the oligosaccharyltransferase (OST) complex that transfers oligosaccharides onto the emerging protein in plants and mammalian cells and site occupancy can vary in different expression systems [96]. The incomplete glycosylation of the C-terminal tailpiece is likely mediated by inefficient posttranslational glycosylation of a distinct catalytic subunit of OST [97]. However, in plants it is possible to overcome this limitation by co-expressing LmSTT3D, a single subunit oligosaccharyltransferase from the protozoan *Leishmania major* (see Appendix I) [98].

While both systems were similar in glycosylation efficiency, they differed tremendously in terms of heterogeneity of attached glycans. Due to the limited *N*-glycan processing repertoire in the Golgi, the glycan diversity found on plant-produced recombinant IgAs was clearly reduced. If mammalian glycosylation enzymes are not co-expressed, plants lack tri- and tetra-antennary structures, bisecting GlcNAc, and capping with sialic acid which can all be detected on the HEK293-derived IgA resulting in increased heterogeneity. The site-specific analysis further revealed major differences between the individual *N*-glycosylation sites of each IgA subtype. These distinct features are conserved among the different IgA subtypes and expression systems, although their glycosylation repertoire is very different. The most pronounced difference was the complete lack of core-fucose in the C_H2-resident *N*-glycosylation site in all IgA isotypes. This information would have been lost if the glycans were released from the protein for subsequent analysis and highlights the importance of the more challenging approach of site-specific glycan-analysis.

Compared to the role of the Fc glycosylation of IgG, surprisingly little is known about the role of certain *N*-glycans for the interaction of other antibody subclasses on their structure and interaction with cellular receptors. Therefore, we next aimed to generate distinct IgA1, IgA2m(1) and IgA2m(2) glycoforms which are common in human serum to systematically assess the contribution of glycosylation on biophysical and biochemical properties such as conformational and thermal stability as well as Fc alpha receptor binding.

With the strategy of transiently co-expressing the respective mammalian glycosylation pathways in plants it was possible to generate IgA with the desired glycoform being the most abundant one by a large margin. First, the biophysical properties were investigated, and it was shown that different glycosylation variants of IgA did not differ in their overall conformational integrity and stability as well as antigen binding. However, differential scanning calorimetry

(DSC) experiments showed that although the different glycoforms have identical amino acid sequences they displayed altered thermal stability. We hence concluded that the observed shift in the unfolding temperatures of the different IgA glycoforms might result from the altered glycosylation. The obtained endotherms were fitted as three independent transitions displaying the independent unfolding of the Fab arms, the C_H2 domain and the C_H3 domain as described for IgG. Comparable DSC data for IgA is not available yet. Therefore, in a future study the endotherms for single domain constructs of IgA must be elucidated to verify correct assignment of the deconvoluted peaks to the respective domains.

The role of IgA *N*-glycosylation for the binding to FcαRI was addressed in several studies but remained controversial [11, 99-102]. This might be attributed to the use of serum IgA or recombinant IgA produced in mammalian cells bearing rather heterogenous glycosylation. With our set of homogeneous IgA1, IgA2m(1) and IgA2m(2) glycoforms we wanted to resolve this controversy. Furthermore, the crystal structure of the IgA1-FcαRI complex showed that the receptor glycan at position N58 comes into proximity of the interaction surface. Hence, also receptor glycans could influence binding via carbohydrate-protein or carbohydrate-carbohydrate interaction as it has been described for IgG and FcγRIIIa [15, 48]. In the previous studies FcαRI produced in insect cells has been used, which doesn't display human-like glycosylation. To also account for receptor glycosylation, we generated four different FcαRI glycoforms in HEK293 cells and systematically tested binding of all IgA variants using surface plasmon resonance spectroscopy. Thereby, it was shown that antibody glycosylation only had a subtle influence while the receptor glycans tremendously affected binding. Supported by our molecular model we hypothesized that the differences most likely result from either sterical hindrance by the receptor glycans, different surface charge of the latter or subtle conformational changes observed in circular dichroism spectroscopy in the receptor variant carrying single GlcNAc residues. Considering the high variability of the FcαRI glycosylation status in different cell types [10, 34, 35], receptor glycans could be a tool to modulate immune responses. However, little is known about the exact nature of receptor glycosylation, due to the limited access to receptor from native sources. As an alternative, receptor from cultured neutrophilic or monocytic cell lines which express FcαRI upon stimulation [103-105] could be isolated for subsequent site-specific glycan analysis.

Unexpectedly, we observed a discrepancy in the binding stoichiometry of IgA to FcαRI. In previous studies an IgA-FcαRI stoichiometry of 1:2 was postulated based on the crystal structure and ultra-centrifugation studies of an IgA-Fc construct lacking the tailpiece in

complex with the extra-cellular domain of FcαRI [16, 42]. Here, we tested binding of a full-length IgA to the receptor using three independent methods including SPR, SEC-HPLC-MALS and isothermal titration calorimetry. We suggest that the discrepancy in the stoichiometry could arise from the lack of the tailpiece in the previous studies, which was supported by our molecular model. This model suggests that the tailpiece can exist in different conformations allowing binding of a second FcαRI molecule only if a suitable condition is met. Understanding the mode of the IgA-FcαRI interaction is crucial since it was postulated that very contrary downstream signalling pathways can be triggered upon binding of monomeric IgA or IgA immune complexes to FcαRI expressed on effector cells based on the 1:2 binding model [42, 106]. Therefore, a re-evaluation of the postulated pathways should be considered. Furthermore, our anti-HER2 binding IgA could be used to generate native IgA-antigen immune complexes for signalling studies rather than heat-aggregated IgA and other FcαRI cross-linking mAbs [103, 107-110].

Taken together, in this work we identified distinct glycosylation features of IgA1, IgA2m(1) and IgA2m(2) produced in *N. benthamiana* and HEK293 cells. We were able to demonstrate that *N. benthamiana* is a suitable production host for complex glycoproteins with homogeneous glycosylation and generated distinct anti-HER2 IgA1, IgA2m(1) and IgA2m(2) *N*-glycosylation variants to systematically test the influence of glycosylation on structure-function relationships. Thereby, we were able to show that IgA glycans influence thermal stability, that not IgA but FcαRI glycosylation influences the antibody receptor interaction and that the stoichiometry of interaction is different to the previously postulated one. This system could be further used to investigate glycosylation dependent binding to other more recently identified IgA receptors such as FcRL4, activation of the complement system or other properties such as serum half-life.

REFERENCES

1. Woof, J.M. and M.A. Kerr, *The function of immunoglobulin A in immunity.* J Pathol, 2006. **208**(2): p. 270-82.
2. Woof, J.M. and M.W. Russell, *Structure and function relationships in IgA.* Mucosal Immunology, 2011. **4**(6): p. 590-597.
3. Bonner, A., et al., *Implications of the near-planar solution structure of human myeloma dimeric IgA1 for mucosal immunity and IgA nephropathy.* J Immunol, 2008. **180**(2): p. 1008-18.
4. Mattu, T.S., et al., *The glycosylation and structure of human serum IgA1, Fab, and Fc regions and the role of N-glycosylation on Fcalpha receptor interactions.* J Biol Chem, 1998. **273**(4): p. 2260-72.
5. Royle, L., et al., *Secretory IgA N- and O-glycans provide a link between the innate and adaptive immune systems.* J Biol Chem, 2003. **278**(22): p. 20140-53.
6. Huang, J., et al., *Site-specific glycosylation of secretory immunoglobulin A from human colostrum.* J Proteome Res, 2015. **14**(3): p. 1335-49.
7. Dicker, M., D. Maresch, and R. Strasser, *Glyco-engineering for the production of recombinant IgA1 with distinct mucin-type O-glycans in plants.* Bioengineered, 2016. **7**(6): p. 484-489.
8. Narimatsu, Y., et al., *Effect of Glycosylation on Cis/Trans Isomerization of Prolines in IgA1-Hinge Peptide.* Journal of the American Chemical Society, 2010. **132**(16): p. 5548-5549.
9. Breedveld, A. and M. van Egmond, *IgA and FcalphaRI: Pathological Roles and Therapeutic Opportunities.* Front Immunol, 2019. **10**: p. 553.
10. van Egmond, M., et al., *IgA and the IgA Fc receptor.* Trends in Immunology, 2001. **22**(4): p. 205-211.
11. Gomes, M.M., et al., *Analysis of IgA1 N-glycosylation and its contribution to FcalphaRI binding.* Biochemistry, 2008. **47**(43): p. 11285-99.
12. Yoo, E.M., et al., *Differences in N-glycan structures foundon recombinant IgA1 and IgA2 producedin murine myeloma and CHO cell lines*, in *MAbs*. 2010. p. 320-34.
13. Oortwijn, B.D., et al., *Differential glycosylation of polymeric and monomeric IgA: a possible role in glomerular inflammation in IgA nephropathy.* J Am Soc Nephrol, 2006. **17**(12): p. 3529-39.
14. Field, M.C., et al., *Structural analysis of the N-glycans from human immunoglobulin A1: comparison of normal human serum immunoglobulin A1 with that isolated from patients with rheumatoid arthritis.* Biochem J, 1994. **299 (Pt 1)**: p. 261-75.
15. Ferrara, C., et al., *Unique carbohydrate-carbohydrate interactions are required for high affinity binding between FcgammaRIII and antibodies lacking core fucose.* Proc Natl Acad Sci U S A, 2011. **108**(31): p. 12669-74.
16. Herr, A.B., E.R. Ballister, and P.J. Bjorkman, *Insights into IgA-mediated immune responses from the crystal structures of human FcalphaRI and its complex with IgA1-Fc.* Nature, 2003. **423**(6940): p. 614-20.
17. Arnold, J.N., et al., *The Glycosylation of Human Serum IgD and IgE and the Accessibility of Identified Oligomannose Structures for Interaction with Mannan-Binding Lectin.* The Journal of Immunology, 2004. **173**(11): p. 6831.
18. Borrok, M.J., et al., *Revisiting the role of glycosylation in the structure of human IgG Fc.* ACS Chem Biol, 2012. **7**(9): p. 1596-602.
19. Mimura, Y., et al., *The influence of glycosylation on the thermal stability and effector function expression of human IgG1-Fc: properties of a series of truncated glycoforms.* Mol Immunol, 2000. **37**(12-13): p. 697-706.
20. Rouwendal, G.J., et al., *A comparison of anti-HER2 IgA and IgG1 in vivo efficacy is facilitated by high N-glycan sialylation of the IgA.* MAbs, 2015: p. 0.
21. Maurer, M.A., et al., *Glycosylation of Human IgA Directly Inhibits Influenza A and Other Sialic-Acid-Binding Viruses.* Cell Rep, 2018. **23**(1): p. 90-99.

22. Wines, B.D. and P.M. Hogarth, *IgA receptors in health and disease.* Tissue Antigens, 2006. **68**(2): p. 103-14.
23. Atkin, J.D., et al., *Mutagenesis of the human IgA1 heavy chain tailpiece that prevents dimer assembly.* J Immunol, 1996. **157**(1): p. 156-9.
24. Yoo, E.M., et al., *Structural requirements for polymeric immunoglobulin assembly and association with J chain.* J Biol Chem, 1999. **274**(47): p. 33771-7.
25. Krugmann, S., et al., *Structural requirements for assembly of dimeric IgA probed by site-directed mutagenesis of J chain and a cysteine residue of the alpha-chain CH2 domain.* J Immunol, 1997. **159**(1): p. 244-9.
26. Johansen, F.E., R. Braathen, and P. Brandtzaeg, *The J chain is essential for polymeric Ig receptor-mediated epithelial transport of IgA.* J Immunol, 2001. **167**(9): p. 5185-92.
27. Mostov, K.E., M. Friedlander, and G. Blobel, *The receptor for transepithelial transport of IgA and IgM contains multiple immunoglobulin-like domains.* Nature, 1984. **308**(5954): p. 37-43.
28. Brandtzaeg, P., *Secretory IgA: Designed for Anti-Microbial Defense.* Front Immunol, 2013. **4**: p. 222.
29. Aleyd, E., M.H. Heineke, and M. van Egmond, *The era of the immunoglobulin A Fc receptor FcalphaRI; its function and potential as target in disease.* Immunol Rev, 2015. **268**(1): p. 123-38.
30. Monteiro, R.C., H. Kubagawa, and M.D. Cooper, *Cellular distribution, regulation, and biochemical nature of an Fc alpha receptor in humans.* J Exp Med, 1990. **171**(3): p. 597-613.
31. van Egmond, M., et al., *FcalphaRI-positive liver Kupffer cells: reappraisal of the function of immunoglobulin A in immunity.* Nat Med, 2000. **6**(6): p. 680-5.
32. Mkaddem, S.B., et al., *IgA, IgA receptors, and their anti-inflammatory properties.* Curr Top Microbiol Immunol, 2014. **382**: p. 221-35.
33. de Wit, T.P., et al., *Structure of the gene for the human myeloid IgA Fc receptor (CD89).* J Immunol, 1995. **155**(3): p. 1203-9.
34. Geissmann, F., et al., *A subset of human dendritic cells expresses IgA Fc receptor (CD89), which mediates internalization and activation upon cross-linking by IgA complexes.* J Immunol, 2001. **166**(1): p. 346-52.
35. Morton, H.C., et al., *Alternatively spliced forms of the human myeloid Fc alpha receptor (CD89) in neutrophils.* Immunogenetics, 1996. **43**(4): p. 246-7.
36. Shields, R.L., et al., *High Resolution Mapping of the Binding Site on Human IgG1 for FcγRI, FcγRII, FcγRIII, and FcRn and Design of IgG1 Variants with Improved Binding to the FcγR.* Journal of Biological Chemistry, 2001. **276**(9): p. 6591-6604.
37. Woof, J.M. and D.R. Burton, *Human antibody-Fc receptor interactions illuminated by crystal structures.* Nat Rev Immunol, 2004. **4**(2): p. 89-99.
38. Oortwijn, B.D., et al., *Monomeric and polymeric IgA show a similar association with the myeloid FcalphaRI/CD89.* Mol Immunol, 2007. **44**(5): p. 966-73.
39. Bakema, J.E., et al., *Inside-out regulation of Fc alpha RI (CD89) depends on PP2A.* J Immunol, 2008. **181**(6): p. 4080-8.
40. Bracke, M., et al., *Cytokine-induced inside-out activation of FcalphaR (CD89) is mediated by a single serine residue (S263) in the intracellular domain of the receptor.* Blood, 2001. **97**(11): p. 3478-83.
41. Ginsberg, M.H., A. Partridge, and S.J. Shattil, *Integrin regulation.* Curr Opin Cell Biol, 2005. **17**(5): p. 509-16.
42. Herr, A.B., et al., *Bivalent binding of IgA1 to FcalphaRI suggests a mechanism for cytokine activation of IgA phagocytosis.* J Mol Biol, 2003. **327**(3): p. 645-57.
43. Liu, J., J. Ruppel, and S.J. Shire, *Interaction of human IgE with soluble forms of IgE high affinity receptors.* Pharm Res, 1997. **14**(10): p. 1388-93.
44. Hansen, I.S., D.L.P. Baeten, and J. den Dunnen, *The inflammatory function of human IgA.* Cell Mol Life Sci, 2019. **76**(6): p. 1041-1055.
45. Wines, B.D., et al., *Identification of residues in the first domain of human Fc alpha receptor essential for interaction with IgA.* J Immunol, 1999. **162**(4): p. 2146-53.

46. Wines, B.D., et al., *The interaction of Fc alpha RI with IgA and its implications for ligand binding by immunoreceptors of the leukocyte receptor cluster.* J Immunol, 2001. **166**(3): p. 1781-9.
47. Xue, J., et al., *Deglycosylation of FcalphaR at N58 increases its binding to IgA.* Glycobiology, 2010. **20**(7): p. 905-15.
48. Patel, K.R., et al., *Restricted processing of CD16a/Fc gamma receptor IIIa N-glycans from primary human NK cells impacts structure and function.* J Biol Chem, 2018. **293**(10): p. 3477-3489.
49. van Egmond, M., et al., *Human immunoglobulin A receptor (FcalphaRI, CD89) function in transgenic mice requires both FcR gamma chain and CR3 (CD11b/CD18).* Blood, 1999. **93**(12): p. 4387-94.
50. Morton, H.C., et al., *Functional association between the human myeloid immunoglobulin A Fc receptor (CD89) and FcR gamma chain. Molecular basis for CD89/FcR gamma chain association.* J Biol Chem, 1995. **270**(50): p. 29781-7.
51. Shen, L., et al., *Presentation of ovalbumin internalized via the immunoglobulin-A Fc receptor is enhanced through Fc receptor gamma-chain signaling.* Blood, 2001. **97**(1): p. 205-13.
52. Honorio-Franca, A.C., et al., *Colostral neutrophils express Fc alpha receptors (CD89) lacking gamma chain association and mediate noninflammatory properties of secretory IgA.* J Leukoc Biol, 2001. **69**(2): p. 289-96.
53. Nimmerjahn, F. and J.V. Ravetch, *Fcgamma receptors: old friends and new family members.* Immunity, 2006. **24**(1): p. 19-28.
54. Braathen, R., et al., *The carboxyl-terminal domains of IgA and IgM direct isotype-specific polymerization and interaction with the polymeric immunoglobulin receptor.* J Biol Chem, 2002. **277**(45): p. 42755-62.
55. White, K.D. and J.D. Capra, *Targeting mucosal sites by polymeric immunoglobulin receptor-directed peptides.* J Exp Med, 2002. **196**(4): p. 551-5.
56. Almogren, A., B.W. Senior, and M.A. Kerr, *A comparison of the binding of secretory component to immunoglobulin A (IgA) in human colostral S-IgA1 and S-IgA2.* Immunology, 2007. **120**(2): p. 273-80.
57. Bakos, M.A., et al., *Probing the topography of free and polymeric Ig-bound human secretory component with monoclonal antibodies.* J Immunol, 1991. **146**(1): p. 162-8.
58. Luton, F., et al., *Identification of a cytoplasmic signal for apical transcytosis.* Traffic, 2009. **10**(8): p. 1128-42.
59. Kaetzel, C.S., *The polymeric immunoglobulin receptor: bridging innate and adaptive immune responses at mucosal surfaces.* Immunol Rev, 2005. **206**: p. 83-99.
60. Corthesy, B., *Multi-faceted functions of secretory IgA at mucosal surfaces.* Front Immunol, 2013. **4**: p. 185.
61. van Spriel, A.B., et al., *Mac-1 (CD11b/CD18) is essential for Fc receptor-mediated neutrophil cytotoxicity and immunologic synapse formation.* Blood, 2001. **97**(8): p. 2478-86.
62. Moura, I.C., et al., *Identification of the transferrin receptor as a novel immunoglobulin (Ig)A1 receptor and its enhanced expression on mesangial cells in IgA nephropathy.* J Exp Med, 2001. **194**(4): p. 417-25.
63. Matysiak-Budnik, T., et al., *Secretory IgA mediates retrotranscytosis of intact gliadin peptides via the transferrin receptor in celiac disease.* The Journal of experimental medicine, 2008. **205**(1): p. 143-154.
64. Rochereau, N., et al., *Dectin-1 is essential for reverse transcytosis of glycosylated SIgA-antigen complexes by intestinal M cells.* PLoS Biol, 2013. **11**(9): p. e1001658.
65. Baumann, J., C.G. Park, and N.J. Mantis, *Recognition of secretory IgA by DC-SIGN: implications for immune surveillance in the intestine.* Immunology letters, 2010. **131**(1): p. 59-66.
66. Wilson, T.J., A. Fuchs, and M. Colonna, *Cutting edge: human FcRL4 and FcRL5 are receptors for IgA and IgG.* J Immunol, 2012. **188**(10): p. 4741-5.
67. Davis, R.S., *FCRL regulation in innate-like B cells.* Ann N Y Acad Sci, 2015. **1362**: p. 110-6.
68. Amara, K., et al., *B cells expressing the IgA receptor FcRL4 participate in the autoimmune response in patients with rheumatoid arthritis.* J Autoimmun, 2017. **81**: p. 34-43.

69. Rifai, A., et al., *The N-glycans determine the differential blood clearance and hepatic uptake of human immunoglobulin (Ig)A1 and IgA2 isotypes.* J Exp Med, 2000. **191**(12): p. 2171-82.
70. Shibuya, A. and S. Honda, *Molecular and functional characteristics of the Fcalpha/muR, a novel Fc receptor for IgM and IgA.* Springer Semin Immunopathol, 2006. **28**(4): p. 377-82.
71. Kikuno, K., et al., *Unusual biochemical features and follicular dendritic cell expression of human Fcalpha/mu receptor.* Eur J Immunol, 2007. **37**(12): p. 3540-50.
72. Wang, R., et al., *Human Fcalpha/muR and pIgR distribute differently in intestinal tissues.* Biochem Biophys Res Commun, 2009. **381**(2): p. 148-52.
73. Hamburger, A.E., A.P. West, Jr., and P.J. Bjorkman, *Crystal structure of a polymeric immunoglobulin binding fragment of the human polymeric immunoglobulin receptor.* Structure, 2004. **12**(11): p. 1925-35.
74. Yoo, E.M., et al., *Characterization of IgA and IgM binding and internalization by surface-expressed human Fcalpha/mu receptor.* Mol Immunol, 2011. **48**(15-16): p. 1818-26.
75. Ghumra, A., et al., *Structural requirements for the interaction of human IgM and IgA with the human Fcalpha/mu receptor.* Eur J Immunol, 2009. **39**(4): p. 1147-56.
76. Mantis, N.J., N. Rol, and B. Corthésy, *Secretory IgA's complex roles in immunity and mucosal homeostasis in the gut.* Mucosal Immunology, 2011. **4**(6): p. 603-611.
77. Kadaoui, K.A. and B. Corthesy, *Secretory IgA mediates bacterial translocation to dendritic cells in mouse Peyer's patches with restriction to mucosal compartment.* J Immunol, 2007. **179**(11): p. 7751-7.
78. Yan, H., et al., *Multiple functions of immunoglobulin A in mucosal defense against viruses: an in vitro measles virus model.* J Virol, 2002. **76**(21): p. 10972-9.
79. Wright, A., M.E. Lamm, and Y.T. Huang, *Excretion of human immunodeficiency virus type 1 through polarized epithelium by immunoglobulin A.* J Virol, 2008. **82**(23): p. 11526-35.
80. Heineke, M.H., et al., *Peptide mimetics of immunoglobulin A (IgA) and FcalphaRI block IgA-induced human neutrophil activation and migration.* Eur J Immunol, 2017. **47**(10): p. 1835-1845.
81. van der Steen, L., et al., *Immunoglobulin A: Fc(alpha)RI interactions induce neutrophil migration through release of leukotriene B4.* Gastroenterology, 2009. **137**(6): p. 2018-29.e1-3.
82. Ben Mkaddem, S., et al., *Anti-inflammatory role of the IgA Fc receptor (CD89): from autoimmunity to therapeutic perspectives.* Autoimmun Rev, 2013. **12**(6): p. 666-9.
83. Bakema, J.E. and M. van Egmond, *The human immunoglobulin A Fc receptor FcalphaRI: a multifaceted regulator of mucosal immunity.* Mucosal Immunol, 2011. **4**(6): p. 612-24.
84. Boross, P., et al., *IgA EGFR antibodies mediate tumour killing in vivo.* EMBO Mol Med, 2013. **5**(8): p. 1213-26.
85. Lohse, S., et al., *An Anti-EGFR IgA That Displays Improved Pharmacokinetics and Myeloid Effector Cell Engagement In Vivo.* Cancer Res, 2016. **76**(2): p. 403-17.
86. Jefferis, R., J. Lund, and J.D. Pound, *IgG-Fc-mediated effector functions: molecular definition of interaction sites for effector ligands and the role of glycosylation.* Immunol Rev, 1998. **163**: p. 59-76.
87. Strasser, R., F. Altmann, and H. Steinkellner, *Controlled glycosylation of plant-produced recombinant proteins.* Curr Opin Biotechnol, 2014. **30**: p. 95-100.
88. Heffner, K.M., et al., *Glycoengineering of Mammalian Expression Systems on a Cellular Level.* Adv Biochem Eng Biotechnol, 2018.
89. Strasser, R., et al., *Generation of glyco-engineered Nicotiana benthamiana for the production of monoclonal antibodies with a homogeneous human-like N-glycan structure.* Plant Biotechnol J, 2008. **6**(4): p. 392-402.
90. Strasser, R., *Biological significance of complex N-glycans in plants and their impact on plant physiology.* Front Plant Sci, 2014. **5**: p. 363.
91. Karnoup, A.S., V. Turkelson, and W.H. Anderson, *O-linked glycosylation in maize-expressed human IgA1.* Glycobiology, 2005. **15**(10): p. 965-81.
92. Lin, C.-W., et al., *A common glycan structure on immunoglobulin G for enhancement of effector functions.* 2015.
93. Liu, L., Z.Y. Hong, and C.H. Wong, *Convergent glycopeptide synthesis by traceless Staudinger ligation and enzymatic coupling.* Chembiochem, 2006. **7**(3): p. 429-32.

94. Bennett, C.S., et al., *Sugar-assisted glycopeptide ligation with complex oligosaccharides: scope and limitations.* J Am Chem Soc, 2008. **130**(36): p. 11945-52.
95. Witte, K., et al., *Enzymatic Glycoprotein Synthesis: Preparation of Ribonuclease Glycoforms via Enzymatic Glycopeptide Condensation and Glycosylation.* Journal of the American Chemical Society, 1997. **119**(9): p. 2114-2118.
96. Strasser, R., *Plant protein glycosylation.* Glycobiology, 2016. **26**(9): p. 926-939.
97. Shrimal, S. and R. Gilmore, *Glycosylation of closely spaced acceptor sites in human glycoproteins.* J Cell Sci, 2013. **126**(Pt 23): p. 5513-23.
98. Castilho, A., et al., *An oligosaccharyltransferase from Leishmania major increases the N-glycan occupancy on recombinant glycoproteins produced in Nicotiana benthamiana.* Plant Biotechnol J, 2018. **16**(10): p. 1700-1709.
99. Mattu, T.S., et al., *The Glycosylation and Structure of Human Serum IgA1, Fab, and Fc Regions and the Role of N-Glycosylation on Fcα Receptor Interactions.* 1998.
100. Basset, C., et al., *Glycosylation of immunoglobulin A influences its receptor binding.* Scand J Immunol, 1999. **50**(6): p. 572-9.
101. Carayannopoulos, L., E.E. Max, and J.D. Capra, *Recombinant human IgA expressed in insect cells.* Proc Natl Acad Sci U S A, 1994. **91**(18): p. 8348-52.
102. Pleass, R.J., et al., *Identification of residues in the CH2/CH3 domain interface of IgA essential for interaction with the human fcalpha receptor (FcalphaR) CD89.* J Biol Chem, 1999. **274**(33): p. 23508-14.
103. van Zandbergen, G., et al., *Crosslinking of the human Fc receptor for IgA (FcalphaRI/CD89) triggers FcR gamma-chain-dependent shedding of soluble CD89.* J Immunol, 1999. **163**(11): p. 5806-12.
104. Yin, N., et al., *Intracellular pools of FcalphaR (CD89) in human neutrophils are localized in tertiary granules and secretory vesicles, and two FcalphaR isoforms are found in tertiary granules.* J Leukoc Biol, 2007. **82**(3): p. 551-8.
105. Sibille, Y., et al., *Fc alpha-receptor expression on the myelomonocytic cell line THP-1: comparison with human alveolar macrophages.* Eur Respir J, 1994. **7**(6): p. 1111-9.
106. Brandsma, A.M., et al., *Potent Fc receptor signaling by IgA leads to superior killing of cancer cells by neutrophils compared to IgG.* Front Immunol, 2019. **10**: p. 704.
107. Reterink, T.J., et al., *Size-dependent effect of IgA on the IgA Fc receptor (CD89).* Eur J Immunol, 1997. **27**(9): p. 2219-24.
108. Morton, H.C., et al., *Immunoglobulin-binding sites of human FcalphaRI (CD89) and bovine Fcgamma2R are located in their membrane-distal extracellular domains.* J Exp Med, 1999. **189**(11): p. 1715-22.
109. Diven, S.C., et al., *IgA induced activation of human mesangial cells: Independent of FcαR1 (CD 89).* Kidney International, 1998. **54**(3): p. 837-847.
110. Hostoffer, R.W., I. Krukovets, and M. Berger, *Increased Fc alpha R expression and IgA-mediated function on neutrophils induced by chemoattractants.* The Journal of Immunology, 1993. **150**(10): p. 4532.

APPENDIX I

An oligosaccharyltransferase from Leishmania major increases the N-glycan occupancy on recombinant glycoproteins produced in Nicotiana benthamiana

Castilho A, Beihammer G, Pfeiffer C, **Göritzer K**, Montero-Morales L, Vavra U, Maresch D, Grünwald-Gruber C, Altmann F, Steinkellner H, Strasser R

Research article

Plant Biotechnol J. 2018 Oct;16(10):1700-1709. doi: 10.1111/pbi.12906

Plant Biotechnology Journal

Plant Biotechnology Journal (2018) **16**, pp. 1700–1709 doi: 10.1111/pbi.12906

An oligosaccharyltransferase from *Leishmania major* increases the N-glycan occupancy on recombinant glycoproteins produced in *Nicotiana benthamiana*

Alexandra Castilho[1], Gernot Beihammer[1], Christina Pfeiffer[1], Kathrin Göritzer[1], Laura Montero-Morales[1], Ulrike Vavra[1], Daniel Maresch[2], Clemens Grünwald-Gruber[2], Friedrich Altmann[2], Herta Steinkellner[1] and Richard Strasser[1,*]

[1]*Department of Applied Genetics and Cell Biology, University of Natural Resources and Life Sciences, Vienna, Austria*
[2]*Department of Chemistry, University of Natural Resources and Life Sciences, Vienna, Austria*

Received 31 August 2017;
revised 15 December 2017;
accepted 6 February 2018.
*Correspondence (Tel 0043-1-47654-94145; fax 0043-1-47654-94009; email richard.strasser@boku.ac.at)

Keywords: glyco-engineering, N-glycosylation, *Nicotiana benthamiana*, oligosaccharyltransferase, plant-made pharmaceuticals.

Summary

N-glycosylation is critical for recombinant glycoprotein production as it influences the heterogeneity of products and affects their biological function. In most eukaryotes, the oligosaccharyltransferase is the central-protein complex facilitating the N-glycosylation of proteins in the lumen of the endoplasmic reticulum (ER). Not all potential N-glycosylation sites are recognized *in vivo* and the site occupancy can vary in different expression systems, resulting in underglycosylation of recombinant glycoproteins. To overcome this limitation in plants, we expressed LmSTT3D, a single-subunit oligosaccharyltransferase from the protozoan *Leishmania major* transiently in *Nicotiana benthamiana,* a well-established production platform for recombinant proteins. A fluorescent protein-tagged LmSTT3D variant was predominately found in the ER and co-located with plant oligosaccharyltransferase subunits. Co-expression of LmSTT3D with immunoglobulins and other recombinant human glycoproteins resulted in a substantially increased N-glycosylation site occupancy on all N-glycosylation sites except those that were already more than 90% occupied. Our results show that the heterologous expression of LmSTT3D is a versatile tool to increase N-glycosylation efficiency in plants.

Introduction

Asparagine (N)-linked glycosylation is a major co- and post-translational modification of proteins entering the secretory pathway. Many recombinant biopharmaceuticals for therapeutic use in humans are N-glycosylated, and distinct N-glycan structures play crucial roles for their *in vivo* efficacy (Jefferis, 2009; Zacchi and Schulz, 2016). Yet, the extent of N-glycan attachment to a distinct glycosylation site may vary greatly giving rise to the formation of incompletely glycosylated proteins with potentially unwanted characteristics. N-glycans are important for protein folding and protein stability and specifically modulate protein–protein interactions. For erythropoietin (EPO), it has been shown that the *in vivo* biological activity correlates with the number of N-linked glycans (Elliott *et al.*, 2004) and nonglycosylated monoclonal antibodies display reduced or complete loss of immune receptor binding (Nose and Wigzell, 1983; Walker *et al.*, 1989).

In all eukaryotes, a hallmark of N-glycosylation is the *en bloc* transfer of a common preassembled oligosaccharide ($Glc_3Man_9GlcNAc_2$) from the lipid carrier dolichol pyrophosphate to selected asparagine residues in the sequence Asn-X-Ser/Thr (X any amino acid except proline) of nascent polypeptides (Aebi, 2013; Zielinska *et al.*, 2010). The transfer of the oligosaccharide takes place in the lumen of the ER and is catalysed by the oligosaccharyltransferase (OST) complex. In yeast and mammals, OST is a multimeric membrane-bound protein complex (Kelleher and Gilmore, 2006) consisting of one catalytically active subunit (STT3) and several different noncatalytic subunits that contribute to N-glycosylation by regulation of the substrate specificity, stability or assembly of the complex (Knauer and Lehle, 1999; Mohorko *et al.*, 2011; Yan and Lennarz, 2002). The organization of the OST complex is more complex in metazoans than in yeast, and different subunit compositions have been described (Mohorko *et al.*, 2011; Roboti and High, 2012; Shibatani *et al.*, 2005). Mammals harbour two different catalytic STT3 isoforms (STT3A and STT3B) that are present in distinct OST complexes (Ruiz-Canada *et al.*, 2009; Shrimal *et al.*, 2013, 2015). The STT3A/STT3B-containing complexes have overlapping and isoform specific functions and differ in their catalytic activity and acceptor substrate selectivity. While STT3A is predominately involved in co-translational glycosylation, STT3B displays a preference for post-translational glycosylation. By contrast, some unicellular parasites like *Leishmania major* or *Trypanosoma brucei* have several STT3 copies, but lack other noncatalytic subunits of the yeast or mammalian OST complex (Kelleher and Gilmore, 2006; Samuelson *et al.*, 2005). These single-subunit OST enzymes display distinct protein acceptor and oligosaccharide donor specificities (Izquierdo *et al.*, 2009; Nasab *et al.*, 2008).

N-glycosylation in plants requires a similar heteromeric OST complex, which is still poorly described (Strasser, 2016). *Arabidopsis thaliana* has two catalytic subunits, termed STT3A and STT3B (Koiwa *et al.*, 2003). STT3A-deficient plants are viable, but display a protein underglycosylation defect that disturbs the biogenesis of different proteins including the heavily glycosylated pattern recognition receptor EF-TU RECEPTOR (EFR), the endo-β1,4-glucanase KORRIGAN1 (KOR1/RSW2) (Kang *et al.*, 2008) or

the myrosinase TGG1 (Koiwa *et al.*, 2003; Nekrasov *et al.*, 2009; Saijo *et al.*, 2009). Moreover, the *A. thaliana stt3a stt3b* double knockout mutant is gametophytic lethal (Koiwa *et al.*, 2003) highlighting the importance of the catalytic OST subunits for protein N-glycosylation in plants.

Plants are increasingly used as production hosts for recombinant human glycoproteins intended for therapeutic use. The majority of the approved recombinant biopharmaceuticals like monoclonal antibodies are glycoproteins and N-glycosylation modulates, for example, the IgG function by affecting the binding affinity to receptors on immune cells. In recent years, enormous efforts have been made to engineer plant-based expression hosts for the production of glycoproteins with targeted glycan profiles (Dicker *et al.*, 2016; Hanania *et al.*, 2017; Kallolimath *et al.*, 2016; Li *et al.*, 2016; Limkul *et al.*, 2016; Loos *et al.*, 2014; Mercx *et al.*, 2017; Strasser *et al.*, 2014). These advances reduced the variation of N-glycan structures on a given site (microheterogeneity) thereby contributing to product homogeneity and consistency. Besides a recent patent application (WO2014195011A1) little/no attempts have been made that address differences in N-glycosylation site occupancy on recombinant proteins (macroheterogeneity). Here, we present a strategy to overcome underglycosylation at N-glycosylation sites on different recombinant glycoproteins when transiently expressed in *N. benthamiana*. We found that the expression of the single-subunit oligosaccharyltransferase STT3D from *L. major* (LmSTT3D) substantially improves the N-glycosylation efficiency on different transiently expressed recombinant glycoproteins.

Results

Recombinant IgG and an Fc-fusion protein display considerable underglycosylation

Previous studies have shown that the single N-glycosylation site at position Asn297 from the heavy chain of different recombinant IgG molecules is frequently underglycosylated when transiently expressed in *N. benthamiana* (Bendandi *et al.*, 2010; Loos *et al.*, 2015; Strasser *et al.*, 2008; Zeitlin *et al.*, 2016) (Figure 1a). We expressed a monoclonal IgG antibody transiently in wild-type as well as in the glyco-engineered ΔXT/FT *N. benthamiana* line which is widely used as expression host for recombinant glycoproteins (Strasser *et al.*, 2008, 2014). LC-ESI-MS analysis of the proteolytically digested heavy chain showed the presence of considerable amounts of the unglycosylated peptide in both expression hosts (Figure 1b). To investigate this variation in N-glycosylation site occupancy more in detail and to better visualize the difference between glycosylated and nonglycosylated variants, we generated an expression construct where the Fc-domain from the IgG heavy chain lacking a variable region is fused to a signal peptide for targeting to the secretory pathway (SP-Fc). Upon SDS-PAGE under reducing conditions and subsequent immunoblotting, the expressed SP-Fc protein migrates at approximately 35 kDa and a faster migrating band at approximately 33 kDa is clearly detectable (Figure 1c). When digested with PNGase F which cleaves off the single N-glycan, the deglycosylated band co-

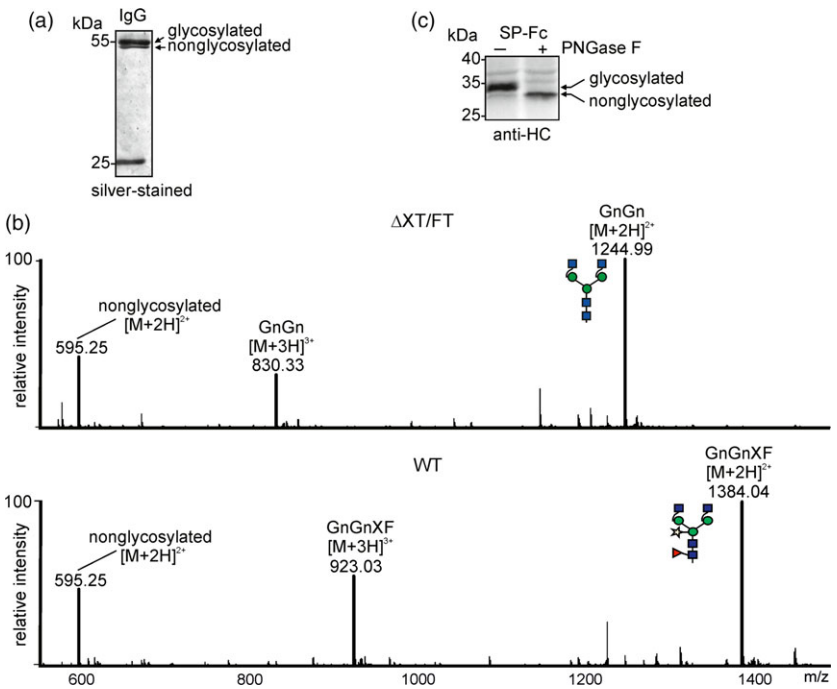

Figure 1 Underglycosylation is observed on transiently expressed IgG and on SP-Fc. (a) A monoclonal IgG antibody was transiently expressed in *N. benthamiana* wild-type plants. The IgG protein was purified 2 days after infiltration, separated by SDS-PAGE and silver-stained. The presence of glycosylated and nonglycosylated variants is indicated. The 25 kDa band represents the light chain. (b) A monoclonal antibody purified from *N. benthamiana* wild-type (WT) or ΔXT/FT was digested with trypsin and subjected to LC-ESI-MS analysis. The mass $[M + 2H]^{2+}$ of the nonglycosylated peptide EEQYNSTYR carrying the Fc-N-glycosylation site (Asn297) and the major glycosylated peaks $[M + 2H]^{2+}$ and $[M + 3H]^{3+}$ are depicted. Peak labels were made according to the ProGlycAn system (www.proglycan.com), and the glycan illustrations are drawn according to the nomenclature from the Consortium for Functional Glycomics. (c) SP-Fc was expressed in *N. benthamiana* ΔXT/FT, and protein was extracted 24 h after infiltration and subjected to PNGase F digestion. Immunoblot detection was performed with anti-IgG antibodies.

migrates with the faster migrating band of the undigested SP-Fc. Mass spectrometry-based analysis of the glycosylation occupancy corroborates these findings for incomplete glycosylation (data not shown).

LmSTT3D from the protist *Leishmania major* is retained in the ER of plants

Leishmania major harbours four paralogues (termed LmSTT3A-D) of the single-subunit OST. In previous studies, it has been shown that the LmSTT3D from the protist *L. major* can rescue the growth and N-glycosylation defects observed in *Saccharomyces cerevisiae* lacking a functional STT3 protein (Nasab *et al.*, 2008) and improves N-glycosylation efficiency of recombinant proteins expressed in *Pichia pastoris* (Choi *et al.*, 2012). Consequently, we hypothesized that LmSTT3D activity may overcome the observed inefficient N-glycosylation of IgG in our plant-based expression system. To test this assumption, we generated a binary vector for expression of a codon-optimized LmSTT3D variant fused to GFP (LmSTT3D-GFP, Figure 2a) and transiently expressed the protein in *N. benthamiana*. According to the proposed topology model for LmSTT3D, the catalytic region close to the C-terminus faces the lumen of the ER, similar to the predictions for *A. thaliana* STT3A (Figure 2b). On immunoblots, a single band of expected size is detectable for LmSTT3D-GFP (Figure 2c). In wild-type leaf epidermal cells, ER-labelling was visible under the confocal microscope 1 day after infiltration (Figure 2d). Two and 3 days after infiltration, ER and additional puncta were detectable which represent Golgi bodies as well as undefined vesicular structures. In contrast to that, *A. thaliana* STT3A-GFP was only observed in the ER. Co-localization with the ER-resident OST4B-mRFP, a subunit of the plant oligosaccharyltransferase complex (Farid *et al.*, 2013), or the *cis*/medial Golgi-marker GnTI-mRFP (Schoberer *et al.*, 2013) confirmed the subcellular localization of LmSTT3D-GFP (Figure 2d) suggesting that LmSTT3D-GFP is incompletely retained in the ER.

LmSTT3D enhances the N-glycosylation occupancy of recombinant SP-Fc and IgG

In the next experiments, we examined whether LmSTT3D-GFP can improve the N-glycosylation efficiency of SP-Fc and IgG when transiently co-expressed in *N. benthamiana*. In the presence of LmSTT3D-GFP, the faster migrating band of SP-Fc disappeared, indicating an enhanced occupancy of glycosylation site Asn297 (Figure 3a and b). MS-based analysis of peptides/glycopeptides derived from proteolytically digested SP-Fc expressed in ΔXT/FT demonstrated that the co-expression of LmSTT3D-GFP drastically reduced the amount of the nonglycosylated variant (Figure 3c, Table 1). The N-glycan composition of the recombinantly expressed proteins was not altered upon LmSTT3D-GFP co-expression. The major N-glycan peak corresponds to processed complex N-glycans (GnGn: $GlcNAc_2Man_3GlcNAc_2$) (Figure 3c) indicating that LmSTT3D-GFP co-expression does not interfere with complex N-glycan processing of SP-Fc in the Golgi. The same result was obtained for an IgG co-expressed with LmSTT3D-GFP (Figure S1 and Table 1). Intact MS analysis of the fully assembled IgG 2G12 revealed further that in the absence of LmSTT3D-GFP, nonglycosylated as well as hemi-glycosylated (only one of the two heavy chains carries an N-glycan) forms are present. Co-expression of LmSTT3D-GFP leads to an increase in fully assembled IgG with two N-glycans, one attached to each heavy chain (Figure 4). In summary, our data show that LmSTT3D-GFP co-expression increases the N-glycosylation site occupancy of SP-Fc and IgG.

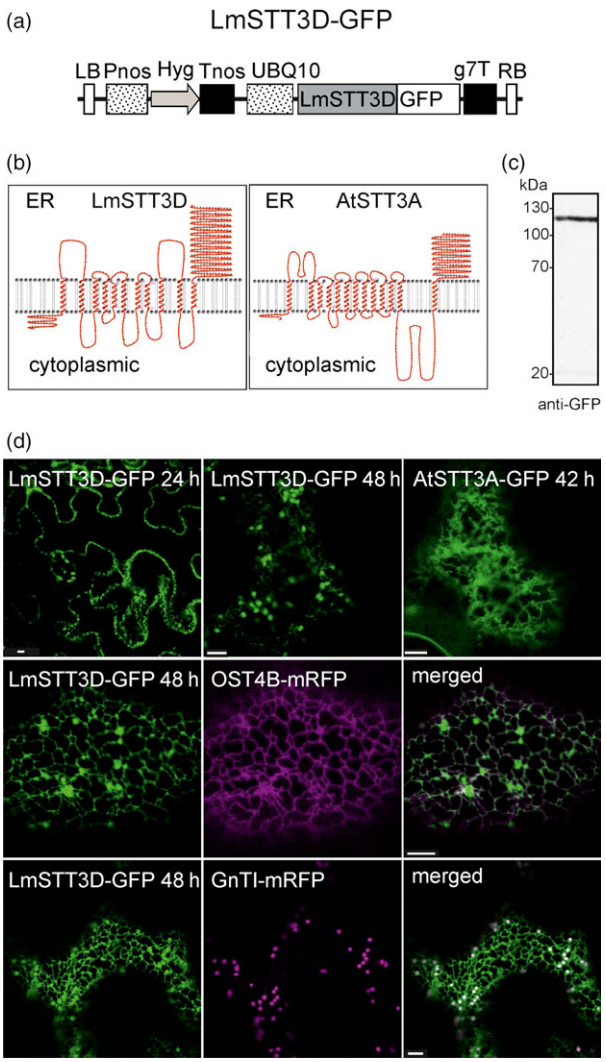

Figure 2 LmSTT3D-GFP accumulates in the ER and Golgi. (a) Schematic representation of the UBQ10:LmSTT3D-GFP expression vector. LB: left border; Pnos: nopaline synthase gene promoter; Hyg: hygromycin B phosphotransferase gene; Tnos: nopaline synthase gene terminator; UBQ10: *A. thaliana* ubiquitin-10 promoter; LmSTT3D: *L. major* catalytic OST subunit STT3D open reading frame; GFP: green fluorescent protein; g7T: agrobacterium gene 7 terminator; RB: right border. (b) Topology of LmSTT3D and *A. thaliana* STT3A (AtSTT3A). The transmembrane domain regions and their topology were obtained using the HMMTop prediction program (http://www.enzim.hu/hmmtop/). The illustration was generated using TMRPres2D visualization (http://bioinformatics.biol.uoa.gr/TMRPres2D/). (c) Immunoblot (with anti-GFP antibodies) of LmSTT3D-GFP transiently expressed in *N. benthamiana*. (d) LmSTT3D-GFP was either expressed alone or in combination with the ER-marker OST4B-mRFP and the Golgi-marker GnTI-mRFP in *N. benthamiana* leaf epidermal cells. Analysis of fluorescent proteins was carried out by confocal laser scanning microscopy at the indicated time after infiltration. Bars = 5 μm. Expression of AtSTT3A-GFP is shown for comparison.

LmSTT3D improves the N-glycosylation efficiency of different recombinant glycoproteins

We found that LmSTT3D-GFP co-expression is a suitable tool to increase the N-glycosylation efficiency of SP-Fc and IgG. To

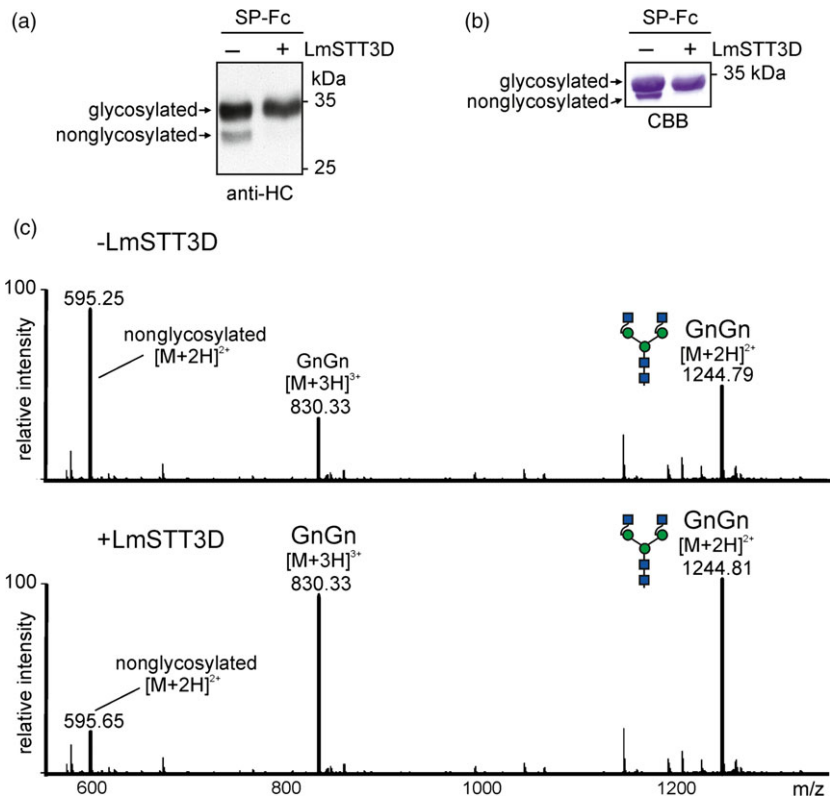

Figure 3 LmSTT3D-GFP co-expression increases the N-glycosylation site occupancy on SP-Fc. SP-Fc was transiently expressed in *N. benthamiana* leaves together with UBQ10:LmSTT3D-GFP. (a) Proteins were extracted from wild-type 2 days postinfiltration and subjected to SDS-PAGE and immunoblotting using anti-IgG heavy chain (HC) antibodies. (b) SDS-PAGE and Coomassie Brilliant Blue staining of SP-Fc purified from ΔXT/FT. (c) LC-ESI-MS analysis of tryptic glycopeptides from SP-Fc expressed in ΔXT/FT. In the shown spectra, the peak at 595.25 ($[M + 2H]^{2+}$) is assigned to the nonglycosylated peptide EEQYNSTYR, and the peaks at 830.33 ($[M + 3H]^{3+}$) and 1244.8 ($[M + 2H]^{2+}$) are assigned to the complex N-glycan GnGn (nomenclature according to the ProGlycAn system: www.proglycan.com).

Table 1 Comparison of the LmSTT3D-GFP effect on N-glycosylation of recombinant glycoproteins expressed in ΔXT/FT.

Protein	N-glycosylation site (GS)	% glycosylated	% glycosylated + LmSTT3D	% increase	Number of repetitions
Fc	GS1 NST	56 ± 3	93 ± 2	66	3
IgG	GS1 NST	87 ± 5	98 ± 4	13	3
IgE	GS3 NKT	20 ± 7	36 ± 3	80	2
	GS5 NLT	40 ± 11	91 ± 3	128	
	GS6 NHS	<2 ± 3	63 ± 4	>1000	
IgA1	GS1 NLT	96 ± 0	94 ± 4		2
	GS2 NVS	59 ± 1	95 ± 4	60	
EPO-Fc	GS1 NIT	60 ± 5	81 ± 3	35	2
	GS3 NSS	95 ± 2	93 ± 0		
	GS4 NST	90 ± 1	99 ± 2	10	
IFN-γ	GS1 + GS2	20 ± 7	67 ± 12	235	5

Mean values + standard deviation from independent experiments (biological replicates) are shown. The glycosylation site occupancy of IFN-γ was calculated by quantification of bands from immunoblots. All other values are derived from MS-based quantification of peptides from purified proteins. Please note, due to an incomplete proteolytic digestion, no reliable quantification of GS2 from EPO-Fc could be performed.

extend our findings, we tested the impact of LmSTT3D-GFP on the N-glycosylation site occupancy of other transiently expressed mammalian glycoproteins carrying multiple glycosylation sites (GS). First, we co-expressed recombinant IgE (7 GS) and IgA1 (2 GS) together with LmSTT3D-GFP. These immunoglobulins have been recently expressed in *N. benthamiana* and contain N-glycosylation sites that were partially occupied (Göritzer *et al.*, 2017; Montero-Morales *et al.*, 2017). GS1, GS2, GS4 and GS7 are fully occupied on recombinant IgE. GS3 and GS5, on the other hand, display partial glycosylation and GS6 is normally not occupied (Montero-Morales *et al.*, 2017; Plomp *et al.*, 2014). In the presence of LmSTT3D-GFP, we observed a slight shift in the migration position of the IgE heavy chain (Figure 5a). MS-based analysis of IgE glycosylation sites confirmed an increase in N-glycosylation site occupancy for the IgE glycosylation sites that were previously found to be incompletely glycosylated in the absence of LmSTT3D-GFP (80% increase for GS3 and 128% for GS5, Table 1). Interestingly, GS6 becomes N-glycosylated in the presence of LmSTT3D-GFP and more than half of the purified IgE is now glycosylated at this particular site (Table 1). The N-glycans found on IgE GS6 were mainly processed complex type N-glycans that are commonly found on plant-produced recombinant glycoproteins indicating that the LmSTT3D-mediated transfer does not lead to altered N-glycan processing (Figure S2). GS2 at the C-terminus of IgA1 is normally incompletely N-glycosylated when expressed in plants or human cells (Göritzer *et al.*, 2017). In the

presence of LmSTT3D-GFP, however, we detected a reduction in the incompletely glycosylated alpha heavy chain from IgA1 (Figure 5b) and MS-based quantification revealed almost complete glycosylation of the sequon in the C-terminal tailpiece (Table 1) without affecting N-glycan processing (Figure S3).

To see whether the positive effect of LmSTT3D can also be observed with recombinant glycoproteins that are not related to immunoglobulins, we transiently expressed human EPO-Fc (Castilho *et al.*, 2011) and the cytokine interferon-γ (IFN-γ). Differences in SDS-PAGE migration of EPO-Fc were observed when LmSTT3D-GFP was co-expressed indicating a reduction in underglycosylation (Figure 5c). Quantification of glycopeptides derived from EPO showed a clear increase at glycosylation site one (Table 1). As observed for Fc glycosylation, the N-glycan profiles were virtually identical in the absence or presence of LmSTT3D-GFP. Mainly the fully processed GnGn glycans were present on all three N-glycosylation sites of EPO as well as on the Fc site when expressed in ΔXT/FT (Figure S4 and data not shown), suggesting that LmSTT3D-GFP expression does not interfere with N-glycan processing.

The effect of LmSTT3D on the N-glycosylation site occupancy of IFN-γ which carries two N-glycosylation sites (Asn25 and Asn97, Figure S5) was examined by immunoblots of a variant carrying a C-terminal HA-tag. IFN-γ-HA shows three bands on immunoblots indicating that it is incompletely glycosylated (no N-glycan, a single N-glycan or fully glycosylated with two N-glycans) when transiently expressed in *N. benthamiana* wild-type and ΔXT/FT. Co-expression of LmSTT3D-GFP resulted in the appearance of a major protein band representing the fully glycosylated protein that could be converted to the nonglycosylated IFN-γ-HA by PNGase F digestion (Figure 5d and e, Table 1). These data show that LmSTT3D co-expression improves the N-glycosylation site occupancy of numerous glycoproteins.

LmSTT3D-GFP-HDEL is efficiently retained in the ER

While the co-expression of LmSTT3D-GFP resulted in a significant improvement of the N-glycosylation efficiency on various proteins, the overlapping occurrence in the ER and Golgi bodies suggests that part of the protein is not functional due to the mislocalization. Consequently, we examined whether a LmSTT3D variant with increased ER accumulation improves its functionality. Thus, a construct was generated which expressed LmSTT3D-GFP with a C-terminal HDEL tetrapeptide for ER retrieval (Figure 6a). Imaging by confocal microscopy showed that the attachment of the HDEL motif leads to an efficient steady-state distribution of LmSTT3D-GFP-HDEL in the ER in *N. benthamiana* leaf epidermal cells (Figure 6b). No signal was observed in Golgi bodies. To analyse the functionality of LmSTT3D-GFP-HDEL, we co-expressed it together with IFN-γ-HA and analysed the glycosylation status. Like LmSTT3D-GFP, the LmSTT3D-GFP-HDEL variant was functional and improved the N-glycosylation site occupancy of IFN-γ-HA. Quantification of bands from immunoblots showed no difference between LmSTT3D-GFP and LmSTT3D-GFP-HDEL (Figure 6c) suggesting that the expression of the fully ER-retained LmSTT3D-GFP-HDEL variant does not increase N-glycosylation efficiency compared to the incompletely retained variant.

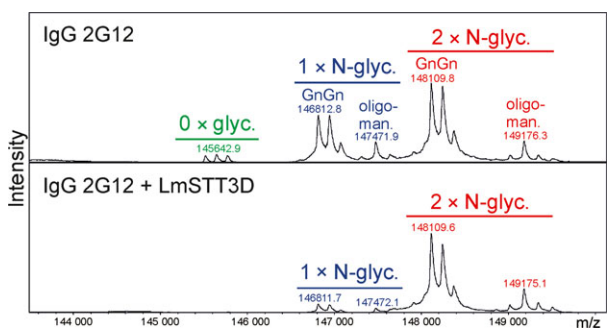

Figure 4 The N-glycan site occupancy of fully assembled IgG in the presence or absence of LmSTT3D-GFP was determined using LC-ESI-MS. The peaks corresponding to unglycosylated (green), hemi-glycosylated (blue, one N-glycan) and fully glycosylated (red, two N-glycans) IgG (HIV-neutralizing antibody 2G12) are highlighted. Multiple peaks represent different glycoforms (complex N-glycan GnGn, oligomannosidic glycans) and variations in the clipping of C-terminal lysine. Please note, the clipping of lysine is not found on variants carrying oligomannosidic N-glycans indicating that this processing reaction occurs in a post-ER compartment.

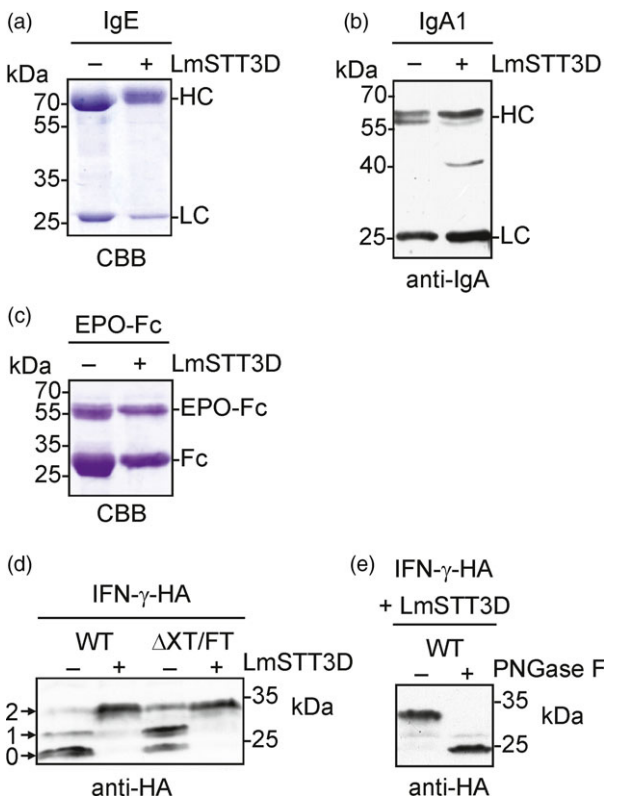

Figure 5 LmSTT3D-GFP enhances the N-glycosylation efficiency of different recombinant proteins when transiently expressed in *N. benthamiana*. (a) Human IgE was expressed in ΔXT/FT in the presence (+) or absence (–) of LmSTT3D-GFP, and the purified IgE was analysed by SDS-PAGE and Coomassie Brilliant Blue (CBB) staining. (b) Human IgA1 was expressed in ΔXT/FT, and total protein extracts were analysed by immunoblotting with antibodies against the alpha heavy chain and the kappa light chain (anti-IgA). (c) EPO-Fc was expressed in ΔXT/FT, purified and subjected to SDS-PAGE and CBB staining. (d) Expression of IFN-γ-HA in the presence (+) or absence (–) of LmSTT3D-GFP. Protein extracts were subjected to SDS-PAGE and immunoblotting using anti-HA antibodies. The migration position of the nonglycosylated (0), mono- (1) and di-glycosylated (2) IFN-γ-HA protein is indicated. (e) PNGase F digestion of IFN-γ-HA co-expressed with LmSTT3D-GFP.

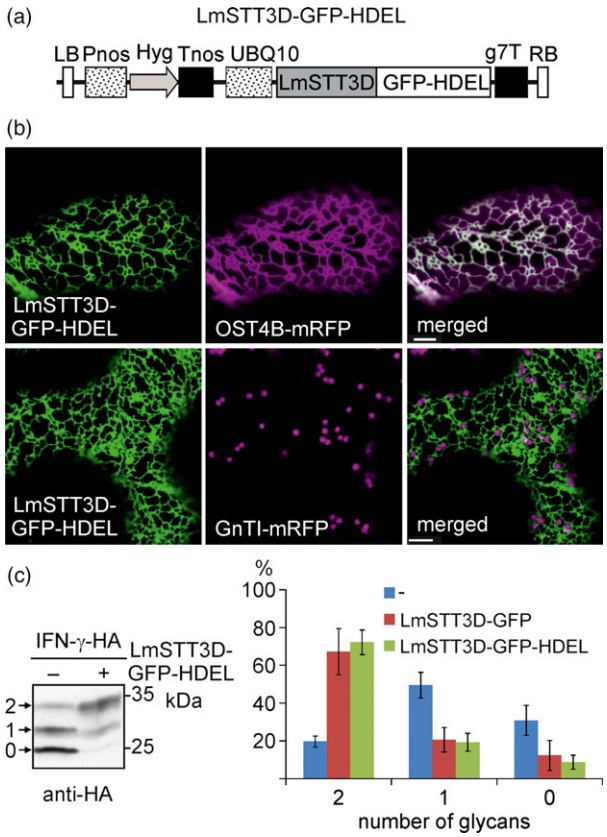

Figure 6 Attachment of the HDEL tetrapeptide improves ER localization of LmSTT3D-GFP and does not interfere with its functionality. (a) Schematic illustration of the UBQ10:LmSTT3D-GFP-HDEL expression vector. For abbreviations, see legend of Figure 2. (b) LmSTT3D-GFP-HDEL was either expressed alone or in combination with the ER-marker OST4B-mRFP in wild-type leaf epidermal cells. Images were acquired two days postinfiltration. Bars = 5 μm. (c) SDS-PAGE and immunoblotting of IFN-γ-HA expressed in ΔXT/FT in the presence (+) or absence (–) of LmSTT3D-GFP-HDEL. Quantification of IFN-γ-HA protein bands upon expression in ΔXT/FT. The diagram shows mean values plus standard deviation from at least five biological replicates.

Discussion

N-glycans have a strong impact on protein folding, stability and influence the interaction with other proteins. N-glycosylation of recombinant biopharmaceuticals is critical for product quality (Reusch and Tejada, 2015). For example, the single N-glycan from the IgG Fc-domain modulates immune effector functions and unglycosylated IgG variants display drastically reduced affinity for Fcγ-receptors (Ferrara *et al.*, 2011; Jefferis and Lund, 2002; Shields *et al.*, 2002). Moreover, the presence of additional N-glycans can improve the *in vivo* half-life and activity of recombinant biopharmaceuticals. This has been impressively demonstrated for a hyperglycosylated EPO variant (darbepoetin alfa) that is glycosylated at two additionally introduced N-glycosylation sites and has been approved for treatment of anaemia (Elliott *et al.*, 2003). EPO or IgG from human serum and recombinant variants thereof expressed in mammalian cells are typically very efficiently glycosylated (Table S1). By contrast, *N. benthamiana* (Table 1) and to a certain degree also other expression systems such as *P. pastoris* (Choi *et al.*, 2012) or insect cells (Sareneva *et al.*, 1995) display more variation in N-glycosylation efficiency. Despite the documented importance of proper N-glycosylation site occupancy, comparably few studies have so far approached the diversity caused by the absence of glycans at particular sites on recombinant glycoproteins. Previous studies have shown that LmSTT3D, the single catalytic subunit from the protozoan *L. major*, can replace the function of the endogenous STT3 subunit from *S. cerevisiae* and complements growth and N-glycosylation defects associated with OST deficiency (Nasab *et al.*, 2008). Biochemical and genetic evidence indicates that LmSTT3D is functionally independent and not integrated into the native OST complex when heterologously expressed (Hese *et al.*, 2009; Nasab *et al.*, 2008).

Recombinant IFN-γ has been approved for treatment of different human diseases and is a promising candidate for cancer immunotherapy (Razaghi *et al.*, 2016). Glycosylation of IFN-γ is important for its proteolytic stability, secretion and circulatory half-life (Bocci *et al.*, 1985; Sareneva *et al.*, 1993, 1995, 1996). Transient expression in *N. benthamiana* indicates that IFN-γ is inefficiently glycosylated in the absence of LmSTT3D. We currently do not know whether both sites are equally affected or whether Asn97, which is present in an α-helical region, is less occupied as has been suggested for IFN-γ from human cells (Sareneva *et al.*, 1996). In contrast to *N. benthamiana*, approximately two-thirds of native human IFN-γ is fully glycosylated (Rinderknecht *et al.*, 1984; Sareneva *et al.*, 1995) and recombinant IFN-γ expressed in CHO fed-batch cultures displays low amounts of nonglycosylated protein (Wong *et al.*, 2010). The reason for this discrepancy in N-glycosylation efficiency between mammalian cells and plants is currently unknown, but may reflect differences in the composition and function of the OST complex. Notably, in the presence of LmSTT3D, similar levels of fully glycosylated IFN-γ are obtained in plants and on the naturally occurring protein (Table 1 and Table S1).

We found that not all analysed N-glycosylation sites were equally well glycosylated upon LmSTT3D co-expression. Glycosylation of GS3 from EPO-Fc or GS1 from IgA1, which were already efficiently occupied in the absence of LmSTT3D, was not improved. On the other hand, GS2 from IgA1, which is only partially glycosylated when expressed in plants or human cells (Göritzer *et al.*, 2017), could be completely modified with N-glycans upon LmSTT3D expression. This site is likely post-translationally modified in mammalian cells and plays an important role in the assembly of dimeric IgA1 (Atkin *et al.*, 1996). Consequently, our data indicate that LmSTT3D preferentially glycosylates certain N-glycosylation sites which has also been recognized in a previous study (Nasab *et al.*, 2008). The precise sequence or conformational constraints influencing LmSTT3D-dependent glycosylation are unknown. Remarkably, the co-expression of LmSTT3D resulted in the glycosylation of IgE GS6. This is in contrast to native serum or recombinantly produced IgE from human cells (Montero-Morales *et al.*, 2017; Plomp *et al.*, 2014), indicating that LmSTT3D has a more relaxed substrate specificity and recognizes glycosylation sites that are normally not used by the mammalian OST complex. Due to the various biological roles of N-glycans, the functional relevance of an additional N-glycan is difficult to predict. LmSTT3D co-expression facilitates the production of non-natural glycoproteins that can be used to test the influence on physicochemical properties of proteins and known protein interactions in future studies.

A further increase in the glycosylation efficiency may be achieved by stable expression of LmSTT3D in *N. benthamiana* or

incorporation of LmSTT3D into multicassette expression vectors used for transient expression together with a glycoprotein of interest to ensure that all cells express LmSTT3D. The stable expression of the KDEL tagged variant, which is at least equally functional when expressed with IFN-γ or IgG (data not shown), will less likely interfere with N-glycan processing in the Golgi or overall Golgi organization and function.

Apart from the expression levels, interaction with ER-resident proteins, polypeptide substrate specificity or enzyme kinetics of the catalytic STT3 subunit, glycosylation efficiency may be controlled by supply of the preassembled lipid-linked oligosaccharide substrate. Deprivation of glucose from CHO cell cultures reduced the amounts of lipid-linked oligosaccharides resulting in the expression of nonglycosylated monoclonal antibodies (Liu *et al.*, 2014). In addition to optimized metabolic parameters, a limitation in donor substrate availability may be the result of inefficient lipid-linked oligosaccharide transfer into the ER. This shortcoming may be overcome by co-expression of an artificial flippase (Parsaie Nasab *et al.*, 2013). Moreover, it is well known that protein intrinsic structural constraints strongly influence the N-glycosylation efficiency at distinct sites. For example, the presence of a serine instead of a threonine in the consensus site N-X-S/T is less preferred by the OST complex and N-X-T sites are more frequently glycosylated in organisms from different eukaryotic domains of life (Zielinska *et al.*, 2012). Exchange of amino acids in the sequon or at adjacent sites of the polypeptide can drastically alter the glycosylation site occupancy (Murray *et al.*, 2015). For a recombinant elastase expressed in *P. pastoris,* a change of the sequon from N-X-S to N-X-T resulted in an increased glycosylation efficiency that was accompanied by higher production levels of the recombinant glycoprotein (Han *et al.*, 2015). By contrast, mutagenesis of flanking amino acids and generation of an optimized aromatic sequon with increased glycosylation efficiency negatively affected the secretion of IFN-γ expressed in human cells and caused variability in protein expression of another glycoprotein (Huang *et al.*, 2017). Likewise, antibody engineering by generation of an aromatic sequon (FANST instead of the canonical QYNST) improved the thermal stability of the antibody, but reduced the affinity to specific Fcγ-receptors (Chen *et al.*, 2016). These studies highlight impressively that protein engineering at glycosylation sites can have various consequences leading to reduced productivity or altered product quality. Consequently, strategies aiming at an improvement of N-glycosylation by engineering of the OST complex are very promising and relevant for different plant-based expression platforms (Hamorsky *et al.*, 2015; Rademacher *et al.*, 2008; Vamvaka *et al.*, 2016; Van Droogenbroeck *et al.*, 2007). Further advances require a better understanding of the OST complex composition and molecular function of the individual subunits. Taken together, our findings demonstrate that transient LmSTT3D expression is a robust extension of currently existing glyco-engineering approaches and should be integrated into production processes to reduce product heterogeneity and improve biological activities related to N-glycosylation of recombinant glycoproteins.

Experimental procedures

Cloning of expression vectors

The expression constructs for IgG 2G12 (Schähs *et al.*, 2007), EPO-Fc (Castilho *et al.*, 2011), IgE (Montero-Morales *et al.*, 2017) and IgA1 (Göritzer *et al.*, 2017) were described previously. To generate the SP-Fc expression vector, the DNA fragment coding for GCSI-CTS-Fc was amplified from GCSI-CTS-GFPglyc (Schoberer *et al.*, 2009) by PCR using primers GCSI-7F (TATATCTA GAATGACCGGAGCTAGCCGTCGGAGC) and Fc-6R (TATACTC GAGTTATTTACCCGGAGACAGGGAGAGG). The PCR product was digested with XbaI/XhoI and cloned into XbaI/SalI sites of p47 (Hüttner *et al.*, 2014) to generated p71-GCSI-Fc. Subsequently, the chitinase signal peptide was amplified from *N. benthamiana* cDNA by PCR using Nb-Chi-F1 (TATATCTA GAATGAGGCTTAGAGAATTCACAG) and Nb-Chi-R2 (TATAG GATCCTGCCGAGGCAGAGAGTAGGAGAGA), XbaI/BamHI digested and cloned into XbaI/BamHI digested p71-GCSI-Fc, resulting in p71-SP-Fc. For IFN-γ expression, a codon-optimized DNA fragment encoding human IFN-γ was synthetized by GeneArt Gene Synthesis (Thermo Fisher Scientific). The synthetic DNA fragment was XbaI/BamHI digested and cloned into the XbaI/BamHI sites of expression vector p43. The vector p43 is a derivative of expression vector p27 (Strasser *et al.*, 2007) whereby the CaMV 35S promoter was replaced by the *A. thaliana* UBQ10 promoter and a sequence encoding a 3x HA-tag for C-terminal fusion was inserted upstream of the terminator sequence (Figure S5). To generate the LmSTT3D-GFP expression vector a codon-optimized open reading frame coding for *L. major* STT3D (Nasab *et al.*, 2008) was synthetized by GeneArt Gene Synthesis. The LmSTT3D open reading frame was excised by XbaI/BamHI digestion and cloned into XbaI/BamHI sites of p47 or p56. Vector p56 is derived from p47 by replacement of the GFP coding sequence with the one for GFP-HDEL. For generation of the STT3A-GFP expression vector p20-STT3A, the *A. thaliana* STT3A coding region was amplified by PCR as described previously (Farid *et al.*, 2013) and cloned into XbaI/BamHI digested plasmid p20F (Schoberer *et al.*, 2009).

Transient expression and immunoblot analysis

All plant expression vectors were transformed into *Agrobacterium tumefaciens* (strain UIA143) (Farrand *et al.*, 1989). Syringe-mediated agroinfiltration was used for transient expression in leaves of 4- to 5-week-old *N. benthamiana* grown on soil under long-day conditions (16 h light/8 h dark) at 25°C. At the indicated time points, leaf pieces were harvested from infiltrated plants, and total protein extracts were prepared and subjected to SDS-PAGE followed by silver staining (Strasser *et al.*, 2004) or immunoblotting as described in detail previously (Shin *et al.*, 2017). IgG and Fc-containing fragments were monitored with anti-human IgG (H+L)-horseradish peroxidase antibody (Promega, Mannheim, Germany), IgA with anti-alpha chain/anti-kappa-chain antibodies and IFN-γ-HA with anti-HA antibodies. For deglycosylation, protein extracts were incubated with peptide-N-glycosidase F (PNGase F) (New England Biolabs, Frankfurt am Main, Germany) according to the manufacturer's procedure. Quantification of gel bands on immunoblots was performed with a ChemiDoc imager (Bio-Rad, Vienna, Austria) and Quantity One 1D analysis software (Bio-Rad).

For detection of LmSTT3D-GFP on immunoblots, leaf material was harvested 48 h after infiltration of *N. benthamiana* leaves. Proteins were extracted with 1 × Laemmli sample buffer supplemented with 6M urea and incubated at 37°C for 5 min. The fusion protein was detected with anti-GFP horseradish peroxidase (MACS Miltenyi Biotec, Bergisch Gladbach, Germany) antibodies.

Confocal imaging of fluorescent protein fusions

Leaves of 4- to 5-week-old *N. benthamiana* were infiltrated with agrobacterium suspensions carrying binary plant expression vectors for expression of GFP- or mRFP-tagged proteins with the following optical densities (OD_{600}): 0.1 for p47-LmSTT3D (LmSTT3D-GFP), p56-LmSTT3D (LmSTT3D-GFP-HDEL), p20-STT3A (AtSTT3A-GFP). Agrobacteria carrying the expression constructs p31-OST4B (OST4B-mRFP, ER-marker) (Farid *et al.*, 2013) and p31-GnTI (GnTI-mRFP, Golgi-marker) (Schoberer *et al.*, 2013) were infiltrated with $OD_{600} = 0.05$. Confocal images were acquired 1 and 2 days postinfiltration on a Leica SP5 II confocal microscope using the Leica LAS AF software system (http://www.leica.com). Dual-colour image acquisition of cells expressing both GFP and mRFP was performed simultaneously. Postacquisition image processing was performed in Adobe PHOTOSHOP CS5.

LC-ESI-MS analysis

The full-length heavy chain from IgGs and SP-Fc was purified from the protein extract by binding to rProtein A Sepharose™ Fast Flow (GE Healthcare Europe, Vienna, Austria). Purified protein was subjected to SDS-PAGE under reducing conditions and Coomassie Brilliant Blue staining. The corresponding protein band was excised from the gel, destained, carbamidomethylated, in-gel trypsin digested and analysed by liquid chromatography electrospray ionization mass spectrometry (LC-ESI-MS), as described in detail previously (Stadlmann *et al.*, 2008). A detailed explanation of N-glycan abbreviations can be found at http://www.proglycan.com. Protein purification and MS-based analysis of (glyco) peptides from EPO-Fc, IgE and IgA1 were described in detail recently (Castilho *et al.*, 2011; Göritzer *et al.*, 2017; Montero-Morales *et al.*, 2017). Site occupancy was calculated from the peak area of nonglycosylated versus the sum of the peak areas of all glycoforms including relevant adduct ions and observed charged states. The principal suitability of this 'peak sum' approach under the conditions applied was verified in two stages. First, selected samples were subjected to deglycosylation with peptide-N-glycosidase A (ProGlycAn, Vienna, Austria) and the ratio of the Asn vs. the Asp containing glycopeptides, which separate in RP-HPLC, was measured. Peptides differing in charged amino acids may have differing mass spectrometric responses, and hence, in a second stage, the Fc tandem peptide EEQYNSTYREEQYDSTYR (JP peptides, Berlin, Germany) was digested with trypsin to obtain an equimolar mixture of the Asn and the Asp form of the Fc (glyco-)peptide. These measurements showed that the 'peak sum' approach gave reliable values with a possible overestimation of nonglycosylation of a very few percentages especially in the case of low underglycosylation. We assume the situation for other glycoproteins to be comparable to that with IgG Fc.

Mass spectrometric analysis of fully assembled IgGs

The purified IgGs were directly injected to a LC-ESI-MS system (LC: Dionex Ultimate 3000 LC). A gradient from 20% to 80% acetonitrile in 0.05% trifluoroacetic acid (using a Thermo ProSwift™ RP-4H column (0.2 × 250 mm)) at a flow rate of 8 μL/min was applied (30-minute gradient time). Detection was performed with a Q-TOF instrument (Bruker maXis 4G) equipped with the standard ESI source in positive ion, MS mode (range: 750–5000 Da). Instrument calibration was performed using ESI calibration mixture (Agilent). Data were processed using Data Analysis 4.0 (Bruker), and the spectrum was deconvoluted by MaxEnt.

Acknowledgements

We thank Michaela Bogner, Martina Dicker, Thomas Hackl, Jennifer Schoberer, Yun-Ji Shin and Christiane Veit for technical support and the BOKU-VIBT Imaging Centre for access and expertise. We thank Victor Klimyuk from Icon Genetics GmbH for the kind gift of expression vectors used for IgE expression. This work was supported by grants from the Austrian Science Fund (FWF): I2417-B22 (to RS), P28673-B28 (to HS) and the Doctoral Program BioToP (Grant W 1224).

Conflict of interest

The authors declared that they have no conflict of interests.

References

Aebi, M. (2013) N-linked protein glycosylation in the ER. *Biochim. Biophys. Acta*, **1833**, 2430–2437.

Atkin, J.D., Pleass, R.J., Owens, R.J. and Woof, J.M. (1996) Mutagenesis of the human IgA1 heavy chain tailpiece that prevents dimer assembly. *J. Immunol.* **157**, 156–159.

Bendandi, M., Marillonnet, S., Kandzia, R., Thieme, F., Nickstadt, A., Herz, S., Fröde, R. *et al.* (2010) Rapid, high-yield production in plants of individualized idiotype vaccines for non-Hodgkin's lymphoma. *Ann. Oncol.* **21**, 2420–2427.

Bocci, V., Pacini, A., Pessina, G.P., Paulesu, L., Muscettola, M. and Lunghetti, G. (1985) Catabolic sites of human interferon-gamma. *J. Gen. Virol.* **66**, 887–891.

Castilho, A., Gattinger, P., Grass, J., Jez, J., Pabst, M., Altmann, F., Gorfer, M. *et al.* (2011) N-glycosylation engineering of plants for the biosynthesis of glycoproteins with bisected and branched complex N-glycans. *Glycobiology*, **21**, 813–823.

Chen, W., Kong, L., Connelly, S., Dendle, J.M., Liu, Y., Wilson, I.A., Powers, E.T. *et al.* (2016) Stabilizing the CH2 domain of an antibody by engineering in an enhanced aromatic sequon. *ACS Chem. Biol.* **11**, 1852–1861.

Choi, B.K., Warburton, S., Lin, H., Patel, R., Boldogh, I., Meehl, M., d'Anjou, M. *et al.* (2012) Improvement of N-glycan site occupancy of therapeutic glycoproteins produced in *Pichia pastoris*. *Appl. Microbiol. Biotechnol.* **95**, 671–682.

Dicker, M., Tschofen, M., Maresch, D., Konig, J., Juarez, P., Orzaez, D., Altmann, F. *et al.* (2016) Transient Glyco-engineering to produce recombinant IgA1 with defined N- and O-Glycans in plants. *Front Plant Sci.* **7**, 18.

Elliott, S., Lorenzini, T., Asher, S., Aoki, K., Brankow, D., Buck, L., Busse, L. *et al.* (2003) Enhancement of therapeutic protein in vivo activities through glycoengineering. *Nat. Biotechnol.* **21**, 414–421.

Elliott, S., Egrie, J., Browne, J., Lorenzini, T., Busse, L., Rogers, N. and Ponting, I. (2004) Control of rHuEPO biological activity: the role of carbohydrate. *Exp. Hematol.* **32**, 1146–1155.

Farid, A., Malinovsky, F.G., Veit, C., Schoberer, J., Zipfel, C. and Strasser, R. (2013) Specialized roles of the conserved subunit OST3/6 of the oligosaccharyltransferase complex in innate immunity and tolerance to abiotic stresses. *Plant Physiol.* **162**, 24–38.

Farrand, S.K., O'Morchoe, S.P. and McCutchan, J. (1989) Construction of an Agrobacterium tumefaciens C58 recA mutant. *J. Bacteriol.* **171**, 5314–5321.

Ferrara, C., Grau, S., Jäger, C., Sondermann, P., Brünker, P., Waldhauer, I., Hennig, M. *et al.* (2011) Unique carbohydrate-carbohydrate interactions are required for high affinity binding between FcgammaRIII and antibodies lacking core fucose. *Proc. Natl. Acad. Sci. USA*, **108**, 12669–12674.

Göritzer, K., Maresch, D., Altmann, F., Obinger, C. and Strasser, R. (2017) Exploring site-specific N-Glycosylation of HEK293 and plant-produced human IgA isotypes. *J. Proteome Res.* **16**, 2560–2570.

Hamorsky, K.T., Kouokam, J.C., Jurkiewicz, J.M., Nelson, B., Moore, L.J., Husk, A.S., Kajiura, H. *et al.* (2015) N-glycosylation of cholera toxin B subunit in *Nicotiana benthamiana*: impacts on host stress response, production yield and vaccine potential. *Sci. Rep.* **5**, 8003.

Han, M., Wang, W., Wang, X., Liu, X., Cao, H., Tao, Y. and Yu, X. (2015) Enhanced expression of recombinant elastase in *Pichia pastoris* through the substitution of Thr for Ser in Asn-Xaa-Ser sequons. *Appl. Biochem. Biotechnol.* **175**, 428–435.

Hanania, U., Ariel, T., Tekoah, Y., Fux, L., Sheva, M., Gubbay, Y., Weiss, M. *et al.* (2017) Establishment of a tobacco BY2 cell line devoid of plant-specific xylose and fucose as a platform for the production of biotherapeutic proteins. *Plant Biotechnol. J.* **15**, 1120–1129.

Hese, K., Otto, C., Routier, F.H. and Lehle, L. (2009) The yeast oligosaccharyltransferase complex can be replaced by STT3 from *Leishmania major*. *Glycobiology*, **19**, 160–171.

Huang, Y.W., Yang, H.I., Wu, Y.T., Hsu, T.L., Lin, T.W., Kelly, J.W. and Wong, C.H. (2017) Residues comprising the enhanced aromatic sequon influence protein N-glycosylation efficiency. *J. Am. Chem. Soc.* **139**, 12947–12955.

Hüttner, S., Veit, C., Vavra, U., Schoberer, J., Dicker, M., Maresch, D., Altmann, F. *et al.* (2014) A context-independent N-glycan signal targets the misfolded extracellular domain of Arabidopsis STRUBBELIG to endoplasmic-reticulum-associated degradation. *Biochem. J.* **464**, 401–411.

Izquierdo, L., Atrih, A., Rodrigues, J., Jones, D. and Ferguson, M. (2009) *Trypanosoma brucei* UDP-glucose:glycoprotein glucosyltransferase has unusual substrate specificity and protects the parasite from stress. *Eukaryot. Cell*, **8**, 230–240.

Jefferis, R. (2009) Glycosylation as a strategy to improve antibody-based therapeutics. *Nat. Rev. Drug. Discov.* **8**, 226–234.

Jefferis, R. and Lund, J. (2002) Interaction sites on human IgG-Fc for FcgammaR: current models. *Immunol. Lett.* **82**, 57–65.

Kallolimath, S., Castilho, A., Strasser, R., Grunwald-Gruber, C., Altmann, F., Strubl, S., Galuska, C.E. *et al.* (2016) Engineering of complex protein sialylation in plants. *Proc. Natl. Acad. Sci. USA*, **113**, 9498–9503.

Kang, J., Frank, J., Kang, C., Kajiura, H., Vikram, M., Ueda, A., Kim, S. *et al.* (2008) Salt tolerance of Arabidopsis thaliana requires maturation of N-glycosylated proteins in the Golgi apparatus. *Proc. Natl. Acad. Sci. USA*, **105**, 5933–5938.

Kelleher, D. and Gilmore, R. (2006) An evolving view of the eukaryotic oligosaccharyltransferase. *Glycobiology*, **16**, 47R–62R.

Knauer, R. and Lehle, L. (1999) The oligosaccharyltransferase complex from yeast. *Biochim. Biophys. Acta*, **1426**, 259–273.

Koiwa, H., Li, F., McCully, M., Mendoza, I., Koizumi, N., Manabe, Y., Nakagawa, Y. *et al.* (2003) The STT3a subunit isoform of the Arabidopsis oligosaccharyltransferase controls adaptive responses to salt/osmotic stress. *Plant Cell*, **15**, 2273–2284.

Li, J., Stoddard, T.J., Demorest, Z.L., Lavoie, P.O., Luo, S., Clasen, B.M., Cedrone, F. *et al.* (2016) Multiplexed, targeted gene editing in *Nicotiana benthamiana* for glyco-engineering and monoclonal antibody production. *Plant Biotechnol. J.* **14**, 533–542.

Limkul, J., Iizuka, S., Sato, Y., Misaki, R., Ohashi, T. and Fujiyama, K. (2016) The production of human glucocerebrosidase in glyco-engineered *Nicotiana benthamiana* plants. *Plant Biotechnol. J.* **14**, 1682–1694.

Liu, B., Spearman, M., Doering, J., Lattová, E., Perreault, H. and Butler, M. (2014) The availability of glucose to CHO cells affects the intracellular lipid-linked oligosaccharide distribution, site occupancy and the N-glycosylation profile of a monoclonal antibody. *J. Biotechnol.* **170**, 17–27.

Loos, A., Gruber, C., Altmann, F., Mehofer, U., Hensel, F., Grandits, M., Oostenbrink, C. *et al.* (2014) Expression and glycoengineering of functionally active heteromultimeric IgM in plants. *Proc. Natl. Acad. Sci. USA*, **111**, 6263–6268.

Loos, A., Gach, J.S., Hackl, T., Maresch, D., Henkel, T., Porodko, A., Bui-Minh, D. *et al.* (2015) Glycan modulation and sulfoengineering of anti-HIV-1 monoclonal antibody PG9 in plants. *Proc. Natl. Acad. Sci. USA*, **112**, 12675–12680.

Mercx, S., Smargiasso, N., Chaumont, F., De Pauw, E., Boutry, M. and Navarre, C. (2017) Inactivation of the β(1,2)-xylosyltransferase and the α(1,3)-fucosyltransferase genes in *Nicotiana tabacum* BY-2 Cells by a Multiplex CRISPR/Cas9 Strategy Results in Glycoproteins without Plant-Specific Glycans. *Front Plant Sci.* **8**, 403.

Mohorko, E., Glockshuber, R. and Aebi, M. (2011) Oligosaccharyltransferase: the central enzyme of N-linked protein glycosylation. *J. Inherit. Metab. Dis.* **34**, 869–878.

Montero-Morales, L., Maresch, D., Castilho, A., Turupcu, A., Ilieva, K.M., Crescioli, S., Karagiannis, S.N. *et al.* (2017) Recombinant plant-derived human IgE glycoproteomics. *J. Proteomics*, **161**, 81–87.

Murray, A.N., Chen, W., Antonopoulos, A., Hanson, S.R., Wiseman, R.L., Dell, A., Haslam, S.M. *et al.* (2015) Enhanced aromatic sequons increase oligosaccharyltransferase glycosylation efficiency and glycan homogeneity. *Chem. Biol.* **22**, 1052–1062.

Nasab, F.P., Schulz, B.L., Gamarro, F., Parodi, A.J. and Aebi, M. (2008) All in one: *Leishmania major* STT3 proteins substitute for the whole oligosaccharyltransferase complex in Saccharomyces cerevisiae. *Mol. Biol. Cell*, **19**, 3758–3768.

Nekrasov, V., Li, J., Batoux, M., Roux, M., Chu, Z., Lacombe, S., Rougon, A. *et al.* (2009) Control of the pattern-recognition receptor EFR by an ER protein complex in plant immunity. *EMBO J.* **28**, 3428–3438.

Nose, M. and Wigzell, H. (1983) Biological significance of carbohydrate chains on monoclonal antibodies. *Proc. Natl. Acad. Sci. USA*, **80**, 6632–6636.

Parsaie Nasab, F., Aebi, M., Bernhard, G. and Frey, A.D. (2013) A combined system for engineering glycosylation efficiency and glycan structure in *Saccharomyces cerevisiae*. *Appl. Environ. Microbiol.* **79**, 997–1007.

Plomp, R., Hensbergen, P.J., Rombouts, Y., Zauner, G., Dragan, I., Koeleman, C.A., Deelder, A.M. *et al.* (2014) Site-specific N-glycosylation analysis of human immunoglobulin E. *J. Proteome Res.* **13**, 536–546.

Rademacher, T., Sack, M., Arcalis, E., Stadlmann, J., Balzer, S., Altmann, F., Quendler, H. *et al.* (2008) Recombinant antibody 2G12 produced in maize endosperm efficiently neutralizes HIV-1 and contains predominantly single-GlcNAc N-glycans. *Plant Biotechnol. J.* **6**, 189–201.

Razaghi, A., Owens, L. and Heimann, K. (2016) Review of the recombinant human interferon gamma as an immunotherapeutic: Impacts of production platforms and glycosylation. *J. Biotechnol.* **240**, 48–60.

Reusch, D. and Tejada, M.L. (2015) Fc glycans of therapeutic antibodies as critical quality attributes. *Glycobiology*, **25**, 1325–1334.

Rinderknecht, E., O'Connor, B.H. and Rodriguez, H. (1984) Natural human interferon-gamma. Complete amino acid sequence and determination of sites of glycosylation. *J. Biol. Chem.* **259**, 6790–6797.

Roboti, P. and High, S. (2012) The oligosaccharyltransferase subunits OST48, DAD1 and KCP2 function as ubiquitous and selective modulators of mammalian N-glycosylation. *J. Cell Sci.* **125**, 3474–3484.

Ruiz-Canada, C., Kelleher, D.J. and Gilmore, R. (2009) Cotranslational and posttranslational N-glycosylation of polypeptides by distinct mammalian OST isoforms. *Cell*, **136**, 272–283.

Saijo, Y., Tintor, N., Lu, X., Rauf, P., Pajerowska-Mukhtar, K., Häweker, H., Dong, X. *et al.* (2009) Receptor quality control in the endoplasmic reticulum for plant innate immunity. *EMBO J.* **28**, 3439–3449.

Samuelson, J., Banerjee, S., Magnelli, P., Cui, J., Kelleher, D.J., Gilmore, R. and Robbins, P.W. (2005) The diversity of dolichol-linked precursors to Asn-linked glycans likely results from secondary loss of sets of glycosyltransferases. *Proc. Natl. Acad. Sci. USA*, **102**, 1548–1553.

Sareneva, T., Cantell, K., Pyhälä, L., Pirhonen, J. and Julkunen, I. (1993) Effect of carbohydrates on the pharmacokinetics of human interferon-gamma. *J. Interferon Res.* **13**, 267–269.

Sareneva, T., Pirhonen, J., Cantell, K. and Julkunen, I. (1995) N-glycosylation of human interferon-gamma: glycans at Asn-25 are critical for protease resistance. *Biochem. J.* **308**, 9–14.

Sareneva, T., Mørtz, E., Tölö, H., Roepstorff, P. and Julkunen, I. (1996) Biosynthesis and N-glycosylation of human interferon-gamma. Asn25 and Asn97 differ markedly in how efficiently they are glycosylated and in their oligosaccharide composition. *Eur. J. Biochem.* **242**, 191–200.

Schähs, M., Strasser, R., Stadlmann, J., Kunert, R., Rademacher, T. and Steinkellner, H. (2007) Production of a monoclonal antibody in plants with a humanized N-glycosylation pattern. *Plant Biotechnol. J.* **5**, 657–663.

Schoberer, J., Vavra, U., Stadlmann, J., Hawes, C., Mach, L., Steinkellner, H. and Strasser, R. (2009) Arginine/lysine residues in the cytoplasmic tail promote ER export of plant glycosylation enzymes. *Traffic*, **10**, 101–115.

Schoberer, J., Liebminger, E., Botchway, S.W., Strasser, R. and Hawes, C. (2013) Time-resolved fluorescence imaging reveals differential interactions of N-glycan processing enzymes across the Golgi stack in planta. *Plant Physiol.* **161**, 1737–1754.

Shibatani, T., David, L.L., McCormack, A.L., Frueh, K. and Skach, W.R. (2005) Proteomic analysis of mammalian oligosaccharyltransferase reveals multiple subcomplexes that contain Sec61, TRAP, and two potential new subunits. *Biochemistry*, **44**, 5982–5992.

Shields, R.L., Lai, J., Keck, R., O'Connell, L.Y., Hong, K., Meng, Y.G., Weikert, S.H. *et al.* (2002) Lack of fucose on human IgG1 N-linked oligosaccharide improves binding to human Fcgamma RIII and antibody-dependent cellular toxicity. *J. Biol. Chem.* **277**, 26733–26740.

Shin, Y.J., Castilho, A., Dicker, M., Sádio, F., Vavra, U., Grünwald-Gruber, C., Kwon, T.H. *et al.* (2017) Reduced paucimannosidic N-glycan formation by suppression of a specific β-hexosaminidase from *Nicotiana benthamiana*. *Plant Biotechnol. J.* **15**, 197–206.

Shrimal, S., Trueman, S.F. and Gilmore, R. (2013) Extreme C-terminal sites are posttranslocationally glycosylated by the STT3B isoform of the OST. *J. Cell Biol.* **201**, 81–95.

Shrimal, S., Cherepanova, N.A. and Gilmore, R. (2015) Cotranslational and posttranslocational N-glycosylation of proteins in the endoplasmic reticulum. *Semin. Cell Dev. Biol.* **41**, 71–78.

Stadlmann, J., Pabst, M., Kolarich, D., Kunert, R. and Altmann, F. (2008) Analysis of immunoglobulin glycosylation by LC-ESI-MS of glycopeptides and oligosaccharides. *Proteomics*, **8**, 2858–2871.

Strasser, R. (2016) Plant protein glycosylation. *Glycobiology*, **26**, 926–939.

Strasser, R., Altmann, F., Mach, L., Glössl, J. and Steinkellner, H. (2004) Generation of *Arabidopsis thaliana* plants with complex N-glycans lacking beta1,2-linked xylose and core alpha1,3-linked fucose. *FEBS Lett.* **561**, 132–136.

Strasser, R., Bondili, J., Schoberer, J., Svoboda, B., Liebminger, E., Glössl, J., Altmann, F. *et al.* (2007) Enzymatic properties and subcellular localization of Arabidopsis beta-N-acetylhexosaminidases. *Plant Physiol.* **145**, 5–16.

Strasser, R., Stadlmann, J., Schähs, M., Stiegler, G., Quendler, H., Mach, L., Glössl, J. *et al.* (2008) Generation of glyco-engineered *Nicotiana benthamiana* for the production of monoclonal antibodies with a homogeneous human-like N-glycan structure. *Plant Biotechnol. J.* **6**, 392–402.

Strasser, R., Altmann, F. and Steinkellner, H. (2014) Controlled glycosylation of plant-produced recombinant proteins. *Curr. Opin. Biotechnol.* **30C**, 95–100.

Vamvaka, E., Twyman, R.M., Murad, A.M., Melnik, S., Teh, A.Y., Arcalis, E., Altmann, F. *et al.* (2016) Rice endosperm produces an underglycosylated and potent form of the HIV-neutralizing monoclonal antibody 2G12. *Plant Biotechnol. J.* **14**, 97–108.

Van Droogenbroeck, B., Cao, J., Stadlmann, J., Altmann, F., Colanesi, S., Hillmer, S., Robinson, D.G. *et al.* (2007) Aberrant localization and underglycosylation of highly accumulating single-chain Fv-Fc antibodies in transgenic Arabidopsis seeds. *Proc. Natl. Acad. Sci. USA*, **104**, 1430–1435.

Walker, M.R., Lund, J., Thompson, K.M. and Jefferis, R. (1989) Aglycosylation of human IgG1 and IgG3 monoclonal antibodies can eliminate recognition by human cells expressing Fc gamma RI and/or Fc gamma RII receptors. *Biochem. J.* **259**, 347–353.

Wong, D.C., Wong, N.S., Goh, J.S., May, L.M. and Yap, M.G. (2010) Profiling of N-glycosylation gene expression in CHO cell fed-batch cultures. *Biotechnol. Bioeng.* **107**, 516–528.

Yan, Q. and Lennarz, W.J. (2002) Studies on the function of oligosaccharyl transferase subunits. Stt3p is directly involved in the glycosylation process. *J. Biol. Chem.* **277**, 47692–47700.

Zacchi, L.F. and Schulz, B.L. (2016) N-glycoprotein macroheterogeneity: biological implications and proteomic characterization. *Glycoconj. J.* **33**, 359–376.

Zeitlin, L., Geisbert, J.B., Deer, D.J., Fenton, K.A., Bohorov, O., Bohorova, N., Goodman, C. *et al.* (2016) Monoclonal antibody therapy for Junin virus infection. *Proc. Natl. Acad. Sci. USA*, **13**, 4458–4463.

Zielinska, D.F., Gnad, F., Wiśniewski, J.R. and Mann, M. (2010) Precision mapping of an in vivo N-glycoproteome reveals rigid topological and sequence constraints. *Cell*, **141**, 897–907.

Zielinska, D.F., Gnad, F., Schropp, K., Wiśniewski, J.R. and Mann, M. (2012) Mapping N-glycosylation sites across seven evolutionarily distant species reveals a divergent substrate proteome despite a common core machinery. *Mol. Cell*, **46**, 542–548.

Supporting information

Additional Supporting Information may be found online in the supporting information tab for this article:

Figure S1 Mass spectra of the IgG glycopeptide in the presence or absence of LmSTT3D-GFP.

Figure S2 Mass spectra of IgE glycopeptides in the presence or absence of LmSTT3D-GFP.

Figure S3 Mass spectra of IgA1 glycopeptides in the presence or absence of LmSTT3D-GFP.

Figure S4 Mass spectra of the EPO-Fc glycopeptides harbouring glycosylation site 1 in the presence or absence of LmSTT3D-GFP.

Figure S5 Schematic illustration of the IFN-γ-HA expression construct and the corresponding amino acid sequence.

Table S1 Comparison of the N-glycosylation site occupancy of native and recombinant glycoproteins.

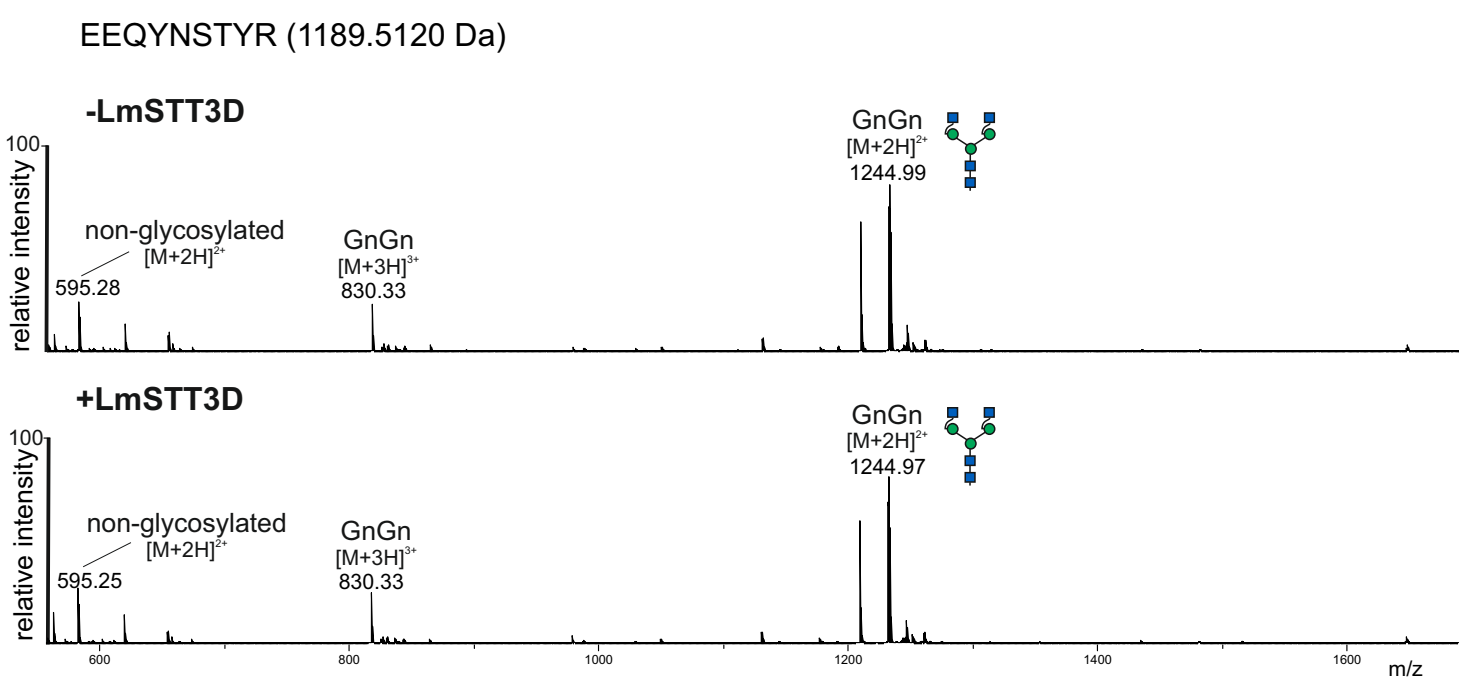

Figure S1 Mass spectra of (glyco)peptides from IgG. IgG was transiently expressed in *N. benthamiana* ΔXT/FT in the presence or absence of LmSTT3D-GFP. Purified IgG was trypsin digested and analysed by LC-ESI-MS.

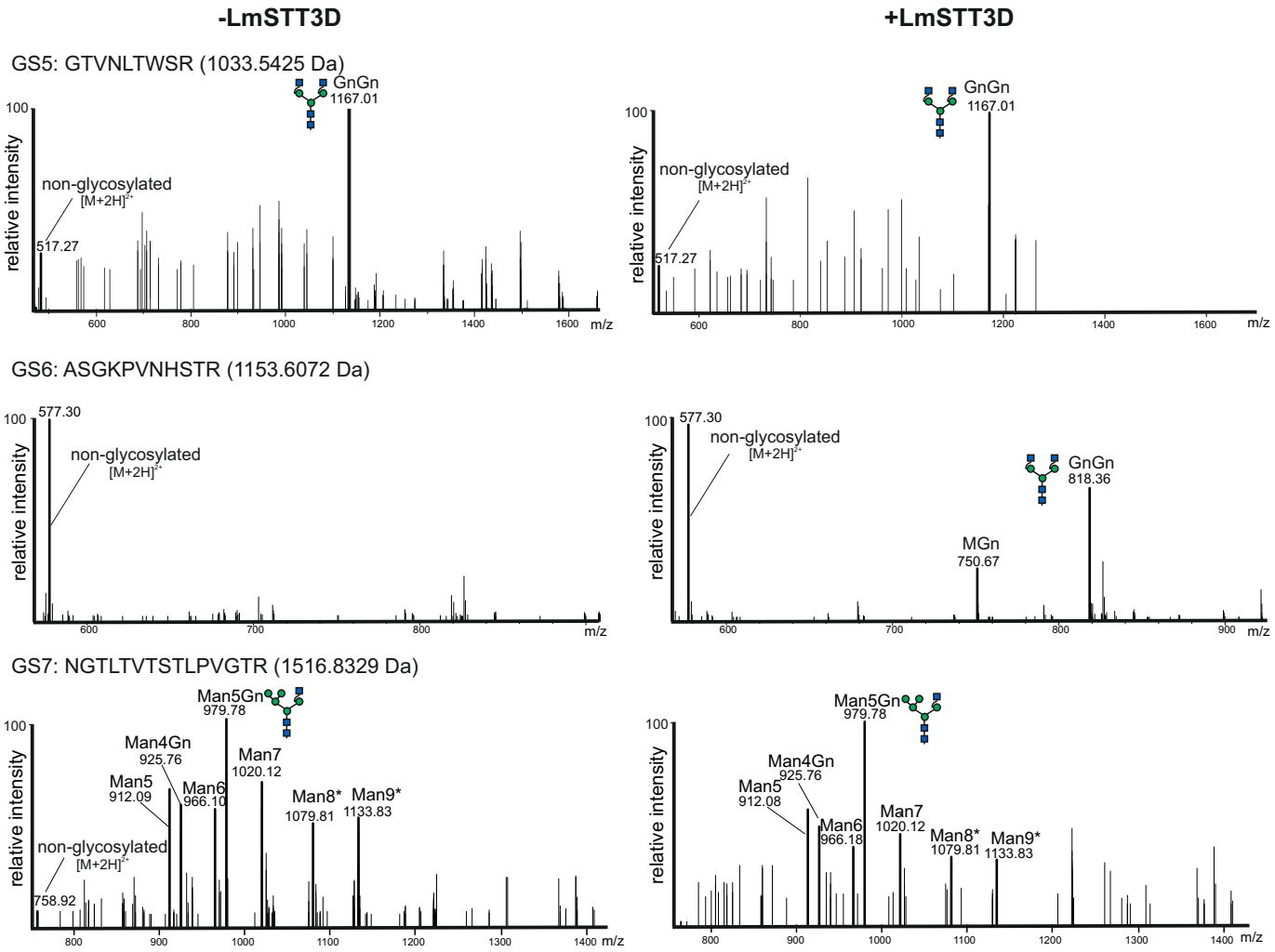

Figure S2 Mass-spectra of IgE (glyco)peptides harbouring glycosylation sites (GS) 5, 6 and 7. IgE was transiently expressed in *N. benthamiana* ΔXT/FT in the presence or absence of LmSTT3D-GFP. Purified IgE was trypsin digested and analysed by LC-ESI-MS. The mass range displays the major glycoforms. Except for the glycopeptides harbouring GS5, the peaks corresponding to triple charged glycopeptides ($[M+3H]^{3+}$) are indicated. The major glycoform on GS5 as well as all non-glycosylated peptides are shown in their double charged ($[M+2H]^{2+}$) state. Ammonia adducts are denoted by an asterisk.

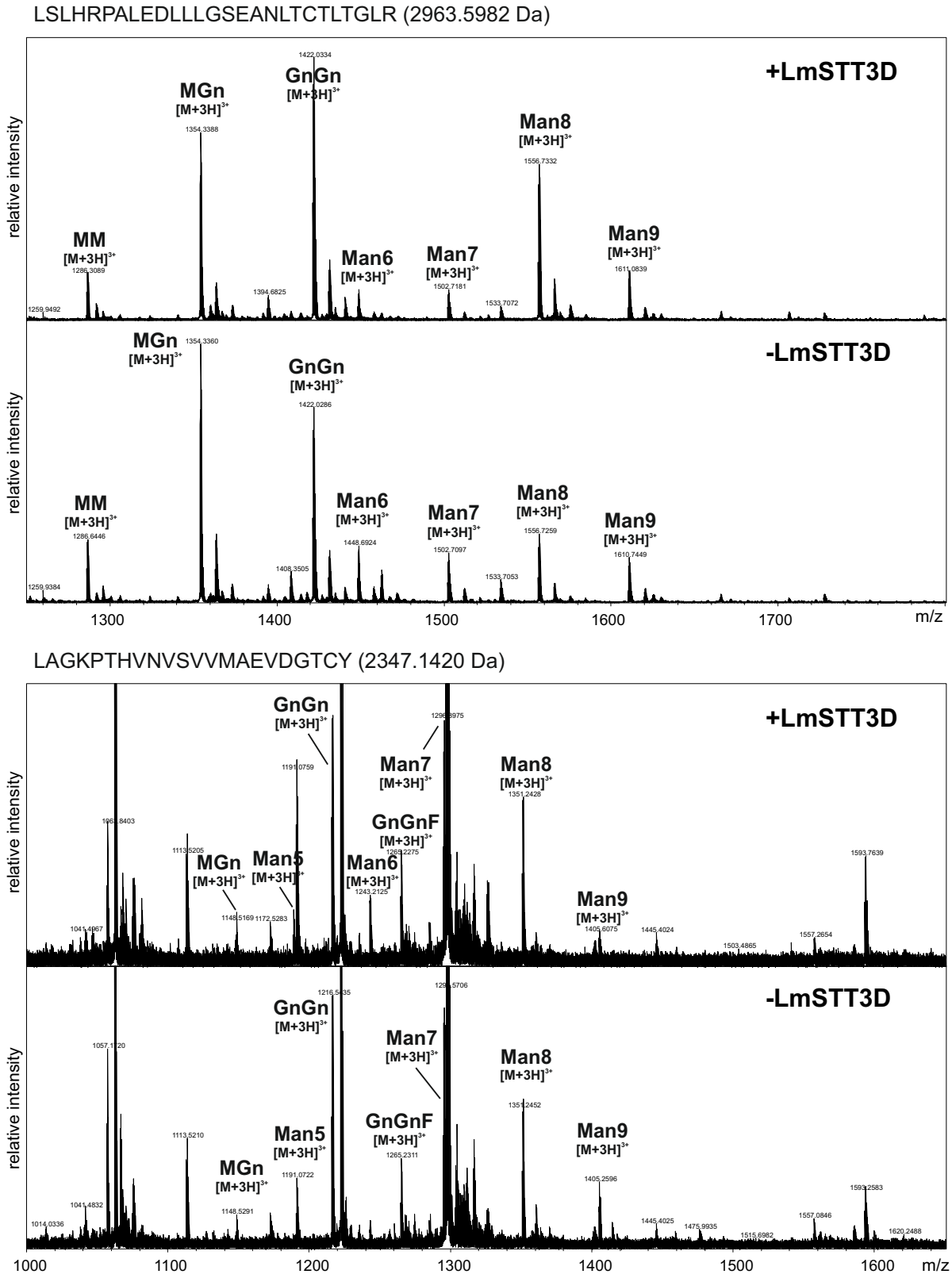

Figure S3 Mass-spectra of IgA1 (glyco)peptides. IgA1 was transiently expressed in *N. benthamiana* ΔXT/FT in the presence or absence of LmSTT3D-GFP. The purified IgA1 heavy chain was trypsin digested and analysed by LC-ESI-MS.

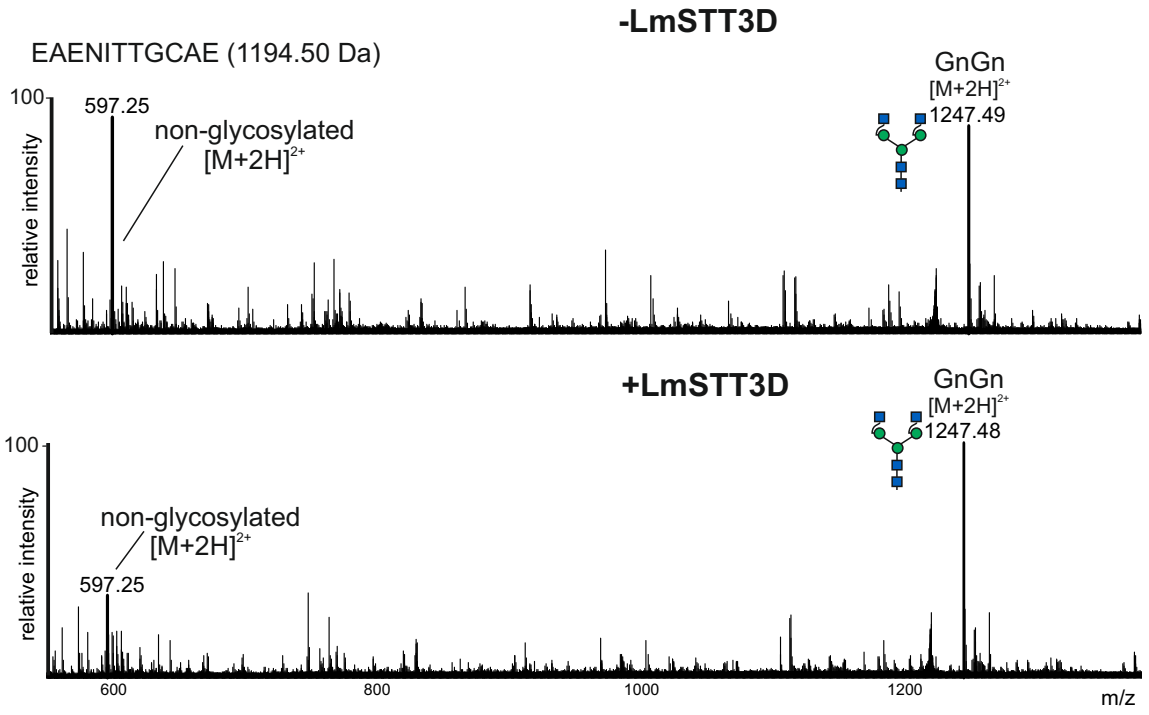

Figure S4 Mass-spectra of EPO-Fc (glyco)peptides. EPO-Fc was transiently expressed in *N. benthamiana* ΔXT/FT in the presence or absence of LmSTT3D-GFP. Purified EPO-Fc was trypsin+GluC digested and analysed by LC-ESI-MS. The mass range displaying the major glycoform from the peptide corresponding to glycosylation site 1 (due to the iodoacetamide treatment the cysteine is present as carbamidomethyl-cysteine) is shown.

(a)

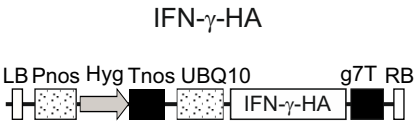

(b)

MANKHLSLSLFLVLLGLSASLAQDPYVKEAENLKKYFNAGHSDVADNGTLFLGILKNWKEESDRKIMQ
SQIVSFYFKLFKNFKDDQSIQKSVETIKEDMNVKFFNSNKKKRDDFEKLTNYSVTDLNVQRKAIHELI
QVMAELSPAAKTGKRKRSQMLFRGRRASQGSYPYDVPDYASLYPYDVPDYASLYPYDVPDYASL

Figure S5 Schematic illustration of the IFN-γ–HA expression construct (a) and the IFN-γ–HA amino acid sequence (b). (a) LB: left border; Pnos: nopaline synthase gene promoter; Hyg: hygromycin B phosphotransferase gene; Tnos: nopaline synthase gene terminator; UBQ10: *A. thaliana* ubiquitin-10 promoter; IFN-γ-HA: coding sequence of human interferon γ fused to a 3x hemagglutinin (HA) tag; g7T: agrobacterium gene 7 terminator; RB: right border. (b) Amino acid sequence of IFN-γ–HA. The signal peptide from barely alpha-amylase is marked in green. The two N-glycosylation sites (NGT and NYS) are marked in blue. A short dipeptide linker is marked in red and the 3x HA tag is highlighted in grey.

Table S1 Comparison of the N-glycosylation site occupancy of native and recombinant glycoproteins.

Protein	N-glycosylation site (GS)	source	% glycosylated	Reference
Fc	GS1 NST	HEK293	> 90	Jez et al. 2012 and unplublished
IgG	GS1 NST	CHO	99	Rustandi et al. 2008
	GS1 NST	human serum	~100	Karnoup et al. 2007
IgE	GS3 NKT	HEK293	80	Montero-Morales et al. 2017
	GS5 NLT	HEK293	91	
	GS6 NHS	HEK293	0	
	GS3 NKT	human serum	75	Montero-Morales et al. 2017
	GS5 NLT	human serum	85	
	GS6 NHS	human serum	0	
	GS3 NKT	human serum	80	Plomp et al. 2014
	GS5 NLT	human serum	98	
IgA1	GS1 NLT	HEK293	99	Göritzer et al. 2017
	GS2 NVS	HEK293	64	
	GS1 NLT	human colostrum	< 50	Huang et al. 2015
	GS2 NVS	human colostrum	< 10	
	GS1 NLT	human serum	85	Hülsmeier et al. 2016
EPO-Fc	all sites	CHO	100	Taschwer et al. 2012
EPO	all sites	CHO	100	Gong et al. 2013
	all sites	*P. pastoris*	100	
	all sites	human serum	~100	Skibeli et al 2001
IFN-γ	GS1 + GS2	CHO	65	Wong et al. 2010
	GS1 + GS2	human blood cells	~67	Rinderknecht et al. 1984

Please note for some glycoproteins no precise data for site-specific N-glycosylation site occupancy could be obtained from literature and for mammalian cells glycosylation efficiency is dependent on culture conditions.

References

Gong, B., Burnina, I., Stadheim, T.A. and Li, H. (2013) Glycosylation characterization of recombinant human erythropoietin produced in glycoengineered Pichia pastoris by mass spectrometry. J Mass Spectrom **48**, 1308-1317.

Göritzer, K., Maresch, D., Altmann, F., Obinger, C. and Strasser, R. (2017) Exploring Site-Specific N-Glycosylation of HEK293 and Plant-Produced Human IgA Isotypes. *J Proteome Res* **16**, 2560-2570.

Huang, J., Guerrero, A., Parker, E., Strum, J.S., Smilowitz, J.T., German, J.B. and Lebrilla, C.B. (2015) Site-specific glycosylation of secretory immunoglobulin A from human colostrum. J Proteome Res **14**, 1335-1349.

Hülsmeier, A.J., Tobler, M., Burda, P. and Hennet, T. (2016) Glycosylation site occupancy in health, congenital disorder of glycosylation and fatty liver disease. Sci Rep **6**, 33927.

Jez, J., Antes, B., Castilho, A., Kainer, M., Wiederkum, S., Grass, J., Rüker, F., Woisetschläger, M. and Steinkellner, H. (2012) Significant impact of single N-glycan residues on the biological activity of Fc-based antibody-like fragments. J Biol Chem **287**, 24313-24319.

Karnoup, A.S., Kuppannan, K. and Young, S.A. (2007) A novel HPLC-UV-MS method for quantitative analysis of protein glycosylation. J Chromatogr B Analyt Technol Biomed Life Sci **859**, 178-191.

Montero-Morales, L., Maresch, D., Castilho, A., Turupcu, A., Ilieva, K.M., Crescioli, S., Karagiannis, S.N., Lupinek, C., Oostenbrink, C., Altmann, F. and Steinkellner, H. (2017) Recombinant plant-derived human IgE glycoproteomics. *J Proteomics* **161**, 81-87.

Plomp, R., Hensbergen, P.J., Rombouts, Y., Zauner, G., Dragan, I., Koeleman, C.A., Deelder, A.M. and Wuhrer, M. (2014) Site-specific N-glycosylation analysis of human immunoglobulin E. J Proteome Res 13, 536-546.

Rinderknecht, E., O'Connor, B.H. and Rodriguez, H. (1984) Natural human interferon-gamma. Complete amino acid sequence and determination of sites of glycosylation. J Biol Chem **259**, 6790-6797.

Rustandi, R.R., Washabaugh, M.W. and Wang, Y. (2008) Applications of CE SDS gel in development of biopharmaceutical antibody-based products. Electrophoresis **29**, 3612-3620.

Skibeli, V., Nissen-Lie, G. and Torjesen, P. (2001) Sugar profiling proves that human serum erythropoietin differs from recombinant human erythropoietin. Blood **98**, 3626-3634.

Taschwer, M., Hackl, M., Hernández Bort, J.A., Leitner, C., Kumar, N., Puc, U., Grass, J., Papst, M., Kunert, R., Altmann, F. and Borth, N. (2012) Growth, productivity and protein glycosylation in a CHO EpoFc producer cell line adapted to glutamine-free growth. J Biotechnol **157**, 295-303.

Wong, D.C., Wong, N.S., Goh, J.S., May, L.M. and Yap, M.G. (2010) Profiling of N-glycosylation gene expression in CHO cell fed-batch cultures. *Biotechnol Bioeng* **107**, 516-528.

APPENDIX II

Curriculum Vitae

Kathrin GÖRITZER

Adress:	Hernalser Hauptstraße 27/11, 1170 Wien
Date of Birth:	02.07.1990
Place of Birth	Lienz in Osttirol
Nationality:	Austria
Tel.:	+43 650 3338887
Email:	kathrin.goeritzer@boku.ac.at

EDUCATION

Since 10/2015 **Member of the international PhD program**
BioToP: Biomolecular Technology of Proteins
University of Natural Resources and Life Sciences Vienna, Austria
PhD thesis: Department of Applied Genetics and Cell Biology,
"Analysis of structure-function relationships of monomeric and dimeric human IgA1 and IgA2 with defined N- and O-glycosylation"

03/2013 – 09/2015 **Master's program: Biotechnology**
University of Natural Resources and Life Sciences Vienna, Austria
Diploma thesis: Department of Chemistry, CD-Laboratory for Antibody Engineering, "***Human epidermal growth factor receptor 2: recombinant production, purification and interaction studies with Fcabs***"

09/2009 – 02/2013 **Bachelor's program: Food Science and Biotechnology**
University of Natural Resources and Life Sciences Vienna, Austria
Bachelor thesis: Department of Biotechnology; "***Fermentation of CHO-cells producing 3D6-Fc and 2F5scFc single-chain antibodies"***

09/2004 – 06/2009 Centrum Humanberuflicher Schulen des Bundes, Villach (High school)

INTERNATIONAL EXPERIENCE

03-06/2018 and 09-12/2018 **University of Alabama at Birmingham, AL, USA**
Department of Microbiology
Research stay as part of the PhD project

07/2013 – 08/2013 **University of Technology, Lodz, Poland**
Department of Food Chemistry
Internship

OTHER RELEVANT WORK EXPERIENCE

05/2014 – 09/2015 **Research assistant**
University of Natural Resources and Life Sciences Vienna, Austria
Department of Chemistry, CD-Laboratory for Antibody Engineering

08/2011 – 09/2011 **Internship**
University of Natural Resources and Life Sciences Vienna, Austria
Institute of Chemistry of Renewable Resources

PUBLICATIONS

SCI publications

Göritzer, K., Turupcu, A., Maresch, D., Novak, J., Altmann, F., Oostenbrink C., Obinger, C., Strasser, R. (2019) Distinct Fc alpha receptor N-glycans modulate the binding affinity to immunoglobulin A (IgA) antibodies. *J Biol Chem*. doi: 10.1074/jbc.RA119.009954

Castilho, A., Beihammer, G., Pfeiffer, C., **Göritzer, K.**, Montero-Morales, L., Vavra, U., Maresch, D., Grünwald-Gruber, C., Altmann, F., Steinkellner, H., Strasser, R. (2018) An oligosaccharyltransferase from Leishmania major increases the N-glycan occupancy on recombinant glycoproteins produced in *Nicotiana benthamiana*. *Plant Biotechnol. J.* doi: 10.1111/pbi.12906

Göritzer, K., Maresch, D., Altmann, F., Obinger, C., Strasser, R. (2017) Exploring Site-Specific N-Glycosylation of HEK293 and Plant-Produced Human IgA Isotypes. *J. Proteome Res.* 16, 2560-2570. doi: 10.1021/acs.jproteome.7b00121

Lobner, E., Humm, A.-S., **Göritzer, K.**, Mlynek, G., Puchinger, M.G., Hasenhindl, C., Rüker, F., Traxlmayr, M.W., Djinović-Carugo, K., Obinger, C. (2017) Fcab-HER2 Interaction: a Ménage à Trois. Lessons from X-Ray and Solution Studies. *Structure* **25**, 878-889.e875. doi: 10.1016/j.str.2017.04.014

Oral presentations at conferences

Göritzer, K., Turupcu, A., Maresch, D., Novak, J., Altmann, F., Oostenbrink, C., Obinger, C., Strasser, R. (2019) A plant-based glyco-engineering approach to elucidate structure-function relationships of distinct Immunoglobulin A glycoforms (Talk) [The 14th Asian Congress on Biotechnology, Taipeh, Taiwan, July 1-4, 2019]

Göritzer, K., Turupcu, A., Maresch, D., Novak, J., Altmann, F., Oostenbrink, C., Obinger, C., Strasser, R. (2019) Unraveling the role of *N*-glycosylation in the IgA-FcαRI interaction (Talk) [Plant-based Vaccines, Antibodies and Biologics, Riga, Latvia, 10-12 June, 2019]

Göritzer, K., Maresch, D., Altmann, F., Obinger, C., Strasser, R. (2016) Investigation of structure-function relationships of different IgA glycoforms (Talk) [21st Austrian Carbohydrate Workshop, Vienna, Austria, February 18, 2018]

Göritzer, K., Maresch, D., Altmann, F., Obinger, C., Strasser, R. (2017) Characterization of monomeric IgA1 and IgA2 produced in Nicotiana benthamiana and HEK293 cells (Talk) [9th International Conference On Recombinant Protein Production, Dubrovnik, Croatia, April 23 - 25, 2017]

Poster presentations at conferences

Göritzer, K., Maresch, D., Altmann, F., Novak J., Obinger, C., Strasser, R. (2018) Elucidating structure-function relationships of Immunoglobulin A with defined glycosylation (Poster) [Benzon Symposium 64 - Glycotherapeutics - Emerging roles of glycans in medicine, Copenhagen, Denmark, August 27-30, 2018]

Göritzer, K., Maresch, D., Altmann, F., Obinger, C., Strasser, R. (2017) Characterization of IgA1 and IgA2 produced in glyco-engineered *Nicotiana benthamiana* and HEK293 cells (Poster) [Plant-based Vaccines, Antibodies& Biologics, Albufeira, Portugal, April 5 - 8, 2017]

Göritzer, K., Maresch, D., Obinger, C., Strasser R. (2016) Expression, purification and characterization of monomeric IgA1 and IgA2 produced in Nicotiana benthamiana (Poster) [ECB2016 - The 17th European Congress on Biotechnology, Krakow, Poland, July 3-6, 2016]

SKILLS

Languages	German	native speaker
	English	fluently
	Italian	basic knowledge

Computer Applications

very good knowledge of Micrososft Office, Adobe Photoshp, corelDRAW, diverse subject-specific software (LabSolutions, Astra 6, Origin Lab, PyMOL, Gene Runner, Sigma Plot, Snap Gene, DNA Star, SeqMan, R), good knowledge in webdesign (HTML, CSS, PHP, JavaScript)

Driving License Austrian B

APPENDIX III

Eidesstattliche Erklärung

Ich erkläre ehrenwörtlich, dass ich die vorliegende Arbeit selbständig und ohne fremde Hilfe verfasst habe, andere als die angegebenen Quellen nicht verwendet habe und die den benutzten Quellen wörtlich oder inhaltlich entnommenen Stellen als solche kenntlich gemacht habe.

_____ _____

Ort, Datum Name